Technical Report
Research Project T9903, Task 41
Seismic Bridge Restrainers

DESIGN OF SEISMIC RESTRAINERS FOR IN-SPAN HINGES

by

Panos Trochalakis
Graduate Research Assistant
Department of Civil Engineering

Marc O. Eberhard
Assistant Professor
Department of Civil Engineering

John F. Stanton
Professor
Department of Civil Engineering

Washington State Transportation Center (TRAC)
University of Washington, Box 354802
University District Building
1107 NE 45th Street, Suite 535
Seattle, Washington 98105-4631

Washington State Department of Transportation
Technical Monitor
Jim Wei
Special Project Engineer

Prepared for

Washington State Transportation Commission
Department of Transportation
and in cooperation with
U.S. Department of Transportation
Federal Highway Administration

May 1996

TECHNICAL REPORT STANDARD TITLE PAGE

1. REPORT NO.	2. GOVERNMENT ACCESSION NO.	3. RECIPIENT'S CATALOG NO.
WA-RD 387.1		

4. TITLE AND SUBTITLE DESIGN OF SEISMIC RESTRAINERS FOR IN-SPAN HINGES	5. REPORT DATE May 1996 6. PERFORMING ORGANIZATION CODE
7. AUTHOR(S) Panos Trochalakis, Marc O. Eberhard, and John F. Stanton	8. PERFORMING ORGANIZATION REPORT NO.
9. PERFORMING ORGANIZATION NAME AND ADDRESS Washington State Transportation Center (TRAC) University of Washington, Box 354802 University District Building; Suite 535; 1107 NE 45th Street Seattle, Washington 98105-4631	10. WORK UNIT NO. 11. CONTRACT OR GRANT NO. Agreement T9903, Task 41
12. SPONSORING AGENCY NAME AND ADDRESS Washington State Department of Transportation Transportation Building, MS 7370 Olympia, Washington 98504-7370	13. TYPE OF REPORT AND PERIOD COVERED Technical Report 14. SPONSORING AGENCY CODE

15. SUPPLEMENTARY NOTES

This study was conducted in cooperation with the U.S. Department of Transportation, Federal Highway Administration.

16. ABSTRACT

Currently, two commonly used restrainer design methods are those mandated by the American Association of State and Highway Transportation Officials (AASHTO) and the California Department of Transportation (CALTRANS). To evaluate these methods and perhaps develop a new method, the Washington State Department of Transportation (WSDOT) sponsored this study.

Using sample WSDOT designs and seismic retrofitting guidelines from WSDOT and CALTRANS, the researchers developed a model of a two-frame bridge with a single in-span hinge. The nonlinear response of the bridge was studied to determine the maximum opening experienced at the in-span hinge and the maximum relative displacements at the abutments.

To identify the parameters most important in restrainer design and in predicting the unrestrained maximum relative abutment displacements, the researchers varied eleven parameters. The parametric study identified the parameters that significantly influenced the maximum relative hinge displacement (MRHD) and the maximum relative abutment displacements (MRAD).

The AASHTO empirical seat width equation and the CALTRANS restrainer design method were compared with the results of nonlinear time history analysis. The empirical seat width equation produced conservative results while the CALTRANS method produced inconsistent results, a large amount of scatter and some significantly unconservative values.

Using the results of the parametric study, the researchers developed a new restrainer design method that predicted the MRHD much more accurately than the CALTRANS method. The researchers also developed a method for estimating the unrestrained MRAD.

17. KEY WORDS	18. DISTRIBUTION STATEMENT
Bridge, design, hinge, earthquakes, evaluation restrainers	No restrictions. This document is available to the public through the National Technical Information Service, Springfield, VA 22616

19. SECURITY CLASSIF. (of this report)	20. SECURITY CLASSIF. (of this page)	21. NO. OF PAGES	22. PRICE
None	None	82	

DISCLAIMER

The contents of this report reflect the views of the authors, who are responsible for the facts and the accuracy of the data presented herein. The contents do not necessarily reflect the official views or policies of the Washington State Transportation Commission, Department of Transportation, or the Federal Highway Administration. This report does not constitute a standard, specification, or regulation.

METRIC CONVERSION
FOR COMMONLY USED UNITS

	From	To	Multiply by
Area	in^2 ft^2	m^2 m^2	0.000 645 160 0.092 903
Force	lbf	N	4.448 222
Force per unit length	lbf/inch	N/mm	0.175 126 8
Length	inch ft	mm m	25.4 0.304 801
Mass	pound (lb)	kg	0.453 592
Mass per unit volume	lb/ft^3	kg/m^3	16.018 460
Pressure	lbf/in^2 (psi) lbf/in^2 (psi)	Pa MPa	6894.757 0.006 894 757
Temperature	°F	°C	$t_C = \frac{(t_F - 32)}{1.8}$

TABLE OF CONTENTS

TABLE OF CONTENTS (Continued)

LIST OF TABLES

LIST OF FIGURES

LIST OF FIGURES (Continued)

Figure **Page**

EXECUTIVE SUMMARY

Since the 1970s, seismic restrainers have been used throughout the United States to prevent bridge superstructures from unseating during earthquakes. To design restrainers, the Washington State Department of Transportation (WSDOT) currently follows restrainer design guidelines mandated by the American Association of Transportation Officials (AASHTO). WSDOT allows designers to use the California Department of Transportation (CALTRANS) design method *in lieu* of elastic analysis. The AASHTO and CALTRANS procedures are consistent with state-of-the-art practice. Indeed, CALTRANS's practice is emulated by many state transportation departments.

The goals of this study were to (1) identify the factors that significantly affect the relative displacement at in-span hinges; (2) identify the factors that significantly affect the superstructure displacements relative to the abutments; (3) determine under what circumstances restrainers are effective in reducing the in-span hinge relative displacement; (4) evaluate the current restrainer design methods; and (5), if necessary, develop a new method to design restrainers.

Because previous studies omitted variables that the University of Washington researchers felt were important in restrainer behavior, the researchers conducted a new parametric study. On the basis of sample WSDOT designs and seismic retrofitting guidelines from WSDOT and CALTRANS, a model of a two-frame bridge with a single in-span hinge was developed. The researchers performed nonlinear time history analyses of this model using the North-South component of the 1940 El Centro ground motion, scaled by a factor of 2.0 (PGA=0.70g). The response of the bridge was studied to determine the maximum opening experienced at the in-span hinge. This opening, termed the maximum relative hinge displacement (MRHD), can be used to predict whether a span will unseat. The maximum relative displacement between the abutment seat and the edge of adjacent superstructure was termed MRAD. This value can be used to predict span unseating at the abutments.

To identify the parameters most important in predicting the MRHD and the unrestrained MRAD, the UW researchers varied eleven parameters. The researchers found the following four parameters to be the most important in predicting the MRHD:

- restrainer stiffness
- restrainer gap
- frame period ratio (ratio of the periods of the two frames adjacent to the hinge of interest)
- frame stiffness ratio (ratio of the stiffnesses of the two frames adjacent to the hinge of interest).

The parametric study identified the following three variables as most important in predicting the unrestrained MRAD:

- abutment stiffness and strength
- sum of frame stiffnesses
- sum of frame weights.

The AASHTO empirical seat width equation and the CALTRANS restrainer design method were compared with the results of nonlinear time history analyses. The empirical seat width equation produced conservative results, even for very strong earthquakes such as El Centro*2 (0.70g). However, the AASHTO restrainer design procedure ignores variables that were shown to be important in the parametric study. In situations where restrainers are required, the procedure does not account for the restrainer gap, frame period ratio, frame stiffness ratio, or hinge seat width. The CALTRANS method produced inconsistent results with a large amount of scatter. In extreme cases, the MRHD was under-predicted by 127 mm (5 inches) and over-predicted by 188 mm (7.4 inches).

Using the results of the parametric study, the UW researchers developed a new restrainer design method that predicted the MRHD more accurately than the CALTRANS method. The average error for over 200 cases was approximately 15 mm (0.6 inches). The largest unconservative error was only 25 mm (1 inch). This method incorporated all of the variables that were shown to be important in the parametric study.

The researchers also developed a method for estimating the unrestrained MRAD. This method produced conservative results. However, its results had more scatter than the method for predicting the MRHD. The average error was 83 mm (3.25 inches).

To verify the proposed methods, the researchers conducted nonlinear time history analyses of three-frame bridges and two-frame bridges with earthquake damaged columns. The proposed methods provided accurate predictions of the nonlinear time history MRHD and MRAD.

WSDOT has been following state-of-the-art procedures in designing its seismic restrainers. The researchers recommend that WSDOT improve its practice by adopting the proposed methods for designing restrainers and for verifying the adequacy of abutment seat lengths.

CHAPTER 1
INTRODUCTION

1.1 CONTEXT

Since their introduction in the early seventies, seismic restrainers have been used throughout the United States to prevent superstructures from unseating during earthquakes. The California Department of Transportation (CALTRANS) began to install cable restrainers in response to the 1971 San Fernando Earthquake (Yang 1994). The CALTRANS procedures and details are widely recognized as representing the state of the art in designing seismic restrainers.

The Washington State Department of Transportation (WSDOT) Bridge Seismic Retrofit Program is currently in its first stage, which addresses superstructure vulnerabilities (Lwin and Henley 1993). The majority of superstructure retrofit work has addressed deficiencies of in-span hinges, simple supports at intermediate piers, and simple supports at abutments. Most of the WSDOT retrofits utilize high-strength steel rods acting as longitudinal restrainers. Currently, WSDOT follows AASHTO restrainer design guidelines (AASHTO 1994) and compares the design with the results of linear dynamic analysis. WSDOT allows substitution of the CALTRANS Design Method (CALTRANS 1989) as an alternative to performing elastic dynamic analysis.

However, researchers at the University of California, San Diego (UCSD), and the University of Nevada, Reno (UNR), have found that the CALTRANS Design Method does not produce results that agree with those of nonlinear analysis. Unfortunately, the UCSD study did not consider the influence of abutments, and the parametric study conducted by the UNR researchers considered only a small number of parameters. To evaluate the current design methods and to perhaps develop a new method, WSDOT sponsored a parametric study with a large number of variables and a more realistic analytical model.

1.2 OBJECTIVES

The objectives of this study were as follows:

1. identify the factors that significantly affect the relative displacement at in-span hinges
2. identify the factors that significantly affect the superstructure displacements relative to the abutments
3. determine under what circumstances, if any, restrainers are effective in reducing the in-span hinge relative displacement
4. evaluate the current restrainer design methods
5. if necessary, develop a new method to design restrainers.

1.3 SCOPE OF REPORT

Chapter 2 provides a summary of previous work on the topic of seismic restrainers. Researchers at the University of California, San Diego, and at the University of Nevada, Reno, have studied the effectiveness of restrainers. The study described in this report considers factors that were not considered in previous studies.

The University of Washington (UW) researchers conducted a parametric study on a nonlinear model of a two-frame bridge with an in-span hinge. The model bridge was developed by examining WSDOT designs and CALTRANS documentation. (CALTRANS 1990). Details of the model and input ground motions are discussed in Chapter 3.

The results of the nonlinear time history analyses were used to identify the factors that are important in estimating the maximum relative hinge displacement (MRHD) and the maximum displacement relative to the abutment (MRAD). The results also allowed the UW researchers to evaluate current design methods and to develop a new design method. The results of the parametric study are outlined in Chapter 4. The current design methods are evaluated in Chapter 5.

Using regression analysis and a database including approximately 200 cases, the researchers developed a design method to estimate the MRHD and MRAD. To keep the model simple, the researchers considered only longitudinal motion of straight bridges, and the motion was assumed to be coherent. These design procedures and their development are described in Chapter 6. Chapter 7 contains the conclusions and recommendations of this study.

CHAPTER 2
PREVIOUS WORK

Researchers at the University of California, San Diego, and the University of Nevada, Reno, conducted studies to evaluate the response of bridges retrofitted with restrainers. This chapter summarizes these studies.

2.1 UCSD

Yang (1994) conducted a parametric study of a two-frame bridge with an in-span hinge. Results of nonlinear dynamic analysis were compared with results of the CALTRANS Equivalent Static Analysis Procedure and with the results of other simpler procedures.

Analytical Models

The analytical model consisted of two nonlinear inelastic oscillators, each representing a bridge frame (Figure 2.1). Each oscillator, modeled as a column, was assumed to support a weight of 22.2 MN (5000 kips). The stiffness of column 1, K_1, remained 105 KN/mm (600 kips/inch), while the stiffness of column 2, K_2, varied from 10.5 KN/mm (60 kips/inch) to 1.05 MN/mm (6000 kips/inch). Each frame's force-deflection relationship was modeled as bilinear with a constant yield force of 4.45 MN (1000 kips) and strain hardening of 5 percent. Abutments were not included in the model.

The hinge model included three components: Coulomb friction, a restrainer, and an impact spring (Figure 2.2). The researchers assumed that a vertical force of 2.23 MN (500 kips) was transferred through the hinge and that the coefficient of kinematic friction was 0.30. Therefore, friction was modeled with a bilinear inelastic element with an initial stiffness of 263 KN/mm (1500 kips/inch) and a yield force of 667 KN (150 kips). The restrainer model contained a linear spring that was effective only in tension. Its stiffness was 17.5 KN/mm (100 kips/inch), and it had an initial gap of 25 mm (1 inch). Collision of the two superstructures was modeled with a linear spring that was effective only in compression. Its stiffness was 17.5 MN/mm (100,000 kips/inch), and it had an initial gap of 25 mm (1 inch).

The model was subjected to synchronous ground motion, and it was assumed to have 5 percent viscous damping in addition to the hysteresis in the nonlinear elements. The ground motion used was 1940 El Centro, with various scale factors. Table 2.1 summarizes the parameters studied and their ranges.

Analysis Methods

Nonlinear Time History (NLTH) analysis was used to compute the response of the idealized bridge. For some of the analyses, the results were compared with the results of the following simpler methods.

1. Time History: Linear column behavior with a nonlinear hinge model.

2. Time History (Linear Compression Model): Linear modeling of all elements. The hinge was modeled as an elastic spring with no gap and with a stiffness equal to the impact stiffness.

3. Time History (Linear Tension Model): Linear modeling of all elements. The hinge was modeled as an elastic spring with no gap and with a stiffness equal to the restrainer stiffness.

4. Response Spectrum (Elastic Compression Model): Same model as (2).

5. Response Spectrum (Elastic Tension Model): Same model as (3).

Conclusions

1. None of the simpler methods was capable of estimating the maximum relative hinge displacements computed with the NLTH method.

2. Except when the stiffness ratio, K_2/K_1, was extremely low, variations in the restrainer stiffness (0.9 to 35.0 KN/mm) did not affect the maximum relative hinge displacement significantly.

3. The influence of Coulomb friction on the maximum relative hinge displacement was small, typically on the order of 10 mm.

Table 2.1. Parameter Variation for UCSD study

PARAMETER	RANGE
K_2/K_1	0.1 to 10
Restrainer Stiffness	0.9 to 35.0 KN/mm (5 to 200 kips/inch)
Coulomb Friction Effects	no friction and standard friction model
Earthquake Intensity	0.08 to 0.66 g
Column Yield Strength	2.22 to 8.88 MN (500 to 2000 kips)
Restrainer Gap	0 to 51 mm (0 to 2.0 inch)

4. A reduction in column yield strength resulted in a reduced maximum relative hinge displacement.

5. A reduction in restrainer gap reduced the maximum relative hinge displacement.

6. When the restrainer was not very stiff, a reasonable estimate of the maximum relative hinge displacement was provided by taking the difference between the absolute maximum displacements of the two columns acting as independent nonlinear oscillators.

7. Greater earthquake intensity increased frame displacements. The maximum relative hinge displacement also increased if the frames remained elastic. However, if the frames yielded and behaved in a ductile manner, the maximum relative hinge displacement was not significantly influenced by the earthquake intensity.

8. In some cases, the CALTRANS Equivalent Static Analysis method is extremely conservative, while in others it underestimates the relative hinge displacement.

2.2 UNR EVALUATION OF THE CALTRANS DESIGN METHOD

Analytical Model

Saiidi et al. (1992) considered a four-frame bridge (Figure 2.3) similar to one described in CALTRANS documentation of its design method. (CALTRANS 1989) The difference between the two models was the type of abutment on the right side of the bridge. The CALTRANS example had a seat-type abutment, while the Reno model had diaphragm-type abutment.

The CALTRANS example did not specify all of the dimensions and properties of the example bridge. Therefore, to perform a nonlinear analysis of the modified CALTRANS model, the UNR researchers made several additional assumptions regarding dimensions and properties of the example bridge. In particular, the UNR researchers assumed that the superstructure was 1.52 m (5 feet) deep, the piers each had three square columns, and the lengths of spans and locations of hinges were those shown in Figure 2.3.

The hinge model consisted of spring elements representing the restrainers and the impact of adjacent superstructures. Friction was not included, and cable restrainers were modeled as bilinear. At the internal hinges, both the restrainer and compression gaps were 19 mm (3/4 inch). The abutments had no restrainers, and the compression gap was 25 mm (1 inch). This bridge represented a typical pre-1971 design with a hinge seat width of 152 mm (6 inches).

The abutment stiffness and capacity were calculated using the CALTRANS values of 115 KN/mm per linear meter (200 kips/inch per linear foot) of abutment width and a maximum soil pressure of 53.1 MPa (7.7 kips per square foot of abutment). Both these values were based on a 2.44 m (8 foot) deep soil wedge. Because the superstructure depth was assumed to be 1.52 m (5 feet), both the stiffness and strength were multiplied by a factor of 5/8.

As in the CALTRANS example, half the columns were assumed to behave as pinned members on both ends because of detailing inadequacies and lightly reinforced footings. The columns were modeled with nonlinear elements.

Parameter Variation

The parametric study considered the following three variables:

1. cross-sectional area of restrainers (Table 2.2 summarizes the six cases analyzed);

2. restrainer gap size (the six cases in Table 2.2 were analyzed with no gap); and

3. earthquake record (all three earthquakes normalized to .60g).

- 1940 El Centro Earthquake, North-South component
- 1954 Eureka Earthquake, North-South component
- 1989 Loma Prieta Earthquake, East-West component

Table 2.2 Variation of Restrainer Area

	# OF 19mm (3/4 inch) DIA. CABLES		
CASE	**HINGE 1**	**HINGE 2**	**HINGE 3**
1	80	60	100
2	70	50	90
3	60	40	80
4	50	30	70
5	40	20	60
6	0	0	0

Sensitivity Study

The CALTRANS Equivalent Static Analysis method requires that several simplifying assumptions be made in calculating the effective stiffness and mass. For example, the restrainer gap used in calculations corresponds to the high ambient temperature condition. To evaluate the effects of varying these assumptions, the process used to calculate the effective stiffness and mass was modified. The modifications are listed below:

1. two or more adjacent frames were allowed to contribute to the stiffness of the "mobilized structure" once the intermediate hinge had closed;

2. the mass of all the mobilized frames was used to calculate the effective period; and

3. the restrainer gap width was set to 0.0 millimeters to represent the extreme low ambient temperature.

Conclusions

1. The number of restrainers became more influential when the restrainer gap was reduced.

2. The CALTRANS Equivalent Static Analysis method did not produce results that agree with results of nonlinear analysis. It predicted the least displacement at the middle hinge, while the dynamic analyses showed the largest displacement at the middle hinge.

3. The restrainer gap width and the number of restrainers at the hinges did not affect the maximum relative displacement at the abutments.

4. Abutment forces were sensitive to the ground motion.

5. The three assumptions incorporated into the CALTRANS design method greatly affect the results.

2.3 UNR CASE STUDIES

Researchers at the University of Nevada, Reno, also performed nonlinear analysis using the computer program NEABS for the four case studies described in Table 2.3. (Saiidi et al. 1993) Ground motions were based on available data in the vicinity of the bridge, adjusted for local soil conditions.

Parameter Variation

The models for the case studies were also used for a modest parametric study. The ground motions were varied for all four bridges, and the restrainer gap width was varied for the San Gregorio Creek Bridge.

Table 2.3. UNR Case Studies

Bridge	Reference	Type	# of spans	# of hinges
Aptos Creek	Abdel-Ghaffar et al. 1993	cast-in-place girder	5	1
Huntington Avenue Overhead	Abdel-Ghaffar et al. 1993	box girder	12	3
Madrone Drive Undercrossing	O'Connor et al. 1993	cast-in-place girder	3	2
San Gregorio Creek	Maragakis et al. 1993	cast-in-place girder	5	3

Conclusions

1. Adequate performance of restrainer systems during the Loma Prieta earthquake was verified. Almost all restrainers survived in good condition, and displacements remained acceptable.

2. The current CALTRANS restrainer design method generally produced conservative results. However, relative hinge displacements were not well estimated.

3. Restrainer design should be based on a restrainer gap of zero. This was shown to be the critical case for restrainer stresses. However, maximum abutment forces can result when the restrainer gap is not zero.

2.4 NEED FOR UW RESEARCH

The UCSD model consists of a two-degree-of-freedom system that does not include abutments. The effect of abutments on the relative hinge displacement is not addressed. Furthermore, the frames were assumed to yield at 4.45 MN (1000 kips) regardless of their stiffness. This assumption does not represent column behavior well. The restrainer stiffness was varied from 0.9 to 35.0 KN/mm (5 to 200 kips/inch). In comparison with the CALTRANS example (CALTRANS 1989) and WSDOT designs, both this range and the values themselves are extremely small.

UNR conducted two limited parametric studies with a total of three variables. In order to produce a credible comparison between the nonlinear time history method and the CALTRANS method, more parameters need to be varied. The model described in Chapter 3 allows the variation of a large number of parameters.

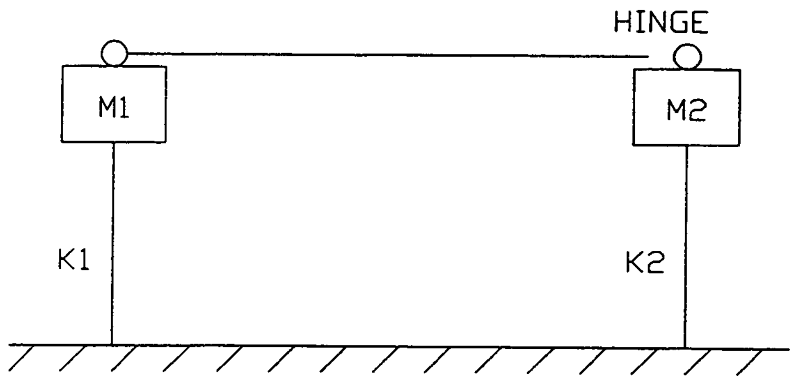

Figure 2.1. Analytical Model for UCSD Parametric Study

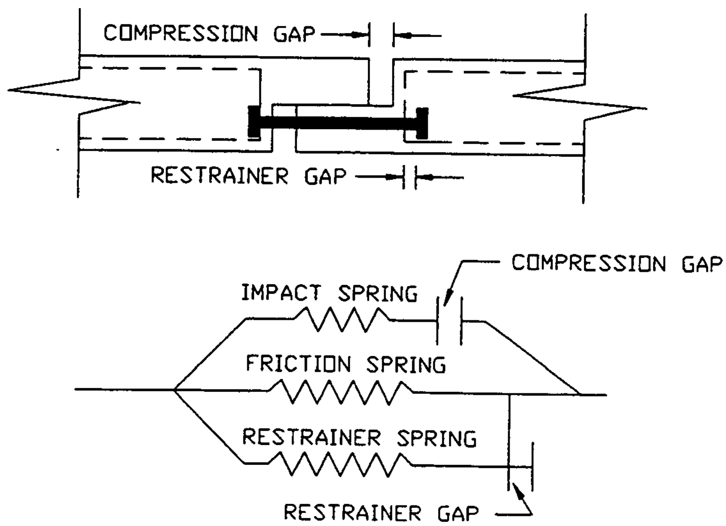

Figure 2.2 Hinge Detail and Model for UCSD Study

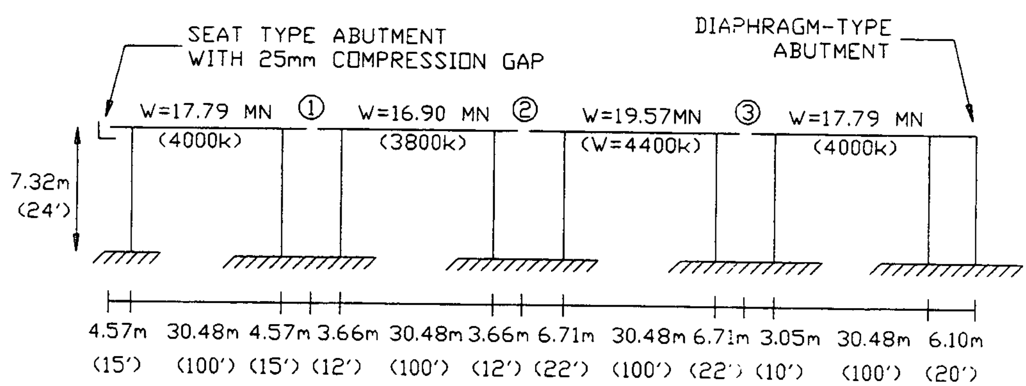

Figure 2.3 Analytical Model for UNReno Study

CHAPTER 3
DEVELOPMENT OF STANDARD BRIDGE MODEL

The model described in this chapter was developed after the researchers examined recent WSDOT seismic retrofit designs, as well as seismic retrofit guidelines from WSDOT and CALTRANS (1990). The model represents a straight, two-frame bridge with a single in-span hinge. (Figure 3.1)

3.1 FRAME PROPERTIES

To represent each frame as a nonlinear oscillator, the mass, stiffness and yield force had to be estimated. Calculation of these values required several assumptions regarding material properties and member geometry. For clarity, the procedure is summarized in Figure 3.2 as a flowchart.

The researchers assumed that all the columns within a frame were 1.22 m x 1.22 m (4 ft x 4 ft), had a concrete compressive strength of 34.5 Mpa (5000 psi), grade 60 reinforcement, and a longitudinal reinforcement ratio of 1 percent. On the basis of a frame weight of 22.2 MN (5000 kips), and a column axial stress of $0.10f'_c$, the number of columns within a frame was estimated to be 4.3. A single column cross section was then examined to determine its moment of inertia and yield moment. The researchers conducted a cracked-section analysis with an axial stress of $0.10f'_c$ to obtain a cracked moment of inertia of 536 m^4 (128,800 in^4). This moment of inertia was approximately 30 percent of the gross-section moment of inertia. The yield moment of the section, which was based on the cracked moment of inertia, was calculated to be 3.57 MN-meter (31,600 kip-inch).

A typical bridge column has a stiffness somewhere between that of a cantilever and a column fixed at both ends. To simplify the procedure of evaluating the frame stiffness, the researchers took the average of the two extremes. Therefore, the elastic stiffness of each frame was calculated as follows:

$$K = (\# \text{ of columns}) * 7.5 * E * I_{cracked} / H^3 \qquad (3.1)$$

where

H = average height of frame, assumed to be 7.62 m (25 feet)

E = modulus of elasticity of concrete

$I_{cracked}$ = cracked moment of inertia

The computed frame stiffness was 105 KN/mm (600 kips/inch).

All the columns within a frame were assumed to yield at both ends. Therefore, the frame yield force was calculated as follows:

$$F = (\# \text{ of columns}) * 2 * M_{yield} / H \qquad (3.2)$$

where

M_{yield} = yield moment based on cracked moment of inertia

The computed frame yield force was 4.00 MN (900 kips).

For the standard case, the two bridge frames were identical. Each frame was modeled as a single mass supported by a bilinear inelastic spring with 2 percent strain hardening.

3.2 ABUTMENT PROPERTIES

Seat abutments with friction-free bearings and no restrainers were included in the model. The abutment backwall was assumed to shear off at the superstructure depth during the earthquake. The computed abutment stiffness and strength were based on a superstructure width of 12.2 m (40 feet) and a superstructure depth of 1.83 m (6 feet). The stiffness and strength were estimated using the CALTRANS values of 115 KN/mm per linear meter (200 kips/inch per linear foot) and a soil strength of 53.1 MPa (7.7 kips per square foot of abutment backwall). Both these values were based on a 2.44 m (8 foot) deep soil wedge. Stiffness and strength were assumed to vary as the height squared, and therefore the above values were multiplied by 36/64. The computed abutment stiffness was 701 KN/mm (4000 kips/inch), and the abutment yield force was 5.56 MN (1250 kips). The abutment was modeled as a bilinear spring effective only in compression.

3.3 HINGE PROPERTIES

The hinge model (Figure 3.3) consisted of three spring components. A linear spring modeled the impact of the two superstructures. This spring was effective only in compression and had an initial gap of 25 mm (1.0 inch). The stiffness of the spring (17.5 MN/mm, 100,000 kips/inch) represented the axial stiffness of the superstructure.

A bilinear elastic spring modeled Coulomb friction. A vertical load of 2.22 MN (500 kips) was assumed to transfer through the hinge. The kinematic coefficient of friction between the bearing pads and the concrete surface was estimated at 0.20. Therefore, the sliding force (i.e., friction yield force) was 0.44 MN (100 kips). The bearing pads were assumed to be 25 mm (1-inch) thick and to have a shear modulus of 1.03 MPa (150 psi). The total area of bearing pads, 0.65 m^2 (1000 in^2), was based on an allowable vertical stress of 3.43 MPa (500 psi) under dead load alone. The stiffness of the friction element before slippage was based on the stiffness of the bearing pads.

$$K_{friction} = G\,A/\,t \tag{3.3}$$

where

G = shear modulus of bearing pads

A = area of bearing pads

t = thickness of bearing pads

The computed stiffness was 26.3 KN/mm (150 kips/inch).

A third linear spring modeled the seismic restrainers. This element had an initial gap and was effective only in tension. The standard case had a restrainer stiffness of 175 KN/mm (1000 kips/inch) and a restrainer gap of 25 mm (1 inch). This restrainer stiffness corresponded to approximately four 38 mm (1.5-inch) diameter high strength steel rods with a length of 5.33 m (17.5 feet).

3.4 DAMPING

Viscous damping was assumed to be 5 percent of critical, and to consist of components proportional to the mass and stiffness. Because it was based on the initial stiffness matrix. Only elements without an initial gap contributed.

3.5 COMPUTED RESPONSE

The standard ground motion was the N-S component of the 1940 El Centro earthquake. The peak ground acceleration was scaled by a factor of 2 to obtain a peak acceleration of 0.70 g. (Figure 3.4)

The displacement responses of frames 1 and 2 are shown in Figure 3.5. It shows that the two frames moved nearly in unison. Frame 1 had a maximum displacement of 147 mm (5.8 inches) away from abutment 1 at approximately 3 seconds. Frame 2 had a maximum displacement of 102 mm (4.0 inches) away from abutment 2 approximately 12 seconds into the earthquake. The amount of opening or closing that the hinge experienced at any time could be determined by calculating the difference between frame 1 and frame 2 displacements at that time. Because the researchers were interested in whether the span unseated, they considered only the largest hinge opening, defined as the maximum relative hinge displacement (MRHD). For the standard case, the MRHD of 14 mm (0.54 inches) occurred at 12.4 seconds.

The responses of the abutments are presented in Figure 3.6. Both abutments yielded within the first two seconds of the earthquake. The final displacement of abutment 1 was slightly over 50 mm (2 inches), and abutment 2 had a final displacement of nearly 90 mm (3.5 inches).

The criterion used to determine the likelihood of unseating at the abutment was the maximum relative displacement between the superstructure and the abutment seat. Because the abutment backwall was modeled as shearing off during the earthquake, the abutment seat was assumed to remain in its initial position. Therefore, the maximum relative abutment displacement (MRAD) was the taken as the maximum displacement of the frame away from the adjacent abutment. This definition is slightly unconservative because the abutment seat would be expected to move during the earthquake. For the standard case, the MRAD for abutment 1 was 147 mm (5.8 inches) and the MRAD for abutment 2 was 102 mm (4 inches).

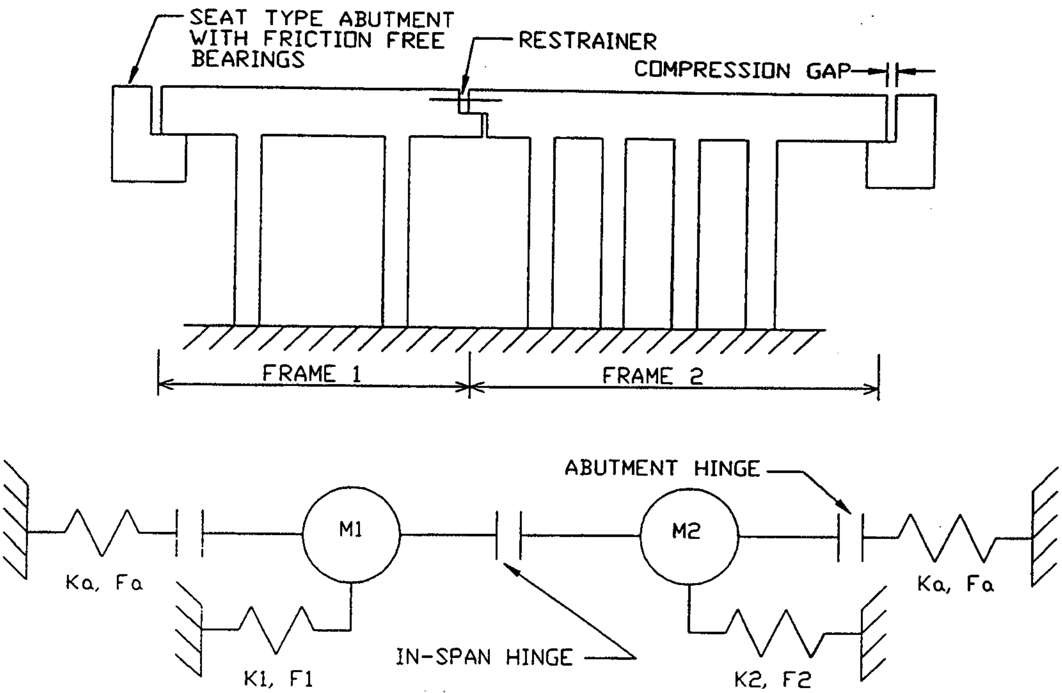

Figure 3.1. Model Used for UW Parametric Study

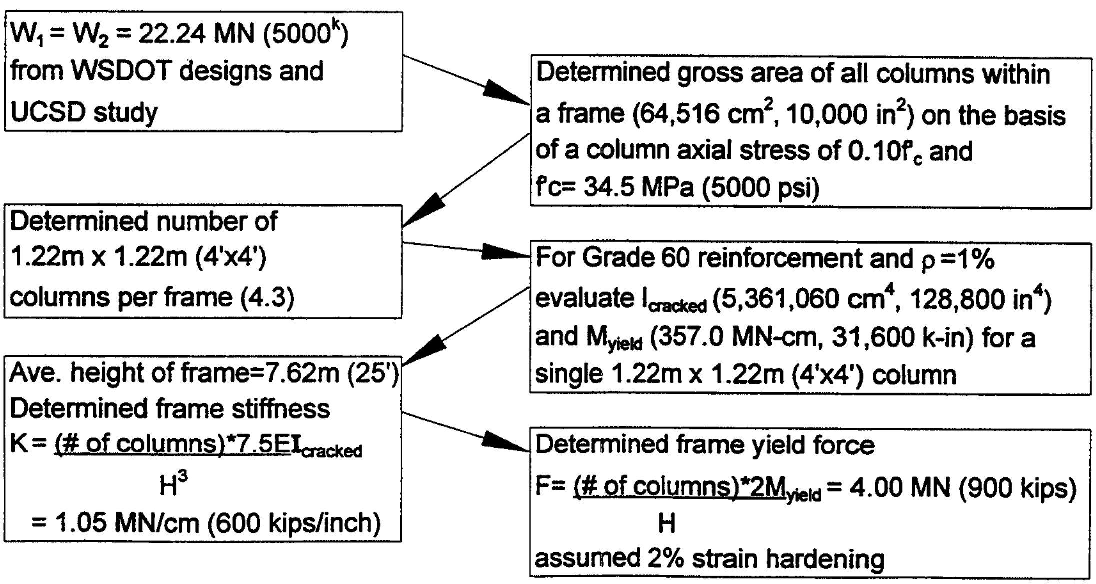

Figure 3.2. Evaluation of Frame Properties for Standard Case

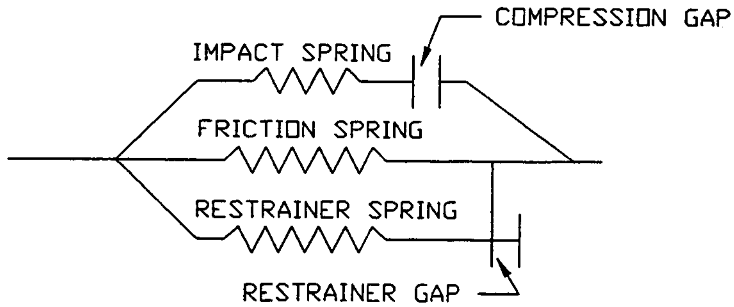

Figure 3.3. Hinge Model for UW Parametric Study

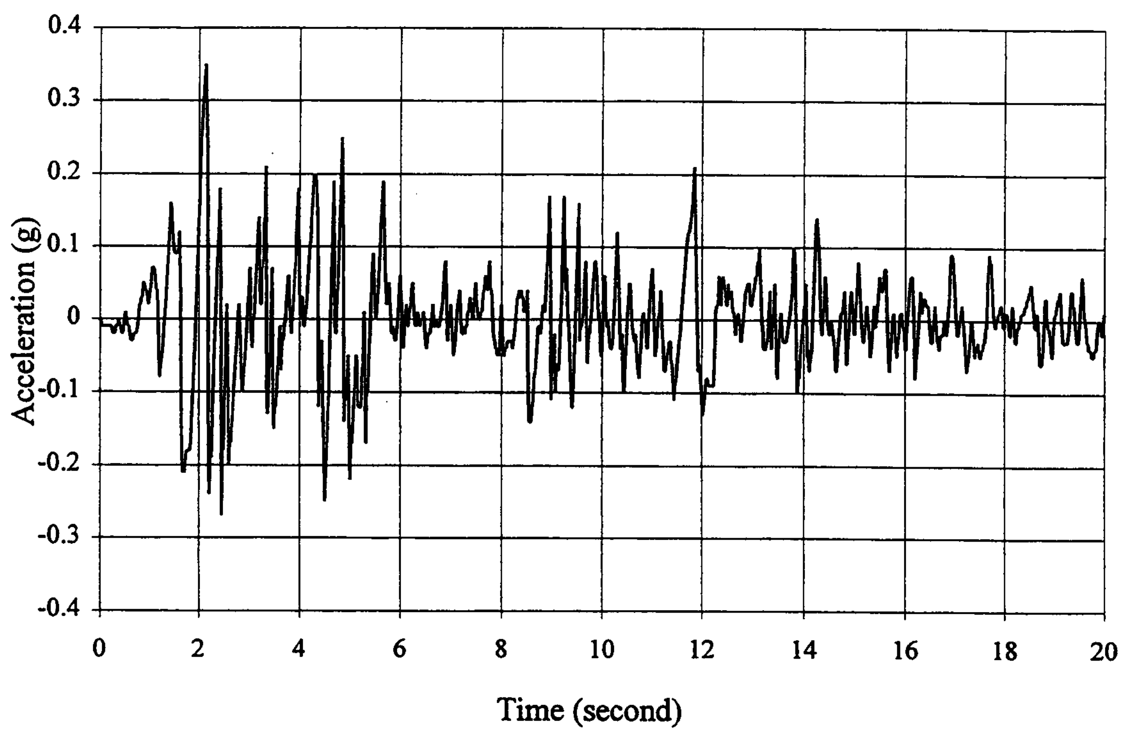

Figure 3.4. N-S Component of 1940 El Centro Earthquake

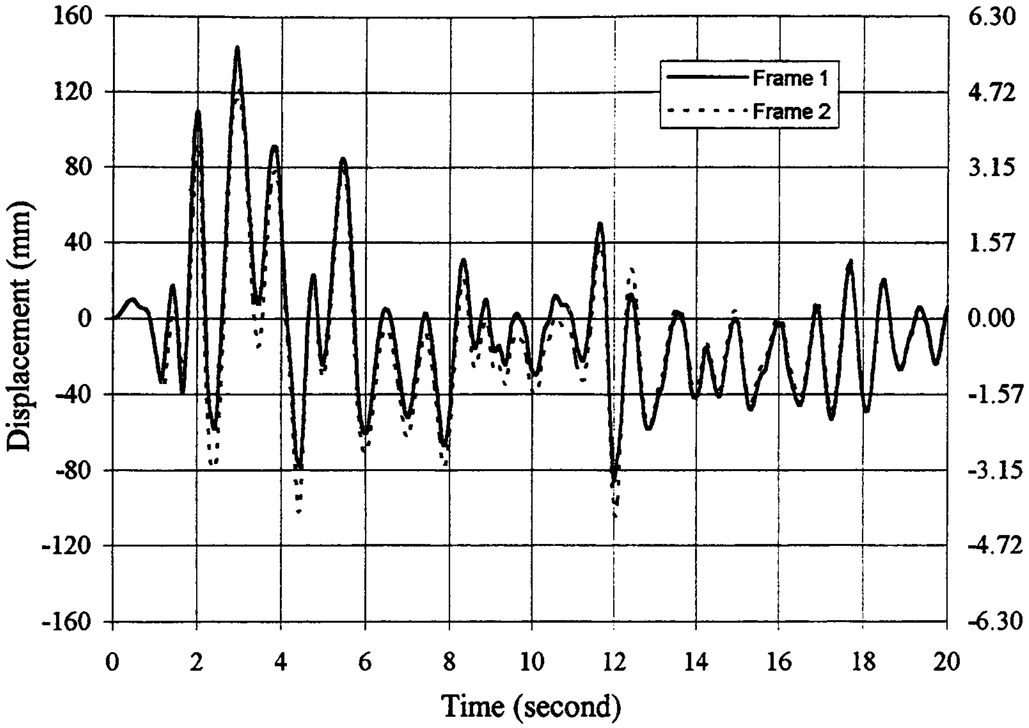

Figure 3.5. Absolute Frame Displacements for Standard Case

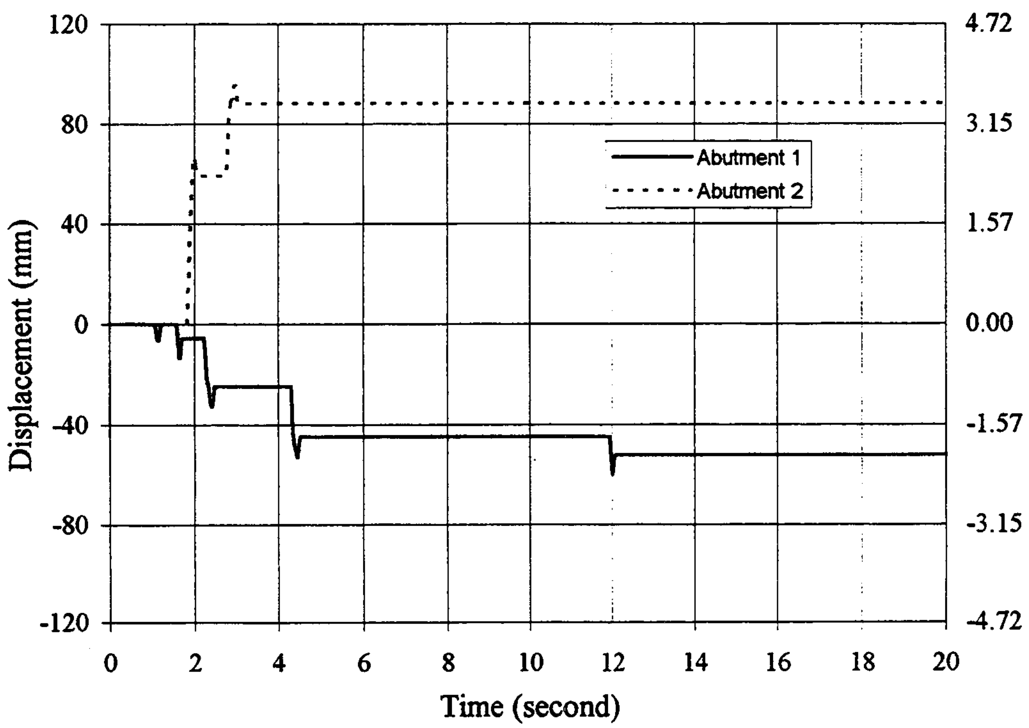

Figure 3.6. Absolute Abutment Displacements for Standard Case

CHAPTER 4
PARAMETRIC STUDY

A parametric study involving eleven variables was conducted to determine the factors most important in restrainer evaluation and design. This chapter summarizes the parameters varied, their ranges, and the results of the variation. Conducting a parametric study allowed the researchers to identify the variables that needed to be incorporated in the proposed design method.

4.1 PARAMETER VARIATION

Table 4.1 lists the eleven parameters varied and their respective ranges. Each parameter, except earthquake record and intensity, was varied independently. The remaining properties were the same as in the standard case. All parameter variations, excluding earthquake record and intensity, were conducted throughout the entire frame stiffness ratio (K_2/K_1) range of 0.1 to 10.

Table 4.1. Parameters and Ranges for UW study

PARAMETER	RANGE
Frame 2 Stiffness (K_2)	10.5 to 1050 KN/mm (60 to 6000 kips/inch)
Restrainer Stiffness (K_r)	0 to 437.8 KN/mm (0 to 2500 kips/inch)
Restrainer Gap (R_g)	0 to 76 mm (0 to 3 inches)
Abutment Factor	K_{abut}=0 & F_{abut}=0 to K_{abut}=787.5 KN/mm (8000 kips/inch) & F_{abut}=11.12 MN (2500 kips)
Hinge Friction	with and without friction
Compression Gap (C_g)	0 to 38 mm (0 to 1.5 inch)
Temperature	22.2° C (40° F) drop to 16.7° C (30° F) rise
Frame 1 Stiffness (K_1)	52.5 to 210.0 KN/mm (300 to 1200 kips/inch)
Frame 1 Weight (W_1)	11.1 to 44.5 MN (2500 to 10,000 kips)
Earthquake Intensity	0.35 to 0.70 g
Earthquake Record	El Centro (1940), Olympia (1949), & James Road (1979)

4.2 RESULTS

For each parameter varied, two plots showing its effect on the maximum relative hinge displacement (MRHD) and the maximum relative abutment displacement (MRAD) are presented. The MRAD plotted was the larger of the two maximum relative abutment displacements.

Effect of Frame 2 Stiffness

The stiffness of frame 1 was held constant at 105 KN/mm (600 kips/inch), while the stiffness of frame 2 varied from 10.5 KN/mm (60 kips/inch) to 1.05 MN/mm (6000 kips/inch). Varying the frame stiffness ratio, K_2/K_1, from 0.1 to 10 resulted in an MRHD that ranged from approximately 12 mm (0.5 inch) to 71 mm (2.8 inch) (Figure 4.1). When the frame stiffness ratio was 1.0, the frames oscillated almost in-phase, resulting in the smallest MRHD. As K_2/K_1 diverged from 1.0, the MRHD increased. As K_2/K_1 increased, the MRAD decreased. This trend was attributed to an increase in the sum of the two frame stiffnesses. In other words, as K_1+K_2 increased, the MRAD decreased.

Effect of Restrainer Stiffness

Figure 4.2 shows the effect of varying the restrainer stiffness from 0 to 350 KN/mm (2000 kips/inch). The largest MRHD of 191 mm (7.5 inches) occurred for a frame stiffness ratio of 0.1 and a restrainer stiffness of 0.0. Even a modest restrainer stiffness (43.8 KN/mm, 250 kips/inch), reduced the largest MRHD to below 127 mm (5 inches). The effectiveness of restrainers in reducing the MRHD is evident in this plot. The MRAD was not significantly affected by changes in the restrainer stiffness.

Effect of Restrainer Gap

Figure 4.3 shows the severe effect that the restrainer gap had on the MRHD. At frame stiffness ratios above or below 1.0, an increase in the restrainer gap resulted in approximately the same increase in the MRHD. The effect of the restrainer gap on the MRAD was negligible.

Effect of Abutment Stiffness and Strength

The effects of multiplying the abutment stiffness and strength by factors of 0.0 and 2.0 are shown in Figure 4.4. Changing the abutment resistance did not significantly affect the MRHD. When the frame stiffness ratio was 1.0 and the abutment stiffness and strength were 0.0, the two frames oscillated in-phase, resulting in an MRHD of 0.0. Removing the abutment stiffness and strength resulted in a large increase in the MRAD for cases with low stiffness ratios. These cases had a low total frame stiffness (K_1+K_2), and they relied on the abutments to limit the frame displacements. The cases with a large total frame stiffness did not rely on the abutments to limit frame displacements. Therefore, the MRADs for large K_2/K_1 ratios were not significantly affected by variations in the abutment properties.

Effect of Coulomb Friction

Removing friction from the in-span hinge did not significantly affect the MRHD (Figure 4.5). The largest increase in MRHD due to removal of friction was 25 mm (1.0 inch). The average increase in MRHD was less than 13 mm (0.5 inches). The effect of friction on the MRAD was negligible.

Effect of Compression Gap

The compression gap was varied from 0 to 38 mm (1.5 inches). Its effects on the MRHD and MRAD were insignificant (Figure 4.6). Typically, the changes in MRHD and MRAD were less than 12 mm (0.5 inches).

Effect of Temperature

To model the effect of temperature variation, the restrainer gap and compression gap were modified simultaneously. As a bridge contracts or expands, the change in restrainer gap is equal and opposite to the change in compression gap. The researchers assumed a superstructure length of 38.1 m (125 feet) and a coefficient of thermal expansion of 1.1×10^{-5} strain/°C (6×10^{-6} strain/°F). The 22.2° C (40° F) drop resulted in a restrainer gap of 15 mm (0.6 inches) and a compression gap of 36 mm (1.4 inches). A restrainer gap of 33 mm (1.3 inches) and a compression gap of 18 mm (0.7 inches) were used for the 16.7° C (30° F) rise. The effect of temperature on both the MRHD and MRAD was negligible (Figure 4.7).

Effect of Frame 1 Stiffness

The stiffness of frame 1 was varied from 52.5 KN/mm (300 kips/inch) to 210.0 KN/mm (1200 kips/inch). The stiffness of frame 2 was determined by multiplying the stiffness of frame 1 by the frame stiffness ratio. Therefore, varying the stiffness of frame 1 was an indirect method of varying the total frame stiffness. The MRHD was not significantly influenced by changes in frame 1 stiffness (Figure 4.8). However, varying K_1+K_2 dramatically changed the MRAD. As K_1+K_2 was increased, the MRAD decreased.

Effect of Frame 1 Weight

The weight of frame 1 was halved and doubled, while the weight of frame 2 was held constant at 22.2 MN (5000 kips). As shown in Figure 4.9, the maximum MRHD increased only slightly. The points of minimum MRHD shifted to occur at a period ratio of 1.0. This result suggests that the important parameter for predicting the MRHD is the period ratio rather than the stiffness ratio. Increasing the weight of frame 1 substantially increased the MRAD, but decreasing the weight of frame 1 only marginally decreased the MRAD.

Effect of Earthquake Record and Intensity

Ten cases were chosen from the database and analyzed for the following combinations of earthquake records and intensities:

- El Centro*2 (.70g)
- El Centro*1 (.35g)
- Olympia*2 (.56 g)
- James Road*1 (.38g)

The ten cases used for variation of earthquake record and intensity are described in Table 4.2. All ten cases included friction within the in-span hinge.

Table 4.2. Cases Analyzed for Variation of Earthquake Record and Intensity

CASE #	K_1 (KN/mm)	K_2 (KN/mm)	W_1 (MN)	W_2 (MN)	R_g (mm)	C_g (mm)	K_r (KN/mm)	K_{abut} (KN/mm)	F_{abut} (KN)
1	105	105	22.24	22.24	25	25	175	700	219
2	105	105	22.24	22.24	25	25	0	700	219
3	105	420	22.24	22.24	25	25	175	700	219
4	105	26	22.24	22.24	25	25	175	700	219
5	105	420	22.24	22.24	51	25	175	700	219
6	105	420	22.24	22.24	25	25	0	700	219
7	105	13	22.24	22.24	25	25	0	700	219
8	105	26	22.24	22.24	25	25	0	700	219
9	105	420	44.48	22.24	25	25	0	700	219
10	105	26	44.48	22.24	25	25	0	700	219

The results of earthquake record and intensity variation are shown in Figure 4.10. El Centro*2 produced the largest MRHDs and MRADs for the majority of the cases. James Road*1 closely followed El Centro*2 for most of the cases. The remaining two records produced substantially smaller MRHDs and MRADs.

4.3 SUMMARY OF RESULTS OF PARAMETRIC STUDY

The parametric study identified the following four variables as important predictors of the MRHD:

- restrainer stiffness
- restrainer gap
- frame period ratio
- frame stiffness ratio.

The following three parameters were identified as important in predicting MRAD:

- abutment stiffness and strength
- summation of frame stiffnesses
- summation of frame weights.

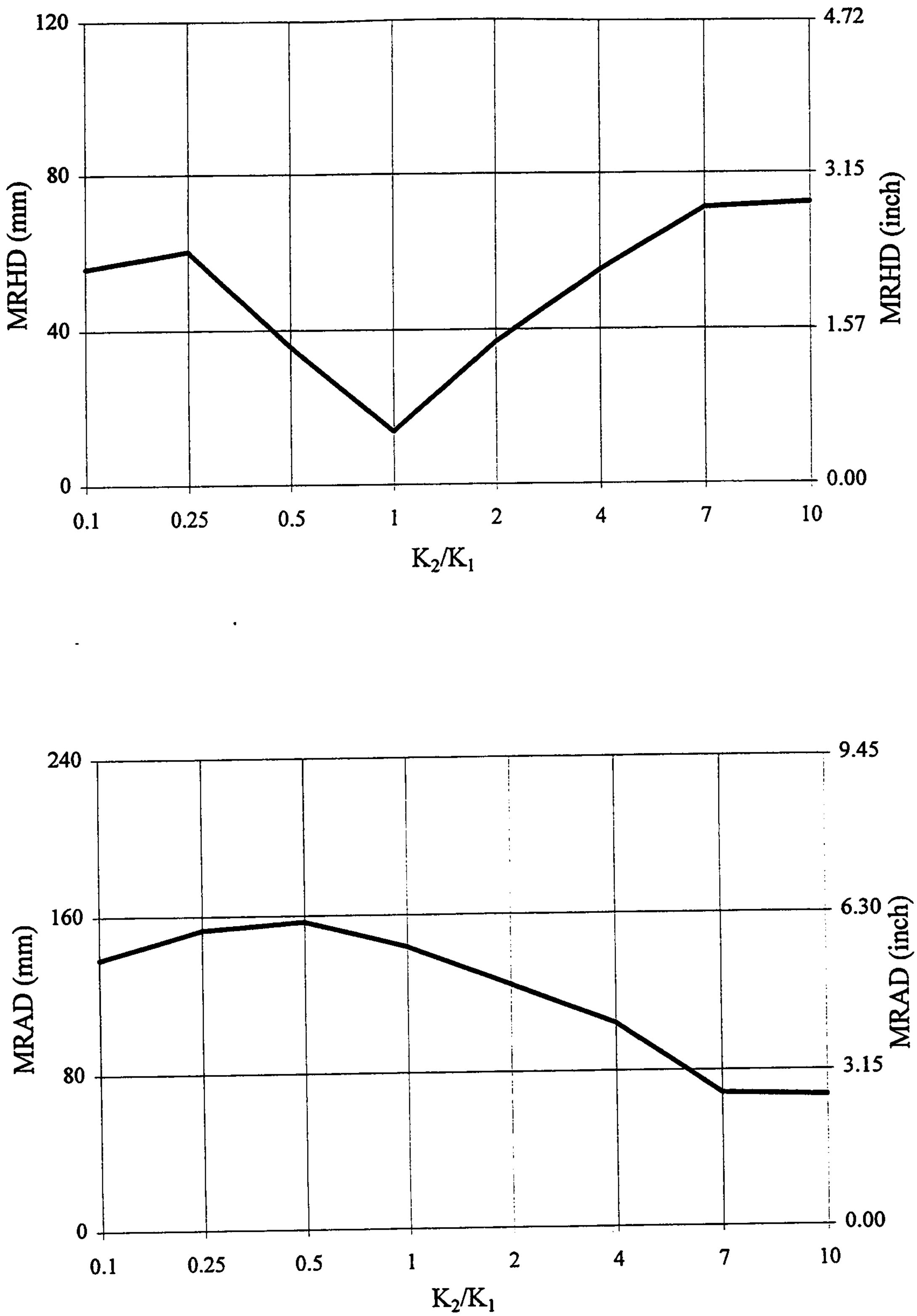

Figure 4.1. Effect of Frame 2 Stiffness on MRHD and MRAD

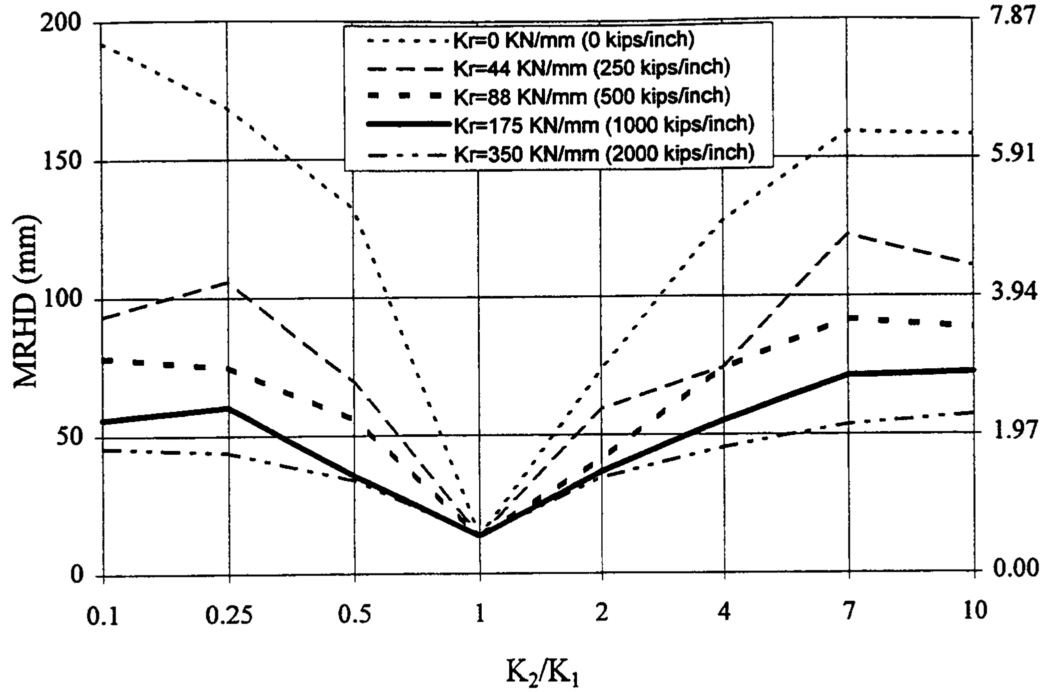

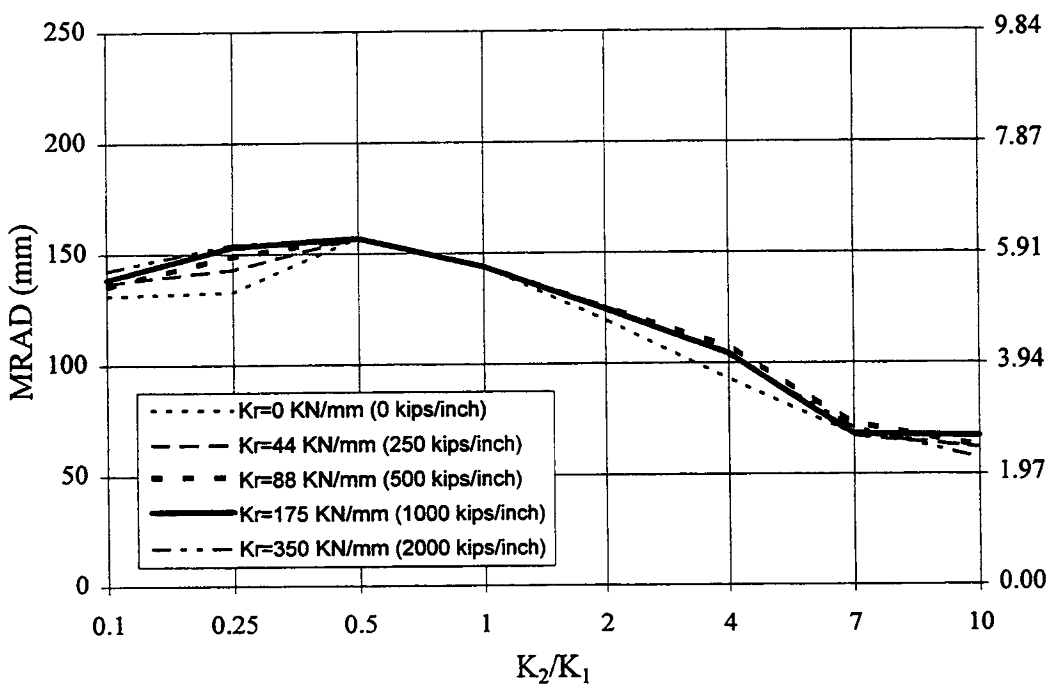

Figure 4.2. Effect of Restrainer Stiffness on MRHD and MRAD

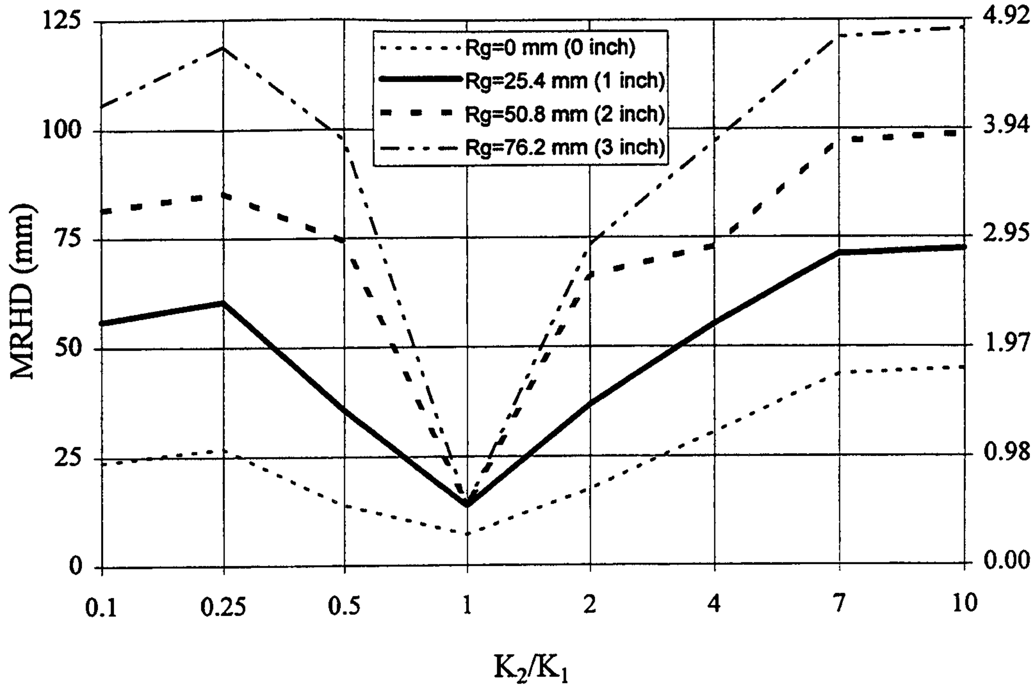

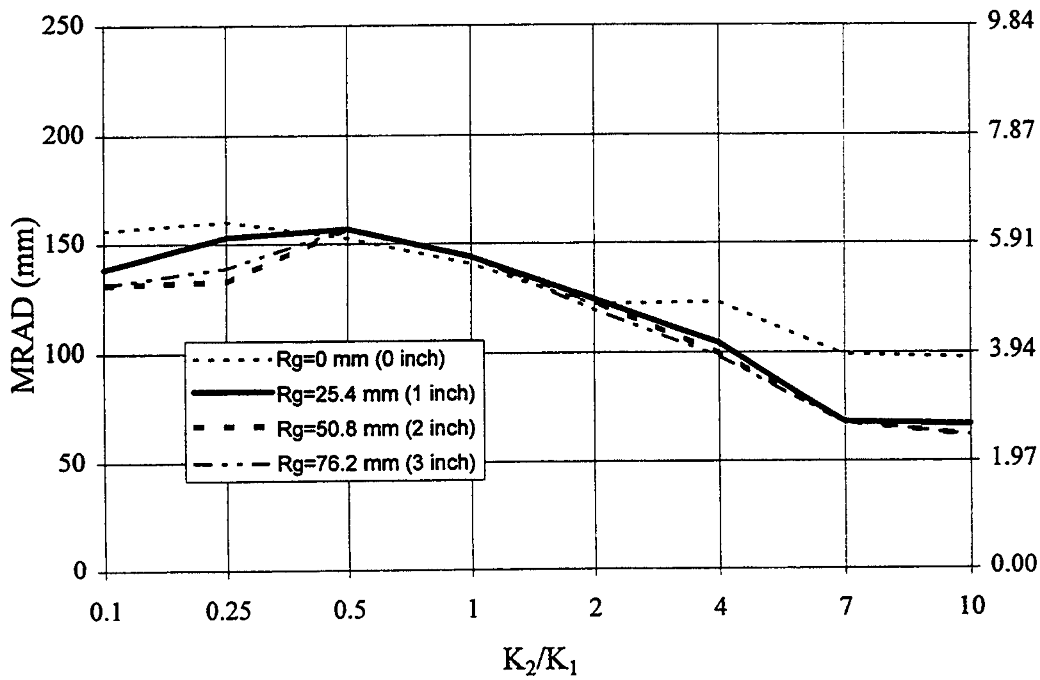

Figure 4.3. Effect of Restrainer Gap on MRHD and MRAD

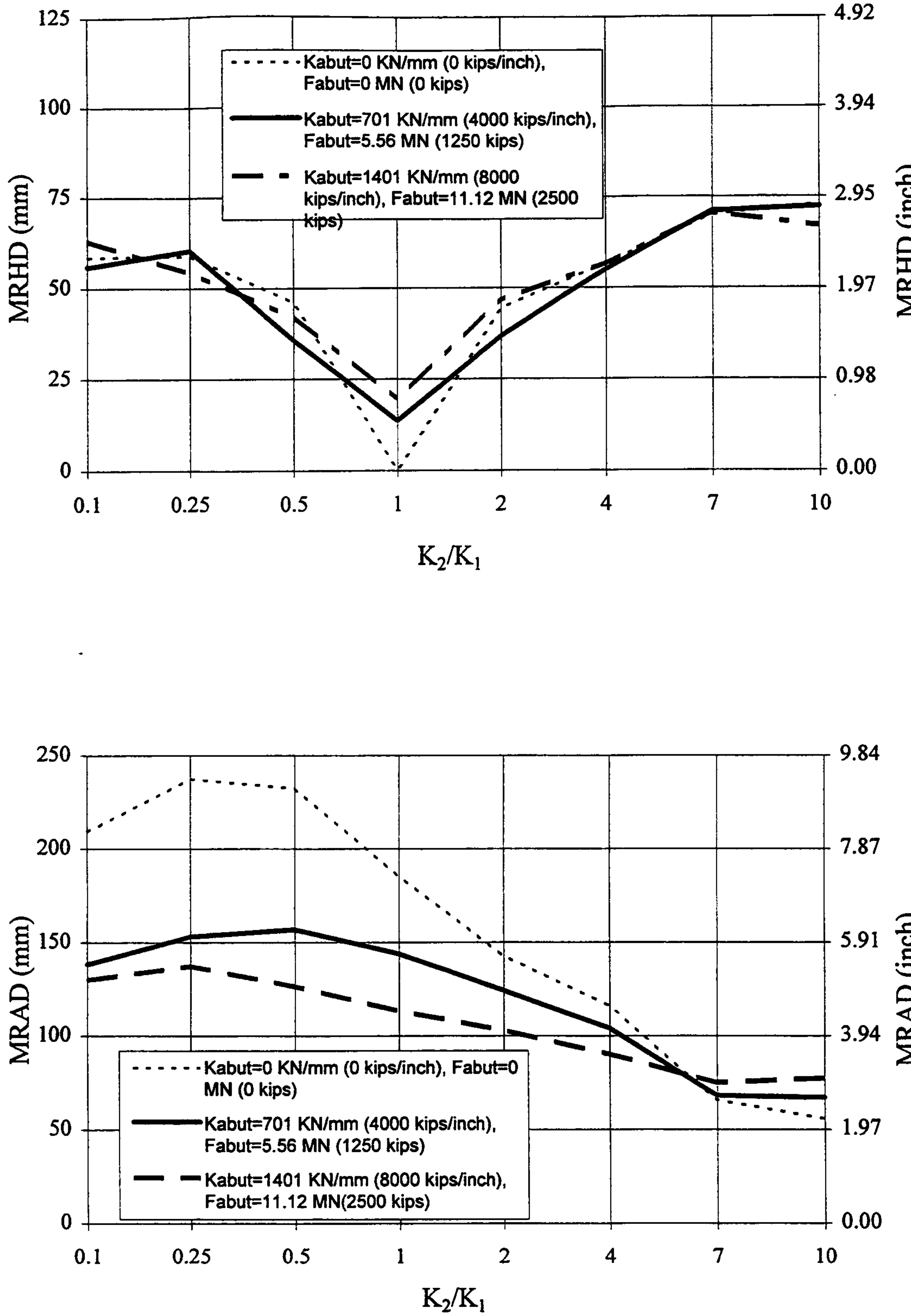

Figure 4.4. Effect of Abutment Factor on MRHD and MRAD

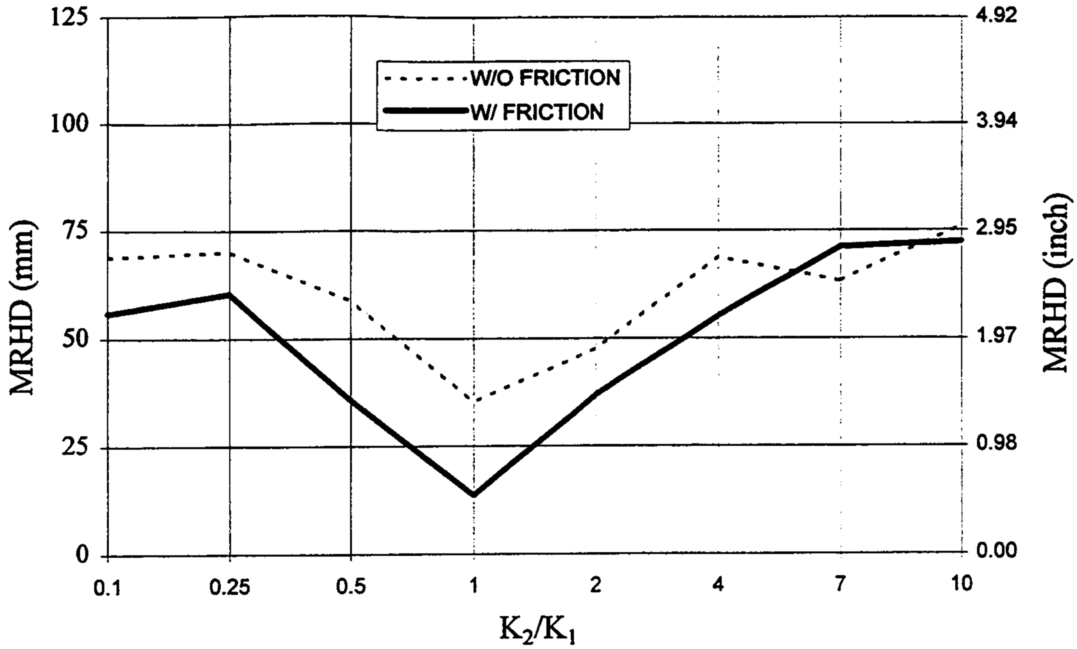

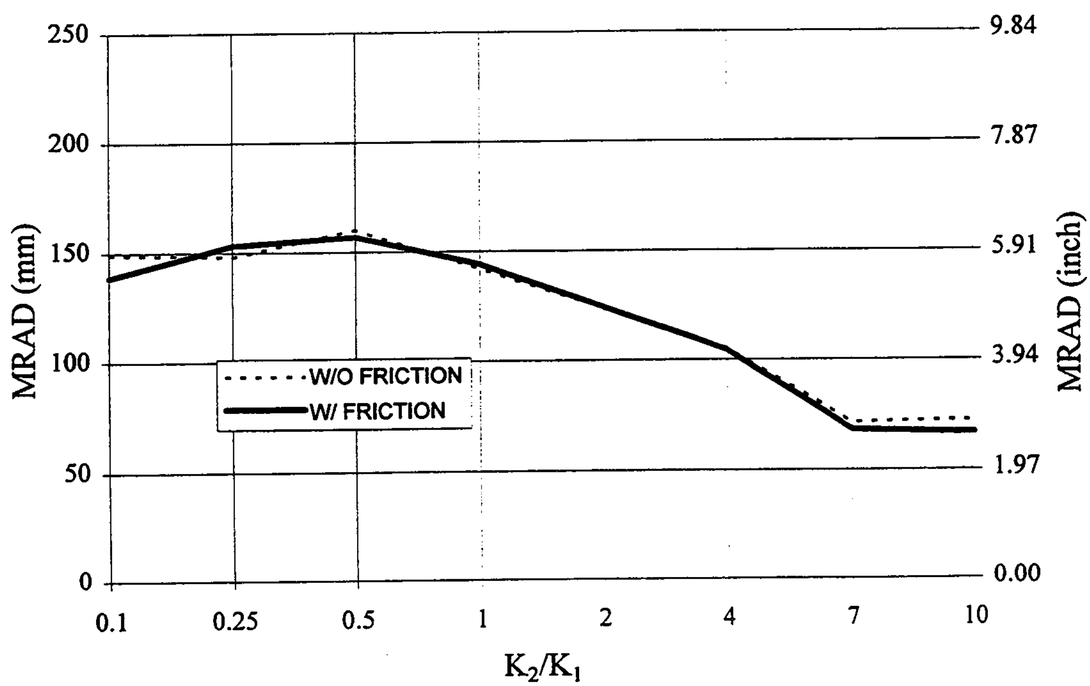

Figure 4.5. Effect of Coulomb Friction on MRHD and MRAD

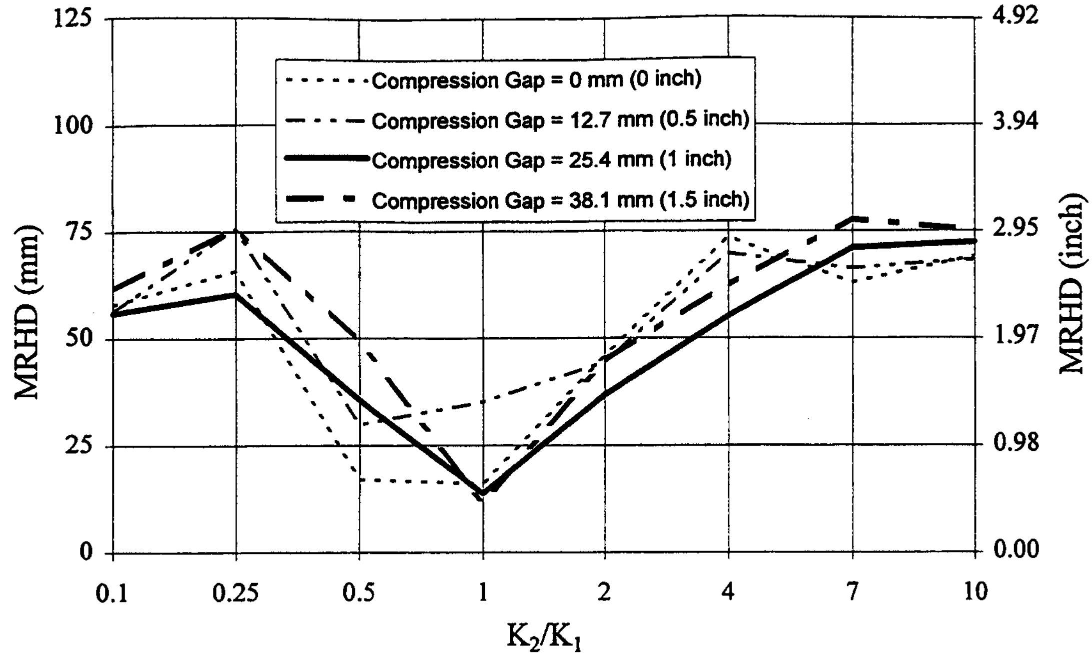

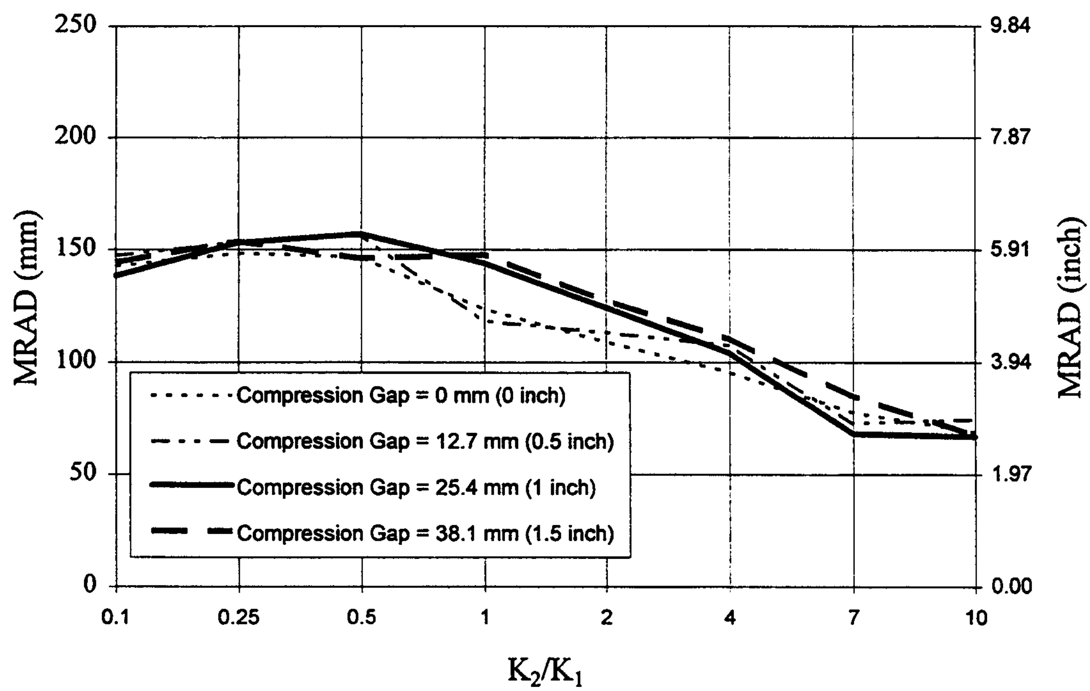

Figure 4.6. Effect of Compression Gap on MRHD and MRAD

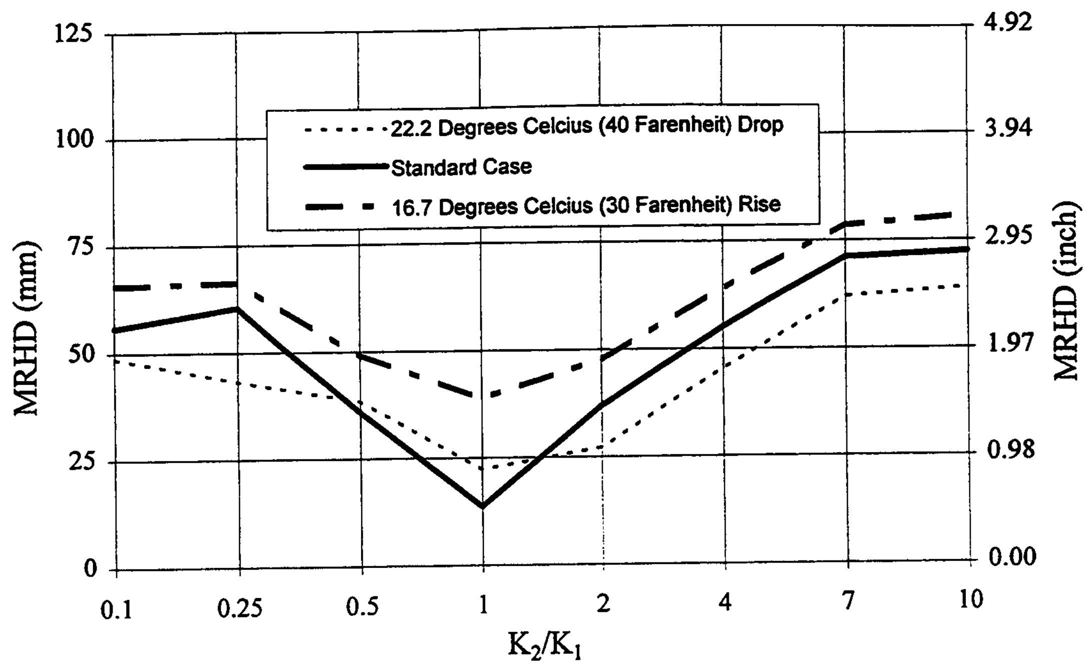

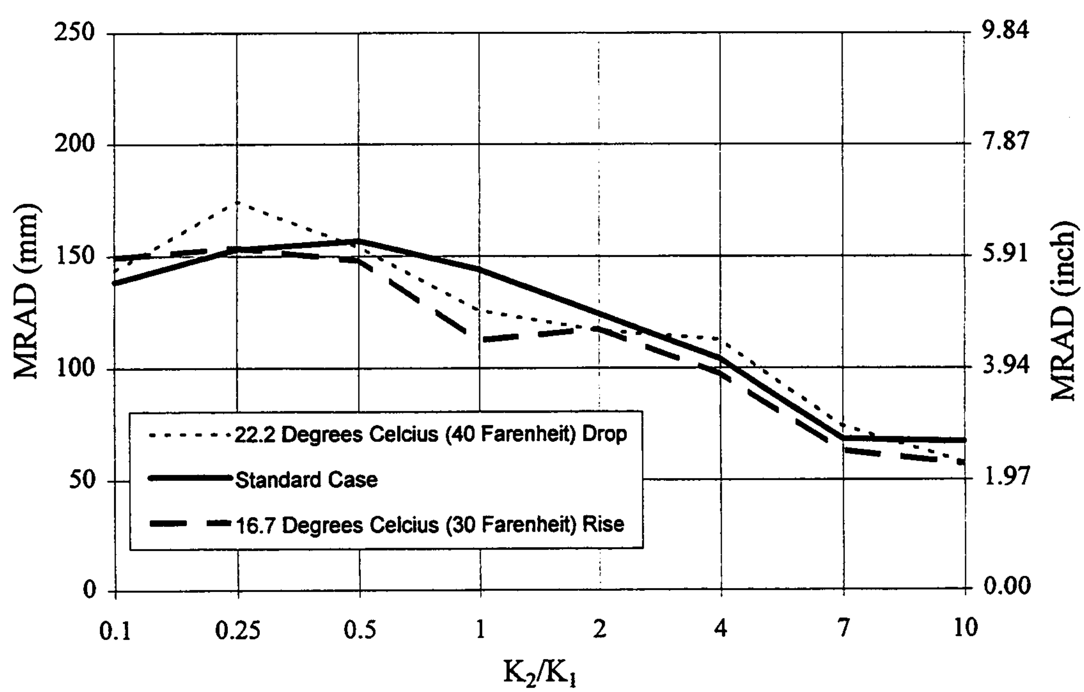

Figure 4.7. Effect of Temperature on MRHD and MRAD

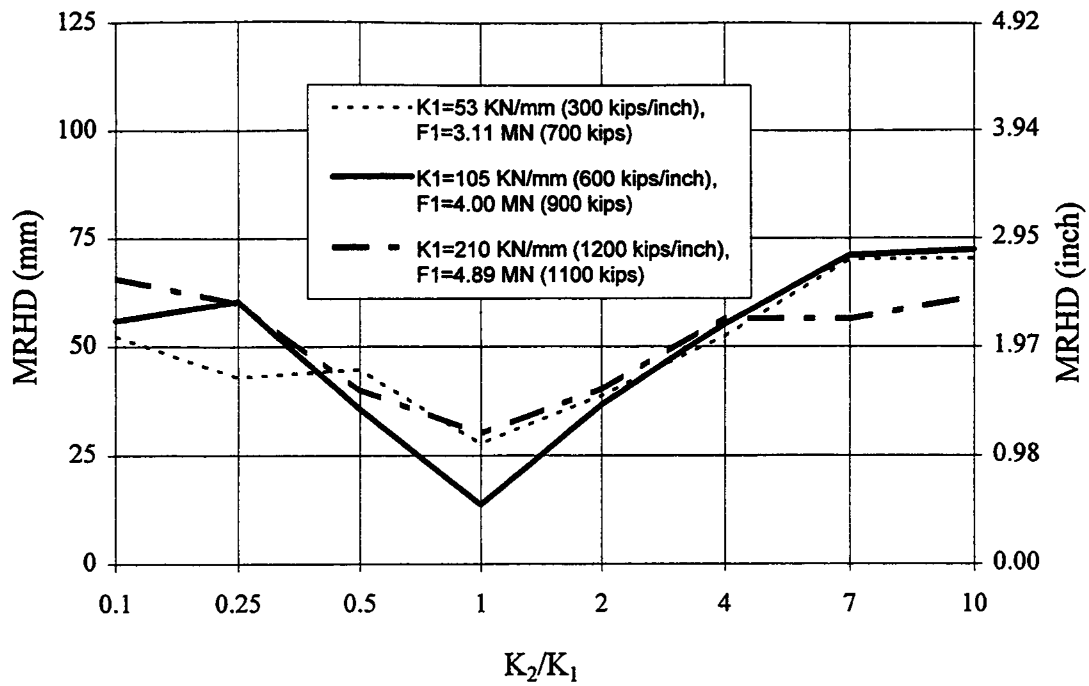

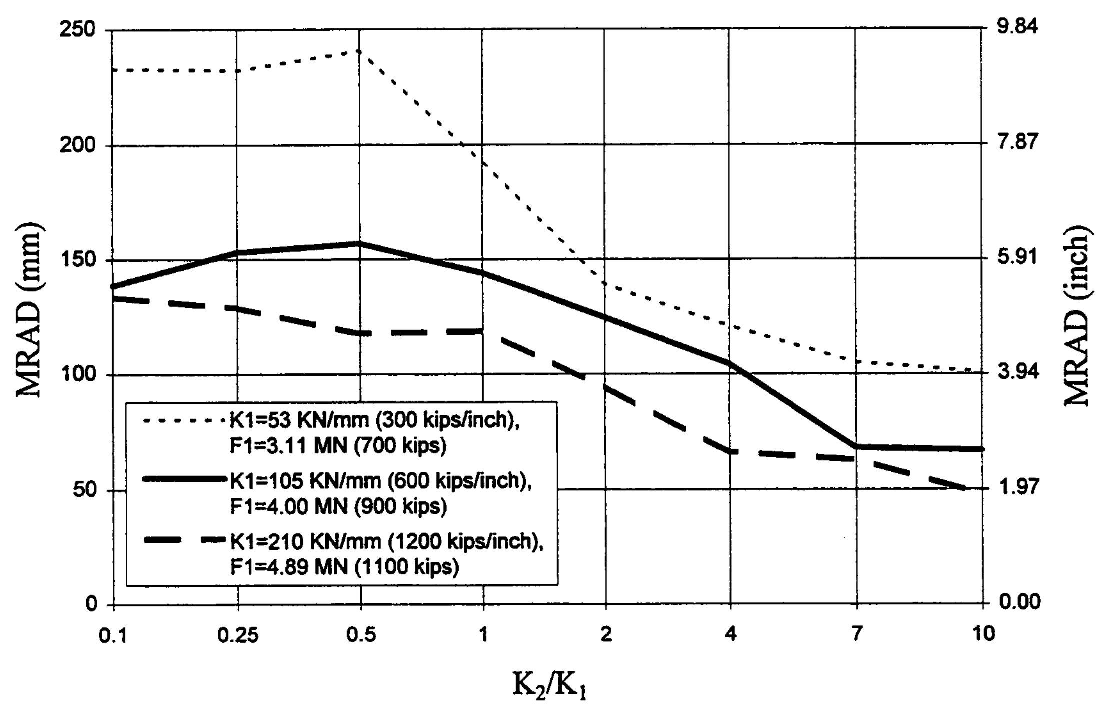

Figure 4.8. Effect of Frame 1 Stiffness on MRHD and MRAD

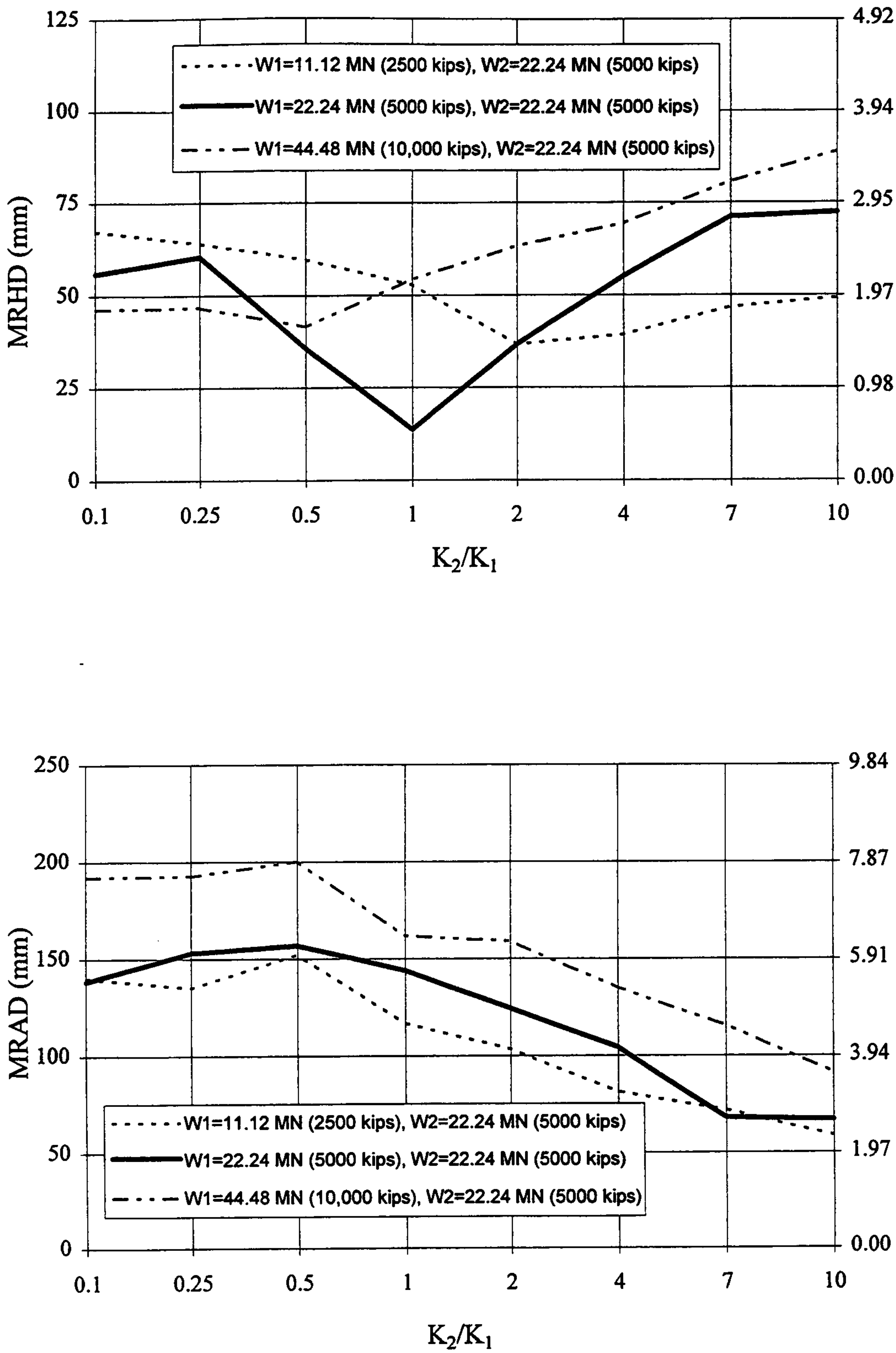

Figure 4.9. Effect of Frame 1 Weight on MRHD and MRAD

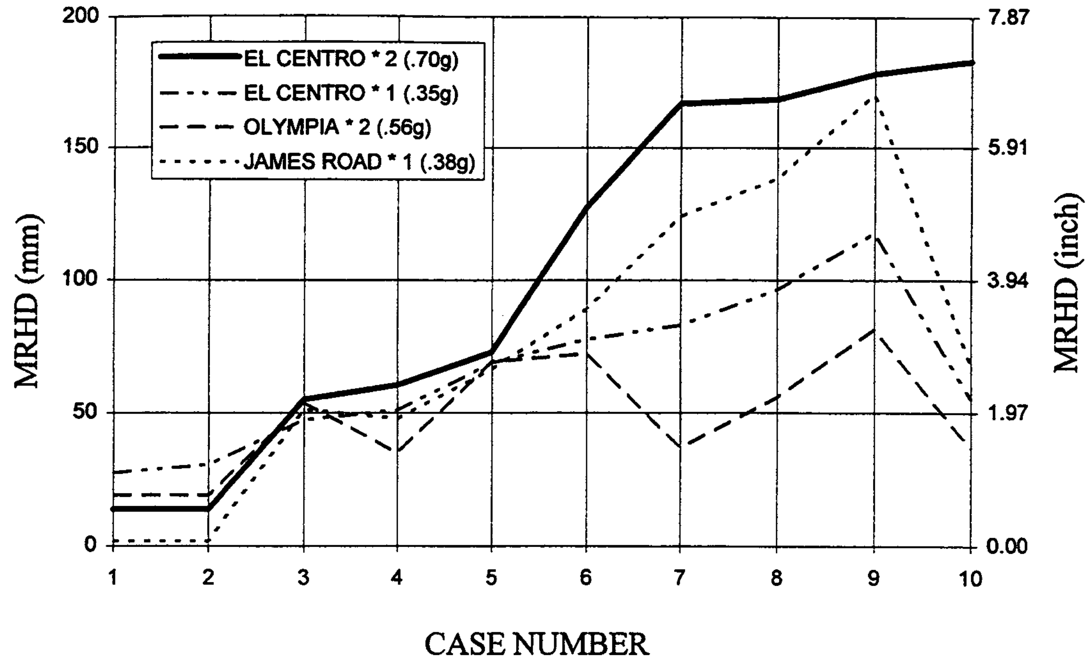

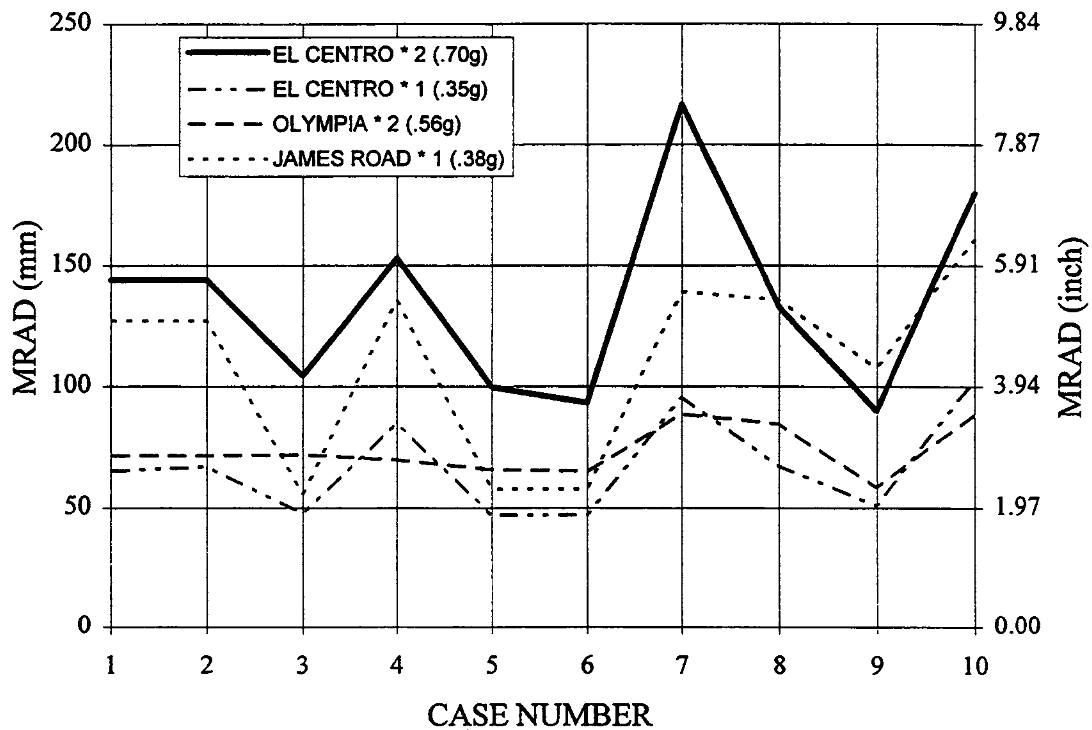

Figure 4.10. Effect of Earthquake Record and Intensity on MRHD and MRAD

CHAPTER 5
EVALUATION OF CURRENT DESIGN METHODS

Both AASHTO and CALTRANS have developed methods for designing restrainers. WSDOT currently uses the AASHTO design procedure, but it supplements the AASHTO method with rules of its own. This chapter describes these procedures and compares their results with those of nonlinear time history analyses.

5.1 AASHTO PROCEDURE

According to the 1994 LRFD Bridge Design Specifications (Section 4.7.4), restrainers are required when the bridge seat width is less than a specified percentage of the empirical seat width. The empirical seat width is calculated as follows:

$$N = (8 + 0.02L + 0.08H)(1 + 0.000125S^2) \qquad \text{U.S. customary units} \qquad (5.1)$$

$$N = (203.2 + 1.7L + 6.7H)(1 + 0.000125S^2) \qquad \text{SI units} \qquad (5.2)$$

where

N = empirical seat width (mm, inches)

L = span length (m, feet)

H = average height of the adjacent two columns or piers (m, feet)

S = skew of support (degrees)

For seismic zones 3 and 4, the minimum seat width for which restrainers are not required is 150 percent of the empirical seat width.

Section 3.10.9 of the 1994 AASHTO LRFD Bridge Design Specification states that "restrainers shall be designed for a force calculated as the acceleration coefficient times the permanent load of the lighter of the two adjoining spans or parts of the structure." WSDOT interprets the "parts of the structure" to mean each separate frame segment between expansion joints. The restrainer must include a gap so that it does not start to act until the design displacement has been exceeded. Friction is not considered.

The minimum seat width was compared with the results of nonlinear analysis for a typical bridge geometry. For a span length of 38.1 m (125 feet), a skew of 0 degrees, and an average frame height of 7.62 m (25 feet), the researchers calculated the empirical seat width to be 318 mm (12.5 inches). This value was multiplied by 1.5 to obtain the minimum unrestrained seat width of 476 mm (18.75 inches) for seismic zones 3 and 4. In comparison, the nonlinear time history analysis predicted a maximum relative hinge displacement (MRHD) of 14 mm (0.54 inches) for the unrestrained case of the standard model described in Chapter 3. The minimum seat width required to prevent span unseating is the sum of the MRHD, the compression gap (25 mm, 1 inch), and a minimum allowable bearing width (Figure 5.1). According to the CALTRANS Bridge Design Aids (1989), a reasonable value for the minimum allowable bearing width is 76 mm (3 inches). Therefore, according to the nonlinear time history, the minimum seat width necessary to prevent unseating would be 115 mm (4.54 inches). This value is much smaller than that required by AASHTO.

The seat widths required by the AASHTO procedure were compared with the displacements predicted by the nonlinear analysis for frame stiffness ratios (K_2/K_1) ranging from 0.1 to 10. The bridge dimensions used for each case and the corresponding calculated minimum seat widths are presented in Table 5.1. Figure 5.2 shows the AASHTO empirical seat width and the minimum seat width predicted by NLTH as K_2/K_1 varies. The empirical seat width, which does not include the 1.5 multiplication factor for seismic zones 3 and 4, was larger than the NLTH minimum seat width throughout the entire K_2/K_1 range. As mentioned in Chapter 3, the standard case was analyzed using the 1940 N-S El Centro ground motion multiplied by a factor of 2 (0.70g). The fact that the empirical seat width was consistently larger than the NLTH minimum seat width for such a strong earthquake suggests that the AASHTO seat width equation is highly conservative; however, in situations where restrainers are required, the procedure is not necessarily conservative.

Table 5.1. Comparison of AASHTO Minimum Seat Widths with results predicted by NLTH

K_2/K_1	H_1 (m)	H_2 (m)	H_{ave} (m)	L (m)	N (mm)	AASHTO min. seat width (mm)	NLTH MRHD (mm)	NLTH min. seat width (mm)
0.1	7.6	14.3	11.0	38.1	340	510	193	295
0.25	7.6	12.1	9.9	38.1	333	500	168	269
0.5	7.6	9.8	8.7	38.1	325	488	132	234
1	7.6	7.6	7.6	38.1	318	477	13	114
2	7.6	6.1	6.9	38.1	312	468	74	175
4	7.6	4.9	6.3	38.1	307	462	127	229
7	7.6	4.3	5.9	38.1	307	460	160	262
10	7.6	4.0	5.8	38.1	305	458	165	267

Another concern about the AASHTO restrainer design method is that, for situations in which restrainers are required, the procedure does not account for the restrainer gap or seat width. The parametric study demonstrated that both of these variables are important in predicting whether a span unseats.

5.2 WSDOT PROCEDURE

WSDOT has supplemented the AASHTO design procedure with its own rules, including the following:

- Orient longitudinal restrainers in the direction of expected movement.
- Use ASTM A722, 1.03 GPa (150 ksi^2) ultimate strength rods for longitudinal restrainers. Design rods to 0.62 GPa (90 ksi^2) maximum in order to act elastically to avoid loss of support at narrow bearing seats.
- Use longitudinal restrainers 4.57 to 6.10 m (15 to 20 feet) in length.
- When determining the restrainer gap allow for 150 percent of the existing bridge temperature displacements or a minimum of 51 mm (2 inches).

The parametric study showed that for cases with substantially different frames on each side of the in-span hinge, an increase in the restrainer gap resulted in approximately the same increase in the MRHD (Section 4.2). Therefore, in order to minimize the MRHD, the restrainer gap should be as small as possible. Rules requiring a minimum restrainer gap (in excess of that required to allow thermal movements) should be avoided.

WSDOT rules attempt to ensure elastic restrainer behavior during the earthquake by limiting the nominal restrainer stress. The restrainer stress, which is computed from the AASHTO forces, is limited to 60 percent of the ultimate stress. However, the restrainer length is determined using empirical guidelines that do not incorporate the expected deformation of the restrainer. The AASHTO/WSDOT procedure does not predict the MRHD. Therefore, the expected restrainer deformation is unknown, and the restrainer length cannot be checked to ensure elastic behavior. The restrainer design should vary with the expected MRHD.

5.3 CALTRANS PROCEDURE

The CALTRANS restrainer design procedure (CALTRANS 1989) attempts to simplify the nonlinear multi-degree-of-freedom dynamic behavior of a bridge by treating all the segments on each side of an in-span hinge as a single-degree-of-freedom (SDOF) oscillator. The procedure involves comparing the predicted MRHD with the available seat width. Restrainers are added until the predicted MRHD is less than or equal to the available seat width. To compute displacements, the procedure assumes that one end of the restrainer is fixed and that the other end is attached to the superstructure segment moving away from the joint. The CALTRANS procedure consists of the following steps.

Step 1: Compute the maximum permissible restrainer deflection, D_r, and the restrainer length required for elastic restrainer behavior.

$$D_r = D_y + D_g \tag{5.3}$$

where

D_y = yield displacement of restrainer

D_g = restrainer gap

D_r must be less than or equal to the available seat width to prevent unseating before the restrainer capacity has been reached. The yield displacement is used to compute the minimum restrainer length required to maintain elastic behavior.

Step 2: Compute the nominal displacements of the equivalent SDOF oscillators on each side of the in-span hinge (D_1 and D_2).

$$D = ARS * W / K_t \tag{5.4}$$

where

ARS = response spectrum acceleration corresponding to the natural period of each SDOF oscillator. Only the weight of the first frame in each system is used in estimating the period.

W = Weight of frame immediately adjacent to the in-span hinge in each SDOF system.

$$K_t = K_u + K_r \tag{5.5}$$

K_u = Equivalent unrestrained stiffness that includes the stiffness of all substructures mobilized and any gaps in the system. CALTRANS allows only the stiffness of one adjacent segment, in addition to the first segment, to be included if the corresponding compression gap closes. The abutment is included as part of the adjacent segment if the abutment compression gap closes. The equivalent stiffness is taken at the maximum permissible restrainer deflection, D_r. An example of computing K_u is provided later in this chapter.

K_r = equivalent restrainer stiffness = restrainer stiffness * D_y / D_r

<u>Step 3:</u> The predicted MRHD (D_t) is the smaller of D_1 and D_2.

<u>Step 4:</u> Determine the number of restrainers required.

If D_t is less than D_r, unseating is not predicted, and only two cable units are required. If D_t exceeds D_r, restrainers are required to reduce D_t and to prevent unseating. The number of required restrainers, N_r, is determined as follows:

$$N_r = K_t * (D_t - D_r) / (F_y * A_r) \tag{5.6}$$

where

F_y = yield stress of restrainers

A_r = area of a single restrainer

Step 5: Check that the predicted MRHD of the retrofitted in-span hinge is less than or equal to the available seat width. Repeat steps 1 through 4 as necessary.

To compare the CALTRANS method with the results of NLTH analysis, the researchers had to make a series of calculations. To implement the CALTRANS procedure, the designer must know the available seat width in order to compute the restrainer yield displacement and restrainer length. In turn, the yield displacement is required to calculate K_u. However, the researchers had not assumed seat widths for their hypothetical cases. Therefore, they iterated until the predicted MRHD was equal to the maximum permissible restrainer deflection. Such an equality corresponded to an optimum design for the CALTRANS procedure.

The two-frame bridge shown in Figure 5.3 can be used to illustrate the iteration. The bridge was analyzed using the idealized El Centro*2 acceleration response spectrum (Figure 5.4). To determine K_u for the left half of the bridge, the force-displacement plot shown in Figure 5.5 was constructed. The bridge frame was modeled as linear, while the abutment was modeled as nonlinear. According to the CALTRANS procedure, the equivalent stiffness is calculated at the maximum permissible restrainer deflection (D_r). Initially, the researchers arbitrarily guessed a restrainer yield displacement of 51 mm (2 inches), which resulted in a maximum permissible restrainer deflection of 76 mm (3 inches). The corresponding equivalent unrestrained system stiffness, K_u, was 178 KN/mm (1017 kips/inch) (K_u = (105(76.2)+5560) / 76.2). The equivalent restrainer stiffness, K_r, was computed as 117 KN/mm (667 kips/inch) (K_r = 175 (50.8 / 76.2)). Therefore, the total stiffness was computed as 295 KN/mm (1684 kips/inch), and the corresponding period was 0.55 seconds.

For this period, the acceleration response , ARS_1, was found to be 15,000 mm/sec^2 (590 inch/sec^2). This acceleration corresponded to a SDOF displacement (D_1) of 115 mm (4.53 inches). The same procedure was repeated for the system on the other side of the in-span hinge, and D_2 was found to be 40 mm (1.59 inches). Therefore, the predicted

MRHD for this iteration was 40 mm (1.59 inches). However, a new iteration was necessary because this value did not match the maximum permissible restrainer deflection of 76 mm (3 inches). The process converged at the value of 15 mm (0.57 inches) for the restrainer yield displacement. This value corresponded to a predicted MRHD of 40 mm (1.57 inches). For this case, the predicted MRHD was less than the NLTH MRHD of 71 mm (2.80 inches).

All 216 cases of the database included in the appendix were analyzed using the CALTRANS procedure. Figure 5.6 compares the results of the nonlinear time history analysis and the CALTRANS procedure. The CALTRANS procedure gave conservative results for many cases, but there was little correlation between the results of the CALTRANS procedure and NLTH analysis. As a result, a large number of displacements were substantially underestimated, and the largest unconservative error was approximately 127 mm (5 inches).

The cases that were underestimated tended to consist of a combination of a flexible frame and a very stiff frame. The CALTRANS method uses the smaller SDOF displacement as the predicted MRHD. Therefore, for bridges with both a flexible and very stiff frame, the predicted MRHD was small. This result contradicted the parametric study, which showed that the MRHD tended to be large for cases with a large frame stiffness ratio. The CALTRANS method was also unable to predict the small MRHD that occurred at frame stiffness ratios near 1.0.

5.4 SUMMARY OF EVALUTION

None of the existing methods was able to produce results that matched those of the nonlinear time history analyses.

The AASHTO empirical seat width equation consistently predicted larger displacements than were calculated with nonlinear analysis. Another limitation of the AASHTO restrainer design procedure is that it does not account for the restrainer gap.

The parametric study showed that the restrainer gap has a large effect on the MRHD. The AASHTO method also does not account for variations in the seat width. Such variations greatly affect the allowable MRHD.

The supplemental WSDOT rules do not produce an ideal restrainer design. As shown in the parametric study, the restrainer gap should be kept to a minimum. However, WSDOT specifies a restrainer gap of at least 51 mm (2 inches). In addition, the restrainers should be designed to remain elastic during the design earthquake. WSDOT tries to ensure elastic behavior by specifying an allowable range for the restrainer length and by limiting the restrainer stress, when subjected to AASHTO specified forces, to 60 percent of the ultimate stress. The minimum restrainer length should be calculated on the basis of a predicted MRHD.

The CALTRANS design method provided inconsistent results. Its inability to capture in-phase and out-of-phase movements of the two adjacent frames resulted in some inaccurate predictions. Important MRHD predictors, such as the frame period ratio, are ignored.

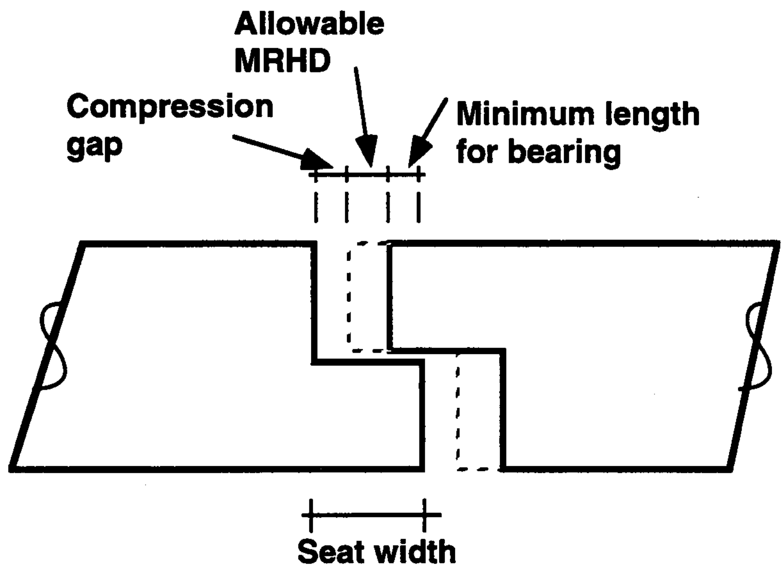

Figure 5.1. Definition of Allowable MRHD

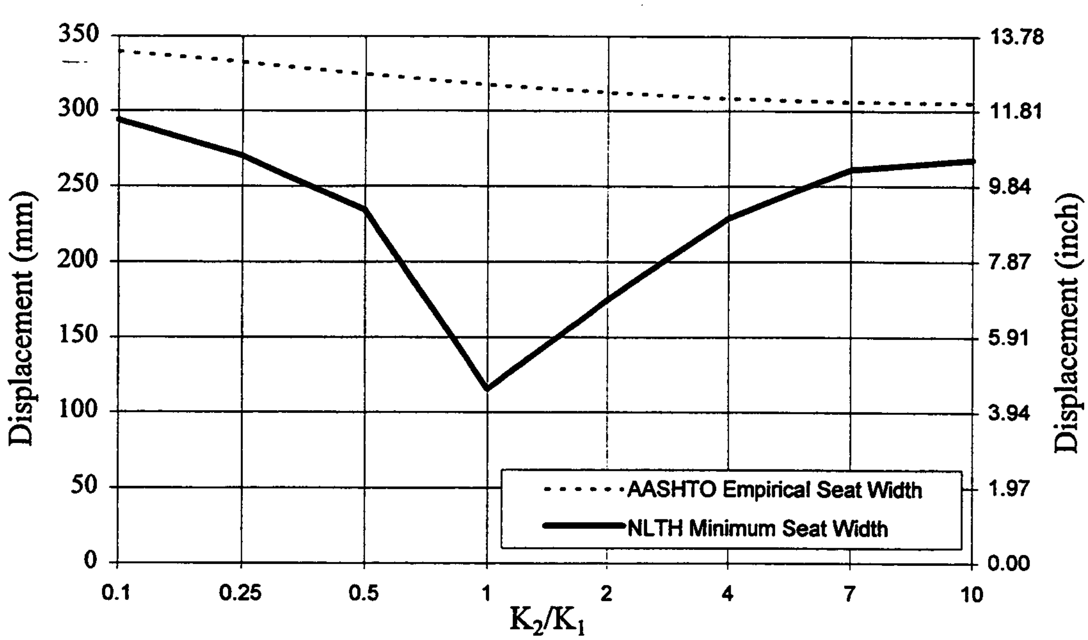

Figure 5.2. AASHTO Empirical Seat Width VS Nonlinear Time History MRHD

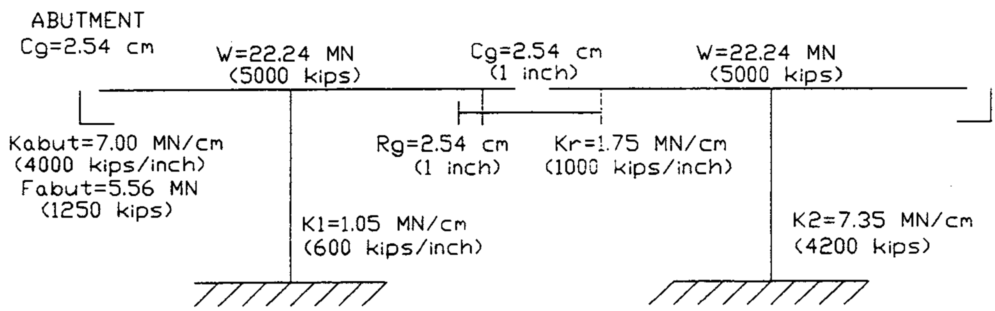

Figure 5.3. Bridge Used for Example of CALTRANS Method

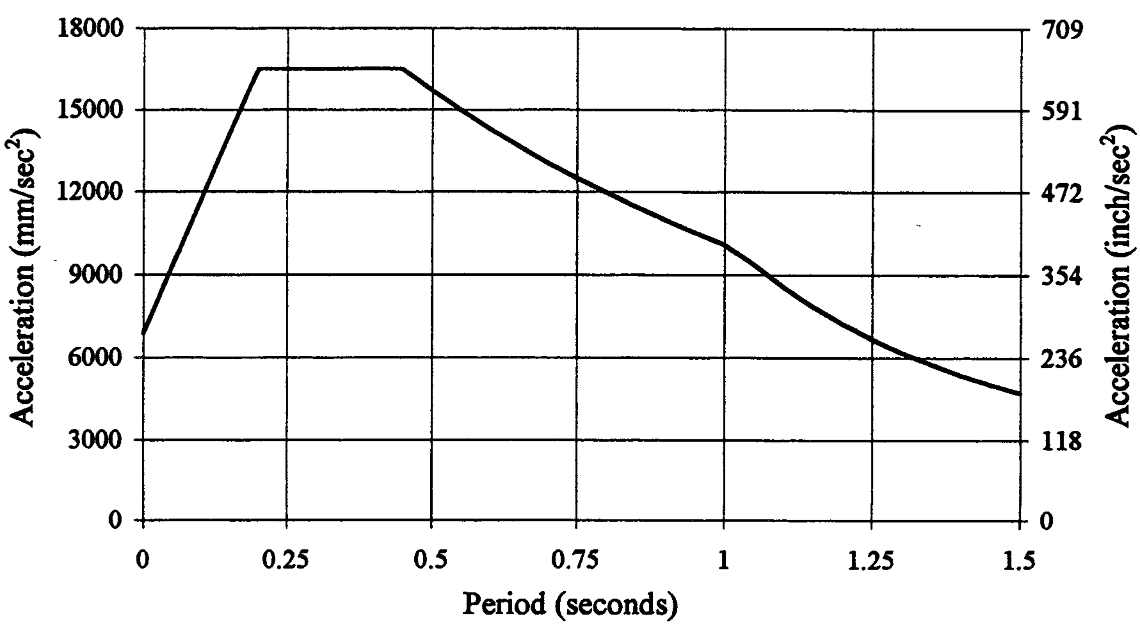

Figure 5.4. Idealized Acceleration Response Spectrum for El Centro*2

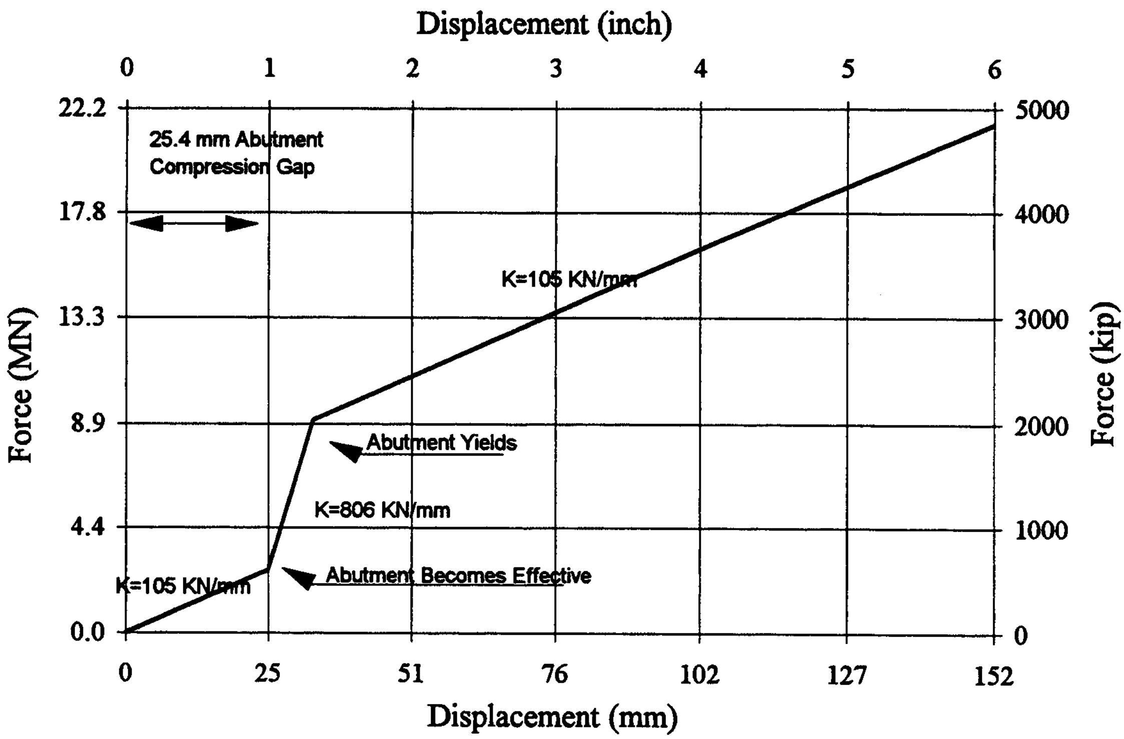

Figure 5.5. Force-Displacement Relationship for Left Half of Example Bridge

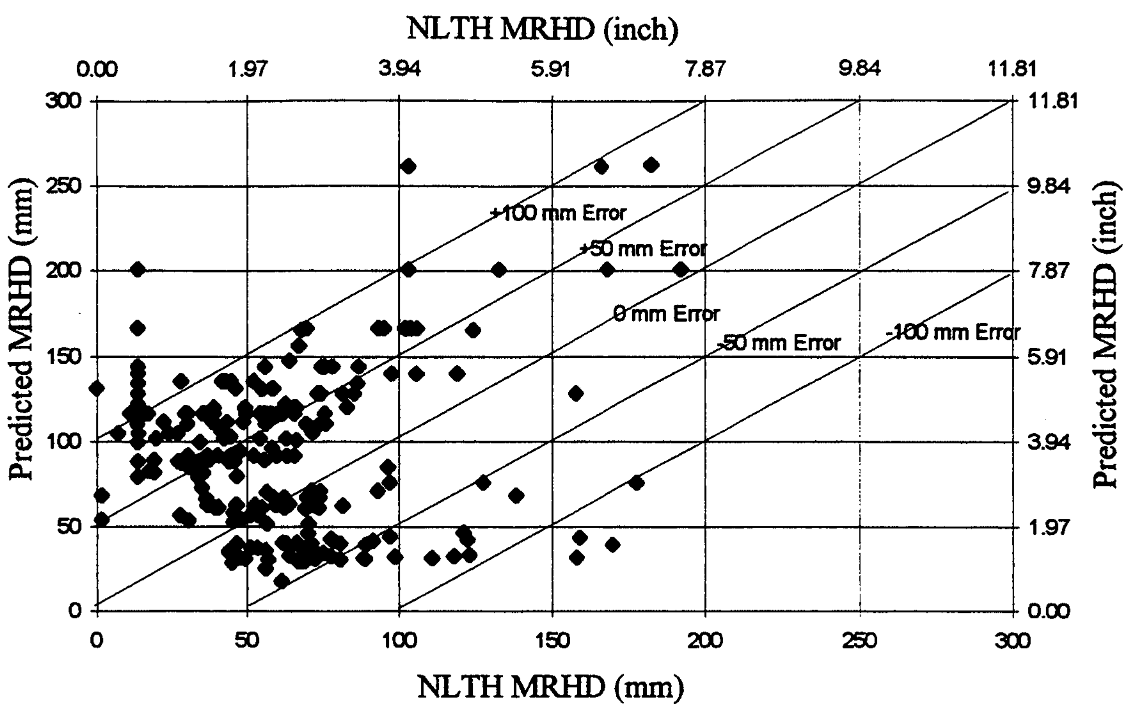

Figure 5.6. Comparison of MRHD Predicted by NLTH and CALTRANS Methods

CHAPTER 6
PROPOSED DESIGN METHOD

This chapter describes a new in-span restrainer design method that was developed by the UW research team. The procedure incorporates many of the assumptions used in the CALTRANS method, but the new procedure relies on a new expression to estimate the MRHD. Furthermore, it considers variables that were ignored by the CALTRANS procedure but were shown to be important in the parametric study. This chapter also describes a new method for estimating the unrestrained maximum relative abutment displacements.

6.1 Development of In-Span Hinge Restrainer Design Method

The parametric study (Chapter 4) showed that the following variables were important in predicting the MRHD:

- restrainer stiffness
- restrainer gap
- frame period ratio (T_L/T_S)
- frame stiffness ratio (K_L/K_S).

The concept of an equivalent stiffness, as implemented by CALTRANS, is attractive because it accounts for the effect of restrainer stiffness, restrainer gap, frame stiffness, frame weight, and abutment resistance. Therefore, the researchers adopted this concept as the basis of their new method. However, it is unreasonable to select the smaller of the displacements computed on each side of an in-span hinge. Therefore, the researchers developed a new expression to combine the displacements (D_1 and D_2) to compute the MRHD. In addition, the new procedure also reflects the influence of frame period ratio.

The effect of the equivalent period ratio (T_L/T_S) on the nonlinear time history MRHD is shown in Figure 6.1. The periods used to compute the equivalent period ratio were calculated using equivalent stiffnesses and masses similar to the ones in the

CALTRANS procedure. As the equivalent period ratio increased, the two systems increasingly oscillated out of phase, and the MRHD increased. By multiplying the system period ratio by the average SDOF displacement ($D_{ave} = (D_1 + D_2) / 2$), the correlation improved even further (Figure 6.2).

As is shown in Figure 6.3, the best fit of the MRHD data was obtained from the following equation:

$$MRHD = \frac{R_g}{3}\sqrt{\frac{K_L}{K_S} - 1} + \frac{D_{ave}}{3}\frac{T_L}{T_S} \leq 2 * D_{ave} \qquad (6.1)$$

where

K_L = larger frame stiffness adjacent to hinge

K_S = smaller frame stiffness adjacent to hinge

D_{ave} = average SDOF displacement

T_L = larger equivalent period

T_S = smaller equivalent period

R_g = restrainer gap

However, although this equation provided the best fit with the results in the database, it is somewhat cumbersome. A fit that is very nearly as good is obtained with

$$MRHD = \frac{D_{ave}}{2}\frac{T_L}{T_S} \leq 2 * D_{ave} \qquad (6.2)$$

This equation is significantly simpler than equation 6.1 and it retains the influence of the relative frame stiffness indirectly within the term T_L/T_S. The influence of R_g is lost, but this is considered relatively unimportant because the researchers recommend using the smallest possible restrainer gap. Equation 6.2 is recommended for design.

6.2 Proposed Design Method for In-Span Hinge Restrainers

The proposed design method idealizes all the components on each side of the in-span hinge as an equivalent SDOF oscillator. Each SDOF oscillator is independently subjected to the earthquake. The two SDOF displacements, along with other parameters, are then used to predict the MRHD. The restrainer stiffness is increased until the predicted MRHD is less than or equal to the allowable seat width. The above procedure is accomplished using the following 14 steps.

Step 1: Compute the allowable MRHD to prevent unseating (Figure 5.1) and to ensure elastic response of the restrainers.

Allowable MRHD = seat width - minimum allowable bearing width - C_g (6.3)

Maximum allowable MRHD = $R_g + F_y L_{max}/E$

where

C_g = compression gap

R_g = restrainer gap

F_y = restrainer yield stress

E = elastic modulus

L_{max} = maximum restrainer length

Step 2: Construct the force-displacement relationship for the equivalent SDOF system.

Step 3: Guess the displacement (Δ_{guess}) of the SDOF system representing all the components on one side of the in-span hinge.

Step 4: Calculate the equivalent frame and abutment stiffness, K_s, on the basis of the guessed displacement.

$$K_s = (\text{force required to produce } \Delta_{guess}) / \Delta_{guess} \quad (6.4)$$

Step 5: Calculate the equivalent restrainer stiffness, K_r.

$$K_r = \text{restrainer stiffness} * (\Delta_{guess} - R_g) / \Delta_{guess} \qquad (6.5)$$

where

R_g = restrainer gap

Step 6: Add the equivalent system and restrainer stiffnesses to obtain the total equivalent stiffness, K_t.

$$K_t = K_s + K_r \qquad (6.6)$$

Step 7: Calculate the equivalent period, T, on basis of K_t and the weight of all mobilized frames.

$$T = 2\pi \sqrt{\frac{W}{K_t * g}} \qquad (6.7)$$

Step 8: Obtain the spectral acceleration corresponding to the equivalent period from the design acceleration response spectrum.

Step 9: Calculate the SDOF displacement.

$$\Delta_{sdof} = ARS * W / K_t \qquad (6.8)$$

where

ARS = response spectrum acceleration corresponding to the equivalent period, T

W = weight of all mobilized frames

Step 10: Repeat steps 3 through 10 until the SDOF displacement equals the guessed displacement.

Step 11: Repeat steps 2 through 10 for the other side of the in-span hinge.

Step 12: Compute the predicted MRHD.

$$\text{MRHD} = \frac{D_{ave}}{2}\frac{T_L}{T_S} \leq 2 * D_{ave} \tag{6.9}$$

where

D_{ave} = average SDOF displacement

T_L = larger equivalent period

T_S = smaller equivalent period

Step 13: Increase the restrainer stiffness until the predicted MRHD is less than or equal to the minimum allowable MRHD.

Step 14: Calculate the minimum restrainer length and area to provide the required stiffness and to ensure elastic behavior of the restrainers.

If the minimum restrainer length is too long, the design procedure can be repeated using a smaller allowable MRHD.

6.3 Example of In-Span Hinge Restrainer Design

The above procedure is illustrated using the example bridge shown in Figure 6.4. The unrestrained case was first examined. The analysis was conducted using the idealized El Centro*2 acceleration response (Figure 6.5) spectrum. The left half of the bridge was first considered.

Step 1: The minimum allowable bearing width was assumed to be 76 mm (3 inches), and the seat width was assumed to be 191 mm (7.5 inches). It was also assumed that the restrainer could be as long as necessary to use the full capacity of the restrainers.

Allowable MRHD = 191 - 76 - 25 = 89 mm (3.5 inches)

Step 2: The system force-displacement relationship for the left half of the bridge is shown in Figure 6.6.

Step 3: Δ_{guess} = 127 mm (5 inches)

Step 4: equivalent system stiffness = (127 * 105 + 5600)/127 = 149 KN/mm (850kips/inch)

Step 5: equivalent restrainer stiffness = (0 * (127 - 25) / 127) = 0 KN/mm

Step 6: K_t = 149 + 0 = 149 KN/mm (850 kips/inch)

Step 7: $T = 2\pi\sqrt{\frac{22{,}240}{(149 \times 9810)}}$ = 0.78 seconds

Step 8: From Figure 6.5, ARS = 12,200 mm/sec^2 (480 inch/sec^2) = 1.24 g

Step 9: Δ_{sdof} = 1.24 * 22.2 / 149 = 185 mm (7.3 inches)

Step 10: $\Delta_{guess} \neq \Delta_{sdof}$ Therefore, steps 3 through 10 must be repeated.

> **Step 3:** Δ_{guess} = 196 mm (7.7 inches)
>
> **Step 4:** equivalent system stiffness = (196 * 105 + 5600) / 196 = 133 KN/mm (760 kips/inch)
>
> **Step 5:** equivalent restrainer stiffness = 0 * (196 - 25) / 196 = 0 KN/mm
>
> **Step 6:** K_t = 133 + 0 = 133 KN/mm (760 kips/inch)
>
> **Step 7:** $T = 2\pi\sqrt{\frac{22{,}240}{(133 \times 9810)}}$ = 0.82 seconds
>
> **Step 8:** ARS = 11,700 mm/sec^2 (460 inch/sec^2) = 1.19 g
>
> **Step 9:** Δ_{sdof} = 1.19 * 22.2 / 133 = 199 mm (7.8 inches)
>
> **Step 10:** $\Delta_{sdof} \cong \Delta_{guess}$ Therefore, OK

Step 11: Repeat steps 2 through 10 for the other side of the in-span hinge.

> **Step 2:** The force-displacement relationship is shown in Figure 6.7.
>
> **Step 3:** Δ_{guess} = 43 mm (1.7 inches)
>
> **Step 4:** equivalent system stiffness = (43 * 736 + 5600) / 43 = 866 KN/mm (4930 kips/inch)
>
> **Step 5:** equivalent restrainer stiffness = 0 * (43 - 25) / 43 = 0 MN/cm
>
> **Step 6:** K_t = 866 + 0 = 866 KN/mm (4930 kips/inch)
>
> **Step 7:** $T = 2\pi\sqrt{\frac{22{,}240}{(866 \times 9810)}}$

Step 8: ARS = 16,500 mm/sec^2 (650 inch/sec^2) = 1.68g

Step 9: Δ_{sdof} = 1.68 * 22.2 / 866,000 = 43 mm (1.7 inches)

Step 10: $\Delta_{sdof} = \Delta_{guess}$ Therefore, OK

Step 12: D_{ave} = (198 + 43) / 2 = 121 mm (4.8 inches)

T_L/T_S = 0.82 / 0.32 = 2.6

MRHD = (121 / 2) * (2.6) = 155 mm (6.12 inches)

The predicted MRHD agreed well with the nonlinear time history MRHD of 160 mm (6.3 inches). The predicted MRHD was larger than the allowable MRHD (Step 1). Therefore, restrainers were required to reduce the predicted MRHD.

Step 13: A restrainer stiffness of 88 KN/mm (500 kips/inch) was used for the next trial. The restrainer gap was set to 25 mm (1.0 inch) to account for temperature changes. By repeating steps 3 through 12, the researchers obtained a predicted MRHD of 95 mm (3.7 inches). This compared favorably with the NLTH MRHD of 91.4 mm (3.6 inches). Since this value exceeded 89 mm (3.5 inches), the restrainer stiffness was further increased. The third trial was conducted using a restrainer stiffness of 175 KN/mm (1000 kips/inch). This resulted in a predicted MRHD of 70 mm (2.8 inches). Since the predicted MRHD was less than the allowable MRHD, a restrainer stiffness of 175 KN/mm (1000 kips/inch) was adequate. In comparison, the nonlinear time history MRHD for a restrainer stiffness of 175 KN/mm (1000 kips/inch) was 71.1 mm (2.8 inches).

Step 14: The minimum area and length of the restrainers were calculated as follows.

Δ_y = MRHD - R_g = 50 mm (1.8 inches) = $F_y L / E$

K = 175 KN/mm (1000 kips/inch) = EA / L

where

E = 206.8 GPa (30,000 ksi) for high strength steel rods and 68.9 GPa (10,000 ksi) for cables

F_y = 827 MPa (120 ksi) for rods, and 1213 Mpa (176 ksi) for cables

For rod restrainers:

$$L_{min} = 206{,}800 * 0.050 / 827 = 12.5 \text{ m (41 feet)}$$

Assuming that the restrainer length L is equal to L_{min} one obtains:

$$A_{min} = 175 * 12.5 / (206{,}800) = 10{,}500 \text{ mm}^2 \text{ (16 inch}^2\text{)}$$

If the restrainer length is excessive, the hinge can be designed for a smaller MRHD.

For cable restrainers:

$$L_{min} = 68{,}900 * 0.050 / 1213 = 2.84 \text{ m (9.3 feet)}$$

Assuming that the restrainer length L is equal to L_{min} one obtains:

$$A_{min} = 175 * 2.84 / (68{,}900) = 7{,}200 \text{ mm}^2 \text{ (11.2 inch}^2\text{)}$$

All the database cases were analyzed with the proposed method to allow comparison with the results of nonlinear time history analysis. The comparison is shown in Figure 6.8. The largest unconservative error was approximately 50 mm (2 inches). The average error was 15.5 mm (0.61 inches).

6.4 Development of Method for Estimating MRAD

The parametric study (Chapter 4) showed that the following variables are important in predicting the MRAD:

- abutment stiffness and strength
- sum of frame stiffnesses
- sum of frame weights.

An approach that incorporated all three variables was first examined. The same procedure used to compute the SDOF displacements for each side of the in-span hinge was used to compute the single unrestrained SDOF displacement for the entire bridge moving away from one of the abutments. The predicted MRAD was equal to the SDOF displacement. The results of this procedure are compared with those of the nonlinear time history in Figure 6.9. This method produced conservative results for almost all the database cases. The largest unconservative error was 28 mm (1.1 inch). The largest conservative error was approximately 203 mm (8 inches).

Another method that was examined consisted of ignoring the abutments and compression gaps and treating the entire bridge as a continuous frame. The SDOF displacement could then be calculated without iteration. The equivalent period used to compute the displacement was based on the sum of all the frame stiffnesses and weights. The results of this procedure are presented in Figure 6.10. For the cases considered in the parametric study, it was possible to ignore the abutments and compression gaps without significantly affecting the predicted MRAD.

The second method was chosen as the proposed method. This method produced results that had the same accuracy as the first method, but does not require iteration. By avoiding iteration, the time required and the chance for error are reduced.

6.5 Proposed Method for Estimating MRAD

The steps involved for estimating the maximum relative abutment displacement are outlined below.

Step 1: Calculate the equivalent SDOF period.

$$T = 2\pi * \sqrt{\frac{\Sigma W}{\Sigma K * g}} \qquad (6.10)$$

where

ΣW = sum of all frame weights

ΣK = sum of all frame stiffnesses

Step 2: Obtain the spectral acceleration corresponding to the equivalent period from the elastic acceleration response spectrum.

Step 3: Calculate the predicted MRAD.

$$MRAD = ARS * (\Sigma W / \Sigma K) \qquad (6.11)$$

where

ARS = spectral acceleration in g

Step 4: Compute the minimum seat width

minimum seat width = C_g + minimum allowable bearing width + MRAD (6.12)

where

C_g = compression gap

6.6 Example

This procedure was demonstrated using the example bridge shown in Figure 6.4. The El Centro *2 acceleration response spectrum (Figure 6.5) was used for the analysis.

Step 1: ΣW = 44.48 MN (10,000 kips)
ΣK = 841 KN/mm (4800 kips/inch)
T = 0.46 seconds

Step 2: From Figure 6.5, ARS = 21,800 mm/sec^2 (860 inch/sec^2)= 2.23 g

Step 3: MRAD = 2.23 * 44.48 / 841 = 118 mm (4.6 inches)

Step 4: minimum seat width = 25 + 76 +118 = 219 mm (8.6 inches)

If such a seat width had not been provided, the seat width should be extended. The nonlinear time history analysis produced an MRAD of 68.3 mm (2.69 inches) for abutment 1 and 45.5 mm (1.79 inches) for abutment 2.

6.7 Effect of Column Damage

The researchers conducted analyses of an additional 12 models to consider the effect of column damage. All analyses were conducted on a two-frame model that was similar to the model described in Chapter 3.

Each frame supported a weight of 22.2 MN (5000 kips). To model earthquake damage, the columns were assumed to be pinned at the bases, and the frame columns were modeled as cantilevers. The frame stiffness was calculated as follows:

$$K = 3\ EI_{cracked} / L^3 \qquad (6.13)$$

The frame yield force was computed as follows.

$$F = M_y / L \qquad (6.14)$$

Using a column height of 7.62 m (25 feet) and the same material properties and geometry as the undamaged case, the stiffness was calculated to be 43.8 KN/mm (250 kips/inch) with a corresponding frame yield force was 2.0 MN (450 kips). The abutment properties remained unchanged from the undamaged two-frame bridge model. The restrainer stiffness was 175 KN/mm (1000 kips/inch).

The above calculations were repeated while the average height of frame 2 was varied from 3.5 m (11.6 feet) to 9.6 m (31.5 feet). The height variation resulted in K_2/K_1 ratios equal to 0.5, 1, 2, 4, 7, and 10. In addition, the entire range was reanalyzed with a restrainer stiffness of 0 KN/mm. All models were analyzed using the El Centro*2 ground motion and a viscous damping ratio of 5 percent.

A comparison between the nonlinear time history MRHD and the predicted MRHD is shown in Figure 6.11. The figure shows the computed MRHD for the damaged columns and for the corresponding undamaged frames. The proposed method provided results that were accurate to within -18 mm (0.7 inches) and +86.4 mm (3.4 inches). For the frames with damaged columns, the majority of the cases had a conservative error of less than 25 mm (1 inch). Figure 6.12 compares the results of the nonlinear time history MRAD and the predicted MRAD. All predicted MRADs were conservative. The largest conservative error was approximately 97 mm (3.8 inches).

6.8 Three-Frame Bridge

Because the parametric study considered only two-frame bridges, it was necessary to check the procedure for a bridge with three frames. The assumptions and properties incorporated in the three-frame model were identical to the ones in the undamaged two-frame model. Table 6.1 summarizes the ten cases analyzed, all of which used the El Centro*2 ground motion.

The predicted MRHD matched the nonlinear time history MRHD to within -25 mm (1 inch) and +46 mm (1.8 inches) (Figure 6.13). Again, the majority of the cases had an error of less than 25 mm (1 inch). Figure 6.14 compares the predicted MRAD to the larger nonlinear time history MRAD. The proposed method produced conservative results for all ten cases. The largest conservative error was 99 mm (3.9 inches). The average error was approximately +58 mm (2.3 inches).

Table 6.1. Cases Analyzed for Three-Frame Bridge

CASE	K_1 (KN/mm)	K_2 (KN/mm)	K_3 (KN/mm)	K_r (KN/mm)
1	105	52	210	0
2	105	52	210	175
3	105	52	52	0
4	105	52	52	175
5	210	105	263	0
6	210	105	263	175
7	210	52	210	0
8	210	52	210	175
9	157	210	52	0
10	157	210	52	175

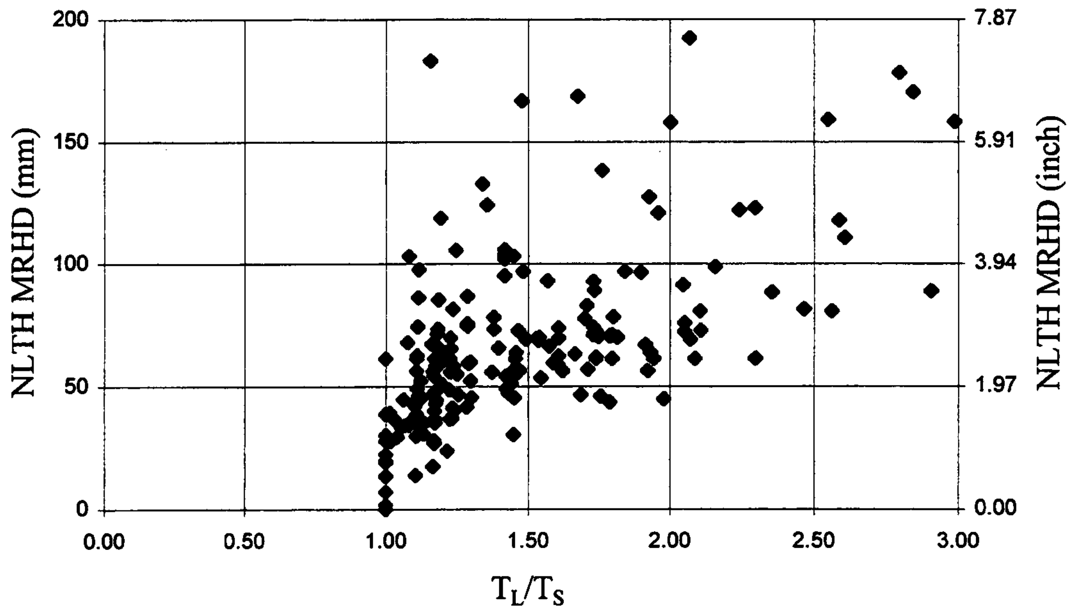

Figure 6.1. Effect of Equivalent Period Ratio on MRHD

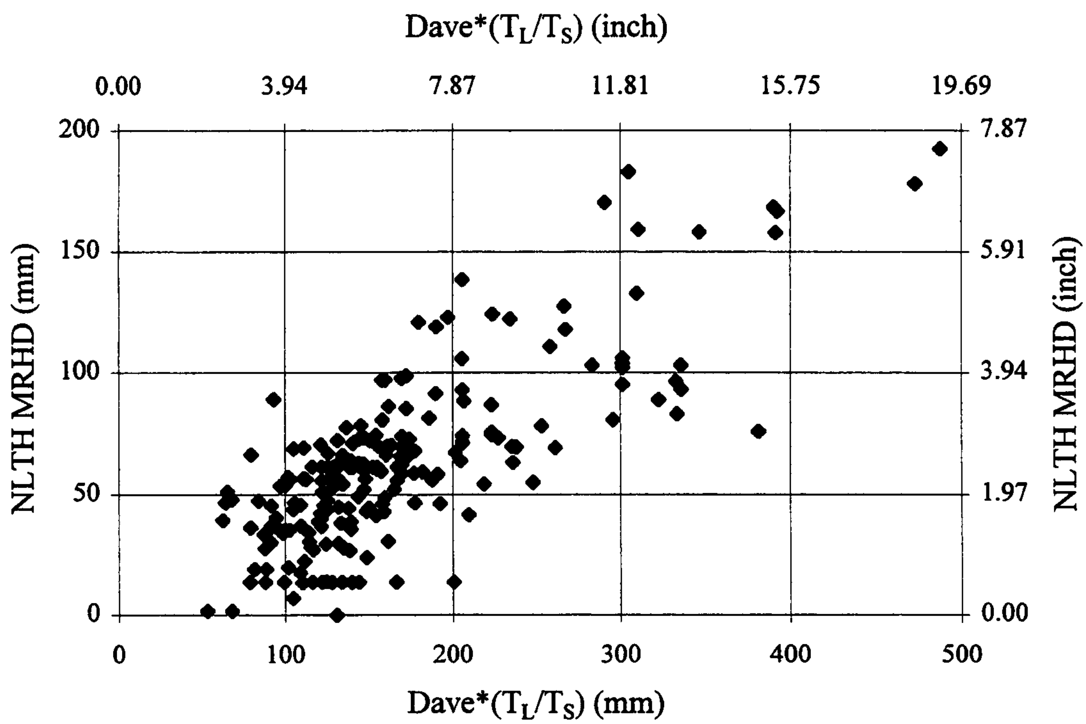

Figure 6.2. Effect of Dave(Tl/Ts) on MRHD

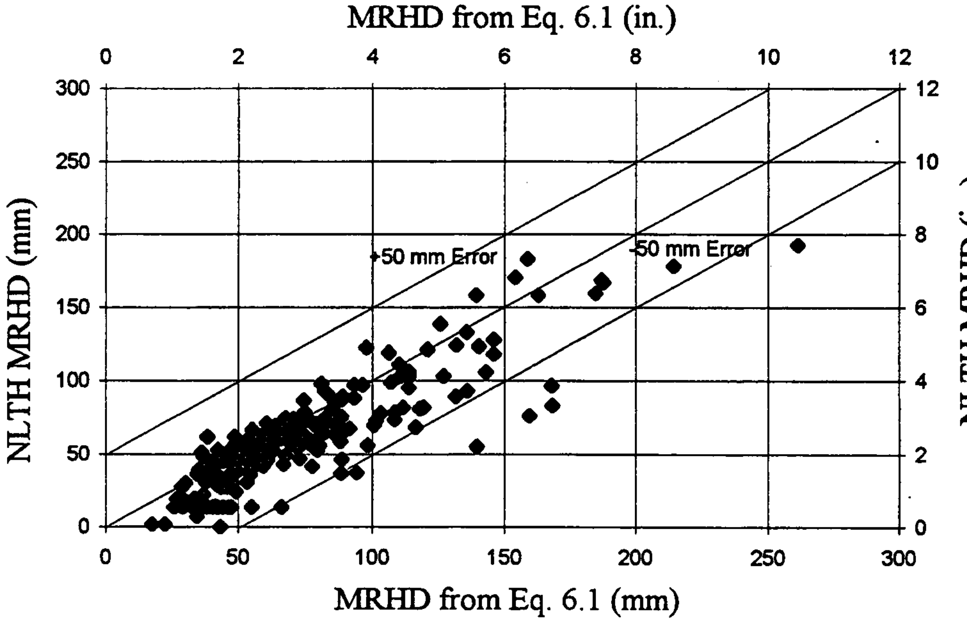

Figure 6.3. Comparison of Equation 6.1 and NLTH

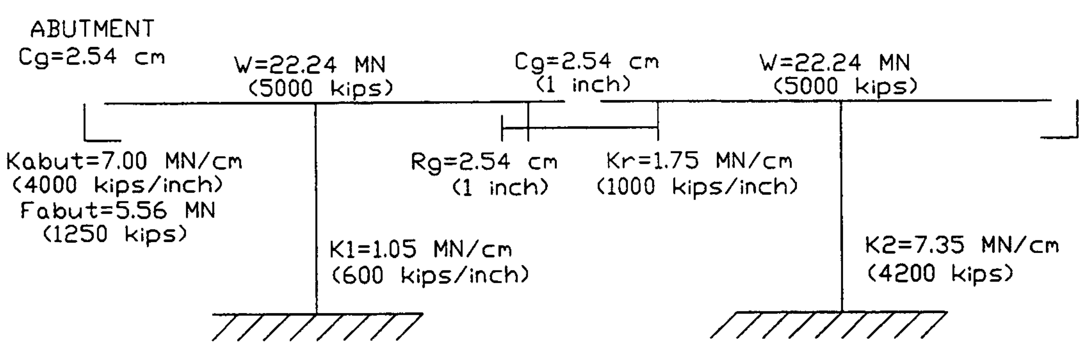

Figure 6.4. Bridge used for Design Example

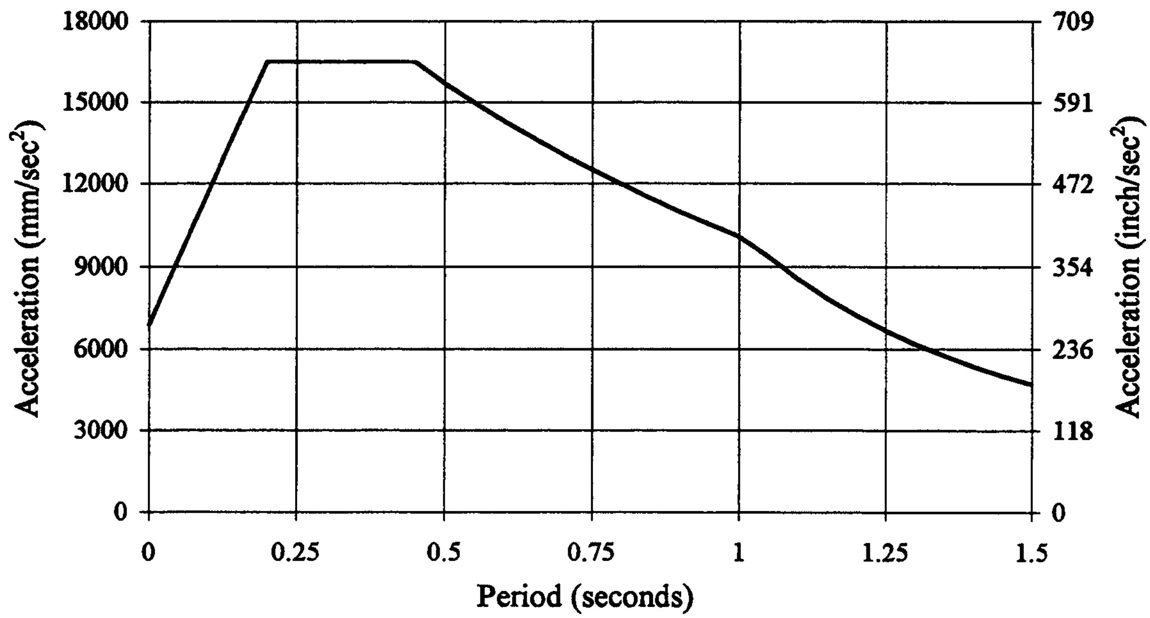

Figure 6.5. Idealized Acceleration Response Spectrum for El Centro*2

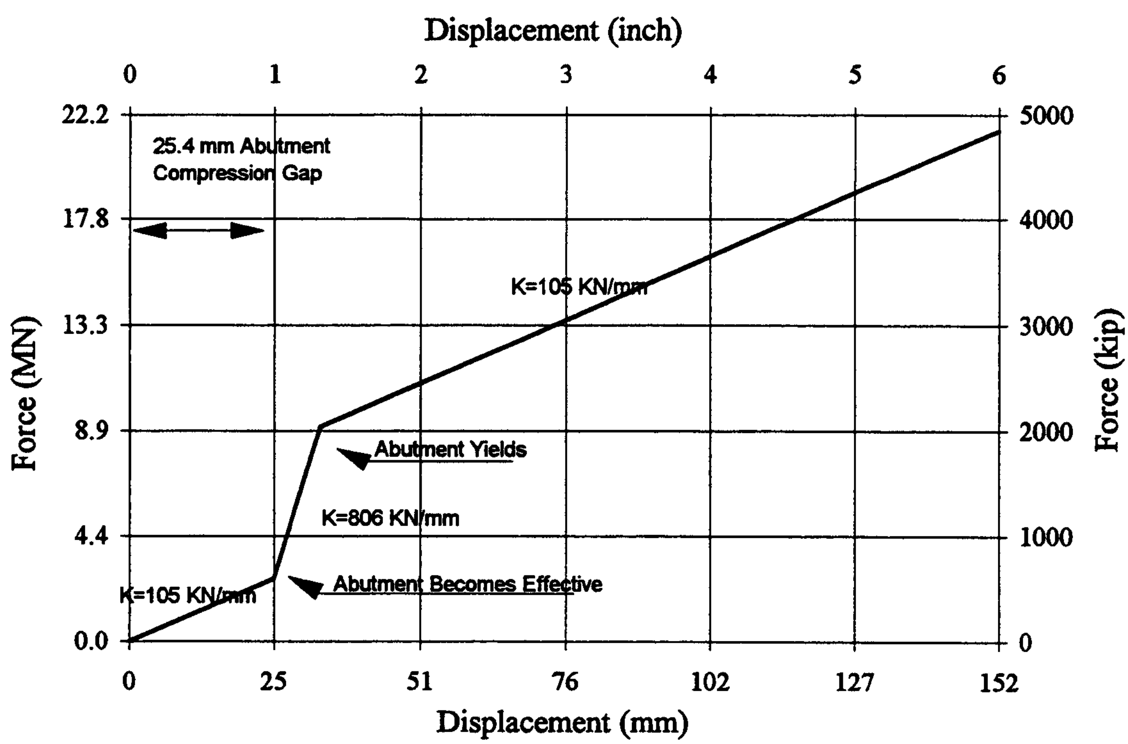

Figure 6.6. Force-Displacement Relationship for Left Half of Example Bridge

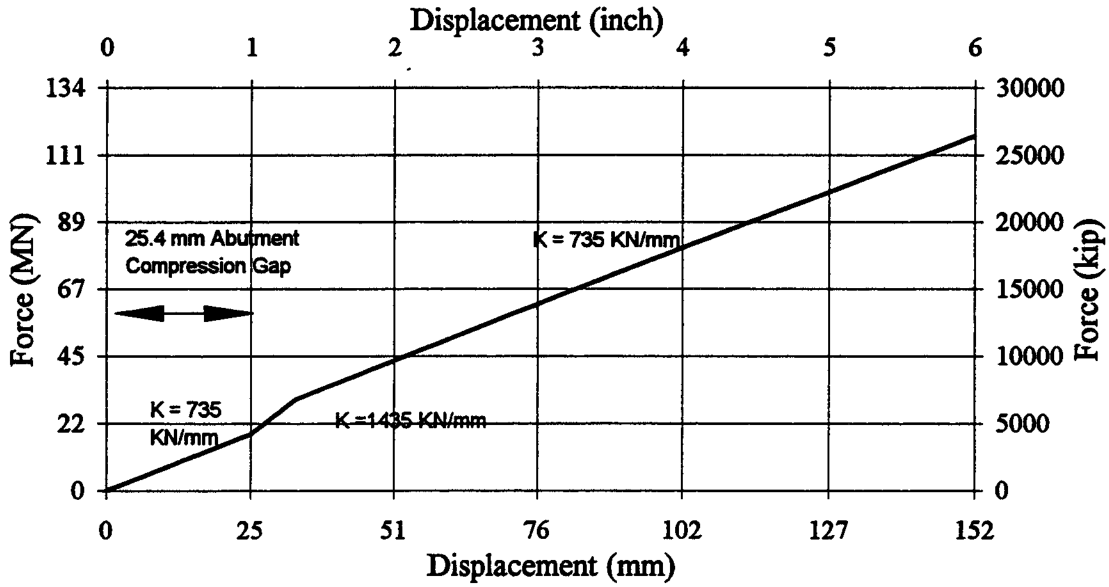

Figure 6.7. Force-Displacement Relationship for Right Half of Example Bridge

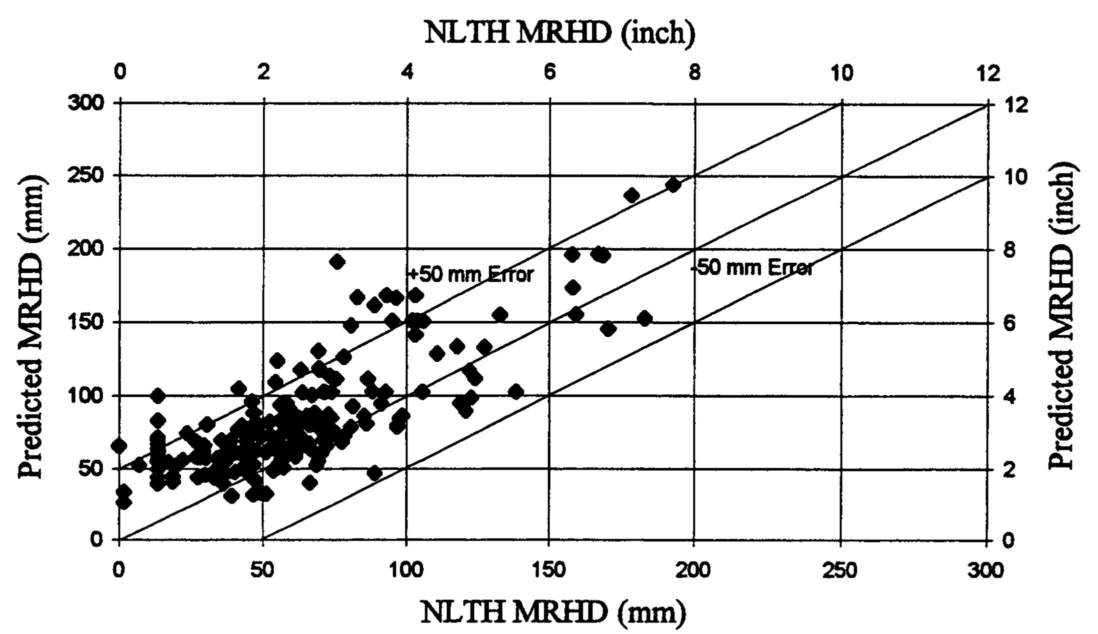

Figure 6.8. Comparison Between Proposed Design Method and NLTH

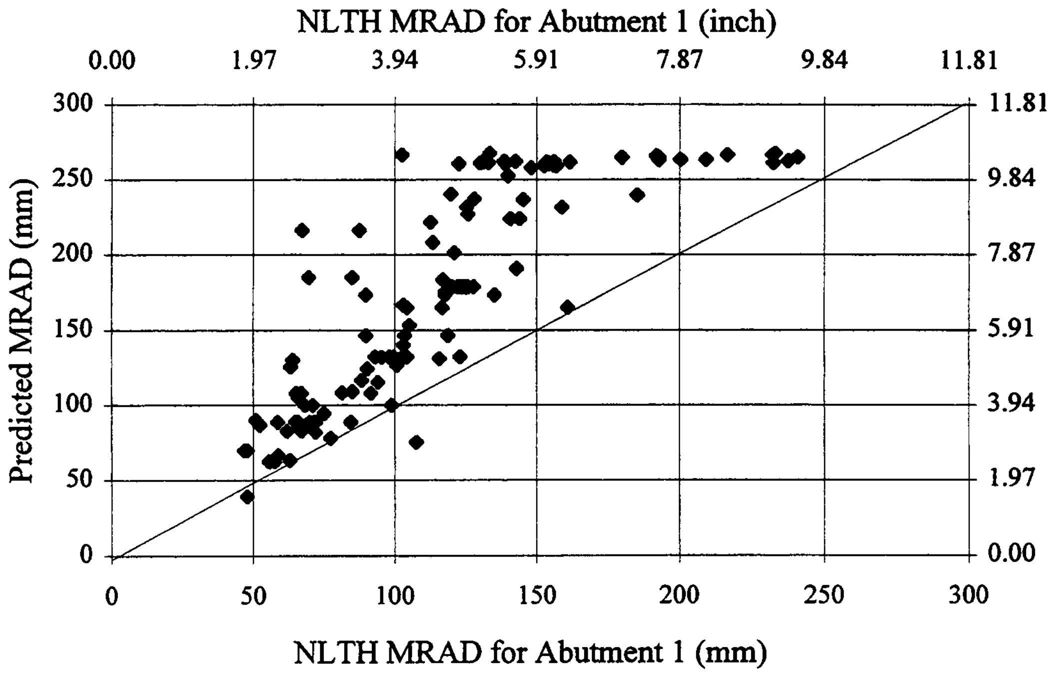

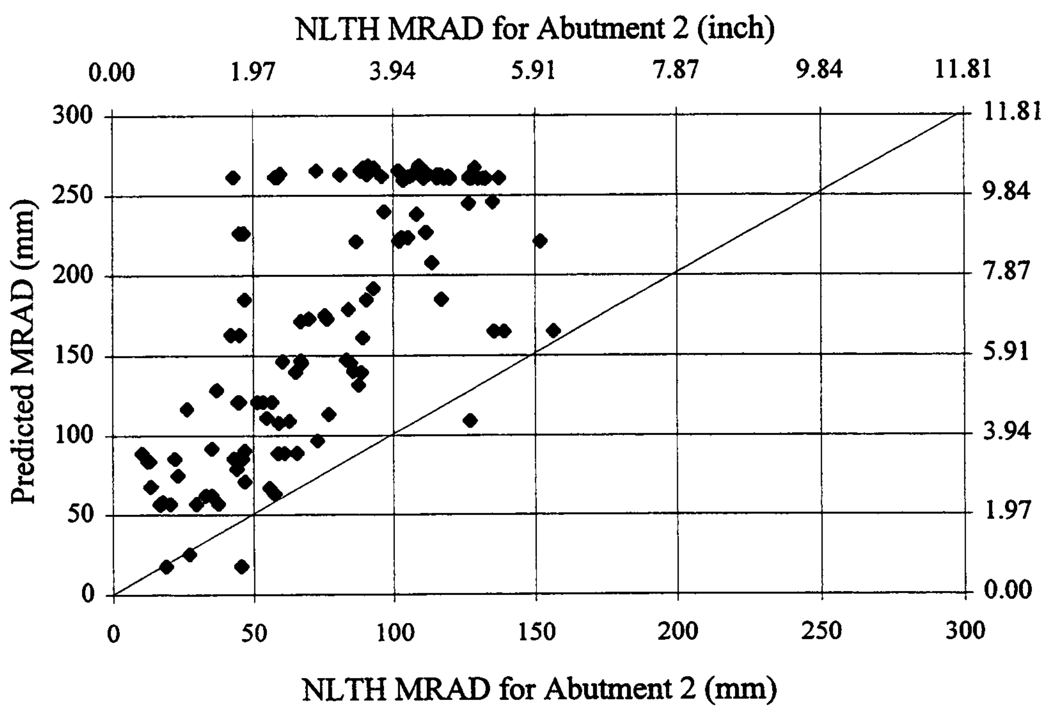

Figure 6.9. Comparison Between Equivalent Static MRAD and NLTH MRAD

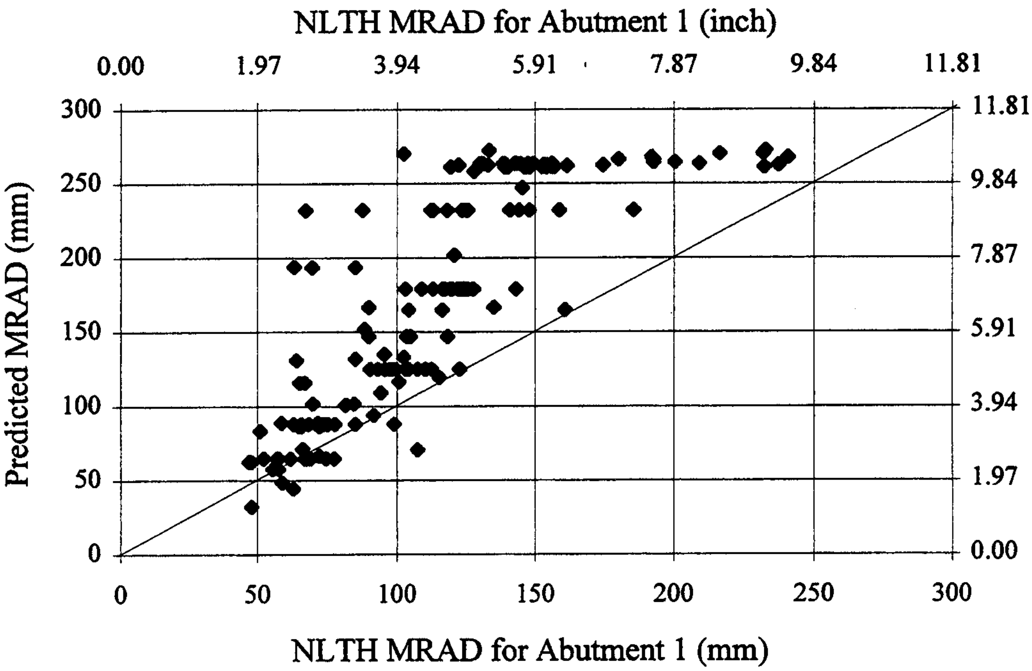

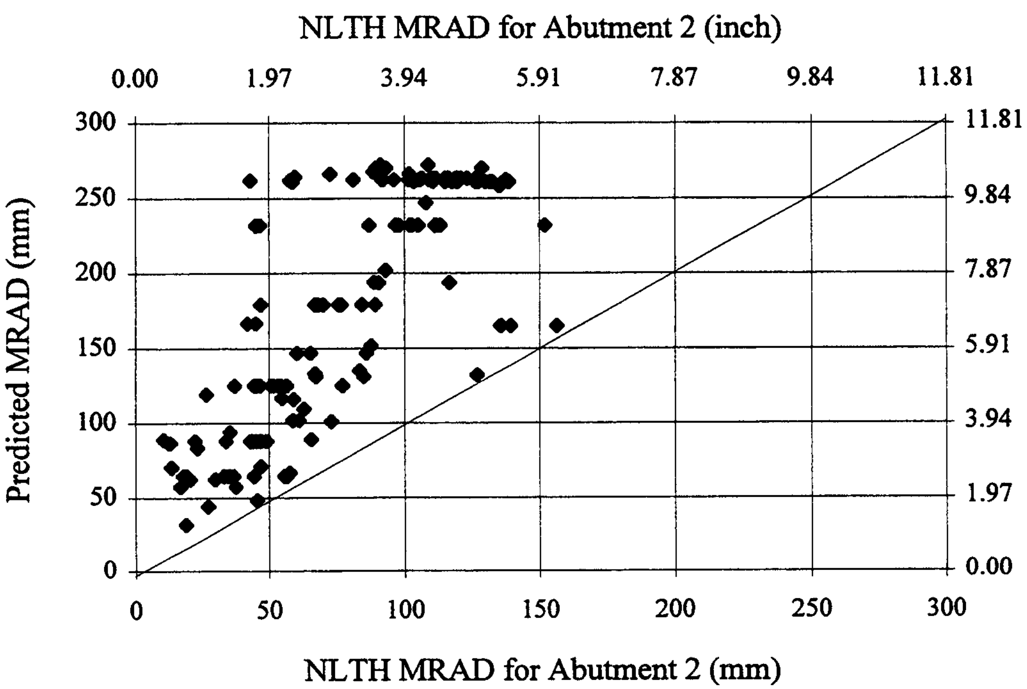

Figure 6.10. Comparison Between Proposed Method MRAD and NLTH MRAD

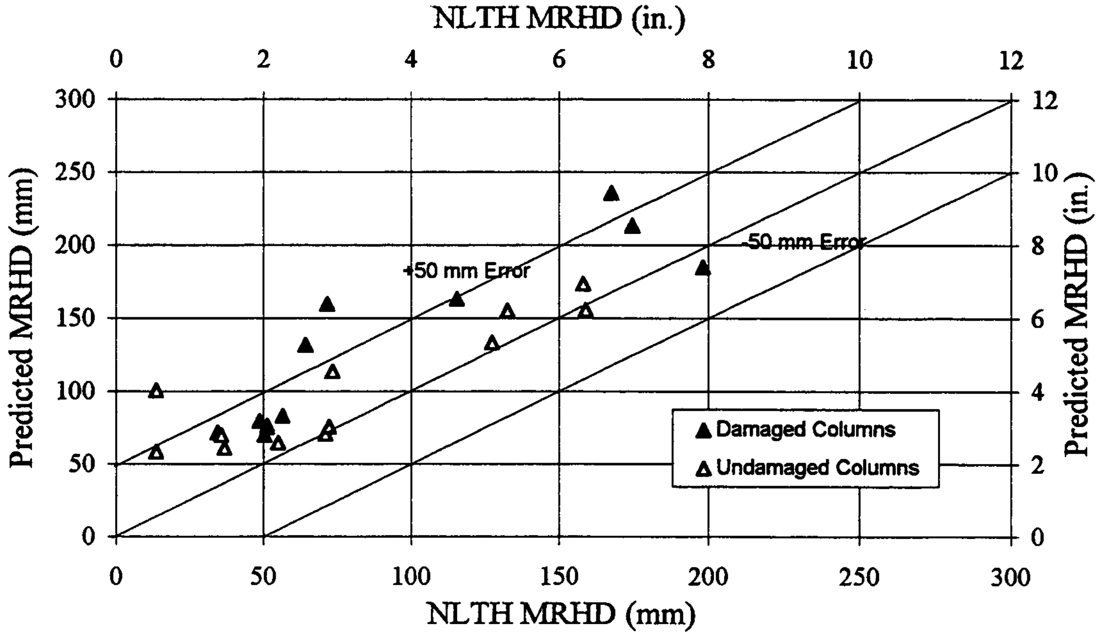

Figure 6.11. Comparison Between Proposed Design Method MRHD and NLTH MRHD for Damaged Two-Frame Bridge

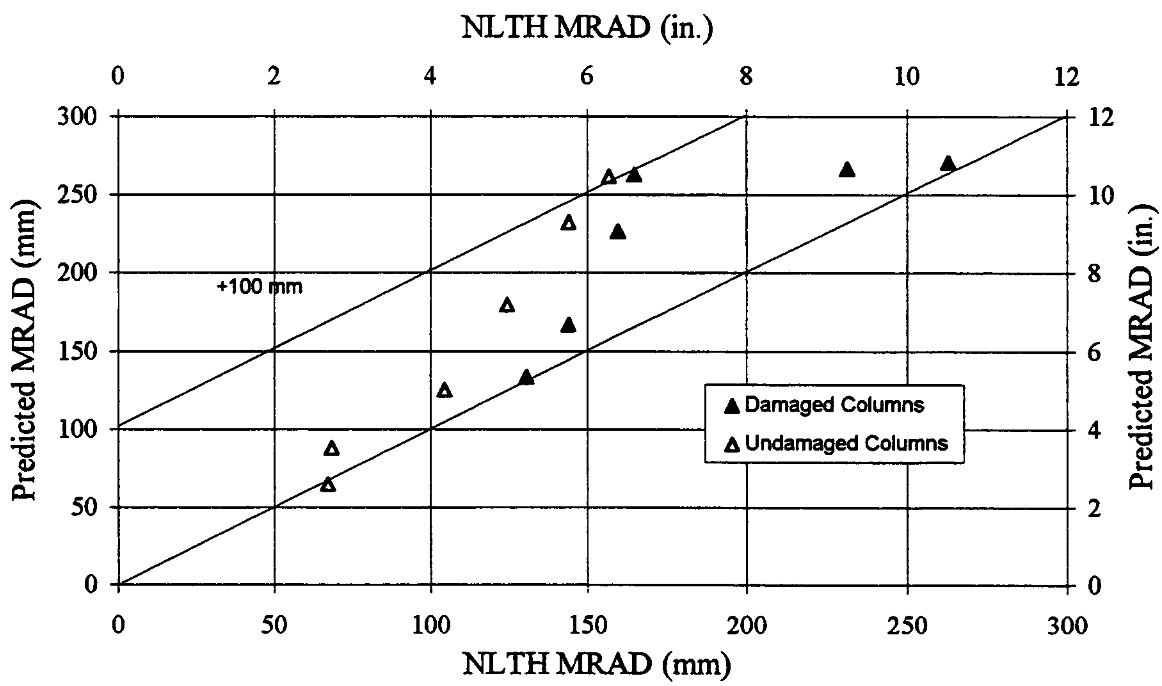

Figure 6.12. Comparison Between Proposed Method MRAD and NLTH MRAD for Damaged Two-Frame Bridge

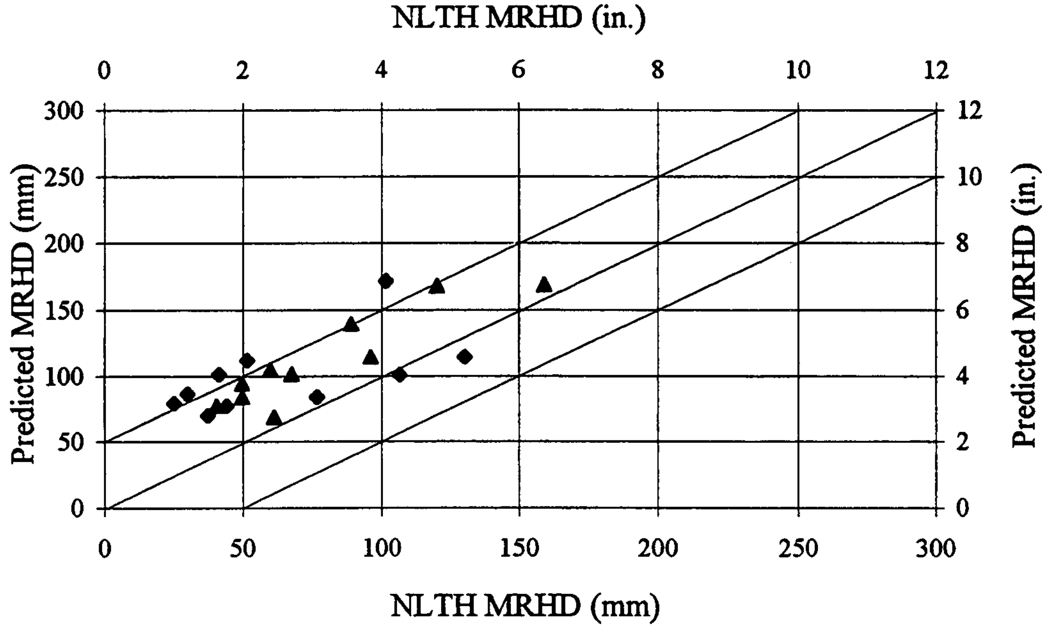

Figure 6.13 Comparison Between Proposed Method MRHD and NLTH MRHD for Three-Frame Bridge

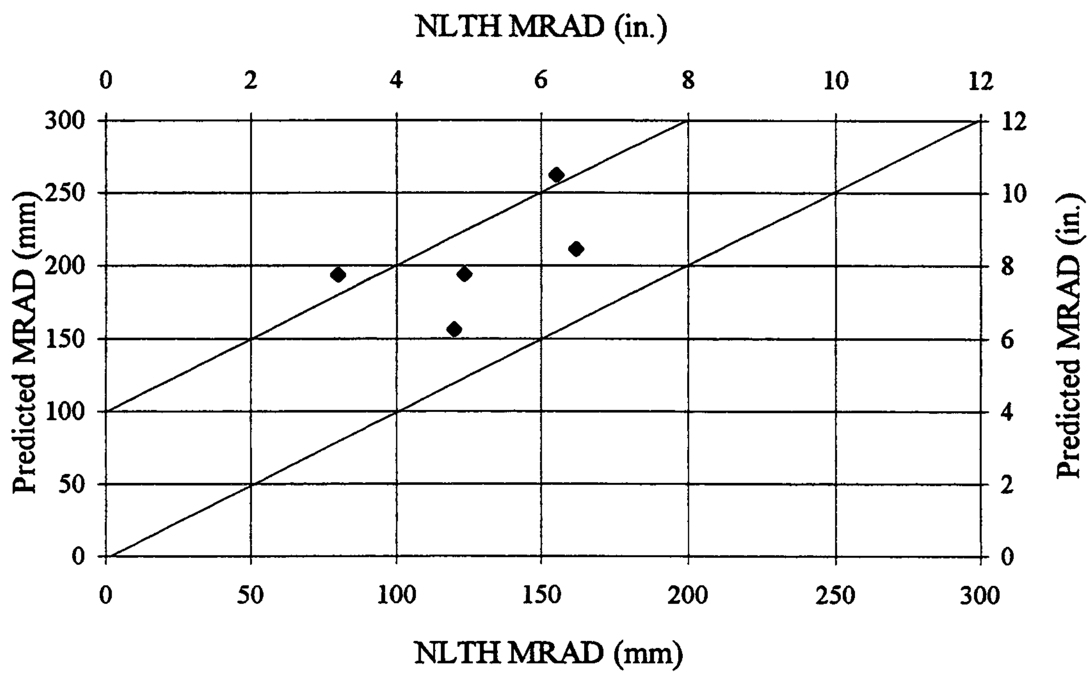

Figure 6.14. Comparison Between Proposed Method MRAD and NLTH MRAD for Three-Frame Bridge

CHAPTER 7

CONCLUSIONS AND RECOMMENDATIONS

The nonlinear analyses conducted for this study allowed the researchers to evaluate current design methods and to identify the parameters most important in predicting maximum relative hinge displacement (MRHD). The researchers also developed a new restrainer design method and a method for predicting the unrestrained maximum relative abutment displacement (MRAD). The conclusions drawn from this work are summarized in this chapter.

7.1 CONCLUSIONS

1. The maximum relative hinge displacement (MRHD) depends greatly on the frame stiffness ratio, frame period ratio, restrainer stiffness, and restrainer gap.

2. The maximum relative abutment displacement (MRAD) depends most on the abutment stiffness and strength, sum of frame stiffnesses, and sum of frame weights.

3. The CALTRANS equivalent static analysis method does not accurately predict the MRHD computed by nonlinear time history analysis. The method was unconservative when applied to a bridge that consisted of a combination of a flexible and stiff frame. At frame stiffness ratios near 1.0, the method produced an MRHD that was substantially larger than the MRHD computed by nonlinear time history analysis (NLTH).

4. Compared with NLTH, the AASHTO minimum seat width equation is conservative, even for very strong earthquakes such as El Centro*2 (0.70g). However, the AASHTO restrainer design procedure does not account for some variables that are important in predicting span unseating, such as the frame stiffnesses. As a result, the factor of safety against failure likely varies greatly among bridges.

5. The parametric study showed that for frame stiffness ratios other than 1.0, an increase in the restrainer gap resulted in approximately the same increase in the MRHD. Therefore, rules requiring large restrainer gaps beyond that necessary to accomodate thermal movements should be avoided.

6. The restrainer length should be large enough to provide a yield displacement that is larger than or equal to the expected MRHD. This will ensure that the restrainer behaves elastically during the design earthquake.

7. A new method for designing restrainers is needed. The current methods do not incorporate variables to account for the out-of-phase movement of the two adjacent frames.

8. WSDOT should consider adopting the proposed restrainer design procedure. This method produced results that were accurate to within -2.5 cm (1 inch) and +5.0 cm (2 inches) of the nonlinear analysis. Further work is needed to account for ground-motion spatial variation and to extend the method to skewed and curved bridges.

9. Abutment seat extensions should be designed to be consistent with the MRAD estimating method developed in this report.

7.2 NEED FOR FURTHER WORK

An effective method for estimating the MRHD of in-span hinges in skewed and curved bridges needs to be developed. Although the CALTRANS procedure addresses such bridges, the method is unlikely to be satisfactory because the CALTRANS method produces unsatisfactory results for regular straight bridges. The response of skewed and curved bridges could be evaluated using two-dimensional nonlinear time history analysis. The effect of spatial variation of the ground motion (incoherency) on the MRHD and MRAD also needs to be investigated.

REFERENCES

AASHTO LRFD Bridge Design Specifications (1994). American Association of State Highway and Transportation Officials, Washington, D.C.

Abdel-Ghaffar, S.M., Emmanuel, M. and Mehdi, S. (1993, June). "Evaluation of the Response of the Aptos Creek Bridge During the 1989 Loma Prieta Earthquake," Report number CCEER 93-1, University of Nevada, Reno, Department of Civil Engineering.

Abdel-Ghaffar, S.M., Maragakis, E. and Saiidi, M. (1993). "Performance of Hinge Restrainers in the Huntington Ave. Bridge during the 1989 Loma Prieta Earthquake," Report number CCEER 93-4, University of Nevada, Reno, Department of Civil Engineering.

California Department of Transportation (1989, October). *Bridge Design Aids.*

Lwin, M. M., and Henley, E.H. (1993, September). "Bridge Seismic Retrofit Program Report." Washington State Department Transportation.

Maragakis, E., Saiidi, M., Feng, S. and Flournoy, L. (1993, July). "Effects of Hinge Restrainers on the Response of the San Gregorio Bridge during the Loma Prieta Earthquake," Report number CCEER 93-05, University of Nevada, Reno, Department of Civil Engineering.

O'Connor, D.N., Saiidi, M. and Margakis, E. (1993, February). "Effect of Hinge Restrainers on the Response of the Madrone Drive Undercrossing during the Loma Prieta Earthquake," Report number CCEER 92-9, University of Nevada, Reno, Department of Civil Engineering.

Saiidi, M., Maragakis, E. and Feng, S. (1992, October). "An Evaluation of the Current Caltrans Seismic Restrainer Design Method," Report number CCEER 92-8, University of Nevada, Reno, Department of Civil Engineering.

Saiidi, M., Maragakis, E., Abdel-Ghaffar, S., Feng, S. and O'Connor, D. (1993, May). "Response of Bridge Hinge Restrainers During Earthquakes -- Field Performance, Analysis, and Design," Report number CCEER 93-6, University of Nevada, Reno, Department of Civil Engineering.

WSDOT, 1993. "Bridge Seismic Retrofit Program Report," September (1993)

Yang, Y-S, (1994). "Aspects of Modeling of Reinfored Concrete Bridge Structures for Dynamic Time History Analysis". Ph.D. thesis, Department of Applied Mechanics and Engineering Systems, University of California, San Diego.

APPENDIX A

DATABASE FOR PARAMETRIC STUDY

DATABASE FOR PARAMETRIC ANALYSIS

CASE	K1 (k/in.)	K2 (k/in.)	K2/K1	W1 (k)	W2 (k)	REST. GAP (inch)	COMP. GAP (inch)	REST. STIFF. (k/in.)	FRICT.	ABUT. STIFF. (k/in.)	ABUT. STREN. (kips)	EARTHQ. RECORD	EARTHQ. INTEN. (g)	MAX REL. DISPL. HINGE (inch)	MAX REL. DISPL. ABUT. 1 (inch)	MAX REL. DISPL. ABUT. 2 (inch)
1	600	60	0.1	5000	5000	1	1	1000	YES	4000	1250	EL CENTRO	0.70	2.20	5.45	4.34
2	600	150	0.25	5000	5000	1	1	1000	YES	4000	1250	EL CENTRO	0.70	2.38	6.03	4.16
3	600	300	0.5	5000	5000	1	1	1000	YES	4000	1250	EL CENTRO	0.70	1.41	6.18	5.19
4	600	480	0.8	5000	5000	1	1	1000	YES	4000	1250	EL CENTRO	0.70	1.16	5.72	4.26
5	600	600	1	5000	5000	1	1	1000	YES	4000	1250	EL CENTRO	0.70	0.54	5.67	4.14
6	600	1200	2	5000	5000	1	1	1000	YES	4000	1250	EL CENTRO	0.70	1.45	4.90	2.75
7	600	2400	4	5000	5000	1	1	1000	YES	4000	1250	EL CENTRO	0.70	2.17	4.11	2.23
8	600	4200	7	5000	5000	1	1	1000	YES	4000	1250	EL CENTRO	0.70	2.80	2.69	1.79
9	600	6000	10	5000	5000	1	1	1000	YES	4000	1250	EL CENTRO	0.70	2.85	2.64	1.30
10	600	60	0.1	5000	5000	1	1	0	YES	4000	1250	EL CENTRO	0.70	7.58	5.16	4.54
11	600	60	0.1	5000	5000	1	1	250	YES	4000	1250	EL CENTRO	0.70	3.67	5.39	4.38
12	600	60	0.1	5000	5000	1	1	500	YES	4000	1250	EL CENTRO	0.70	3.08	5.33	4.61
13	600	60	0.1	5000	5000	1	1	2000	YES	4000	1250	EL CENTRO	0.70	1.80	5.61	4.59
14	600	150	0.25	5000	5000	1	1	0	YES	4000	1250	EL CENTRO	0.70	6.64	5.23	3.78
15	600	150	0.25	5000	5000	1	1	250	YES	4000	1250	EL CENTRO	0.70	4.17	5.63	4.93
16	600	150	0.25	5000	5000	1	1	500	YES	4000	1250	EL CENTRO	0.70	2.94	5.87	4.02
17	600	150	0.25	5000	5000	1	1	2000	YES	4000	1250	EL CENTRO	0.70	1.73	6.07	4.70
18	600	300	0.5	5000	5000	1	1	0	YES	4000	1250	EL CENTRO	0.70	5.23	6.18	4.64
19	600	300	0.5	5000	5000	1	1	250	YES	4000	1250	EL CENTRO	0.70	2.75	6.18	4.93
20	600	300	0.5	5000	5000	1	1	500	YES	4000	1250	EL CENTRO	0.70	2.21	6.18	5.12
21	600	300	0.5	5000	5000	1	1	1500	YES	4000	1250	EL CENTRO	0.70	1.35	6.18	5.21
22	600	300	0.5	5000	5000	1	1	2000	YES	4000	1250	EL CENTRO	0.70	1.34	6.18	5.22
23	600	300	0.5	5000	5000	1	1	2500	YES	4000	1250	EL CENTRO	0.70	1.32	6.18	5.22
24	600	600	1	5000	5000	1	1	0	YES	4000	1250	EL CENTRO	0.70	0.54	5.67	4.14
25	600	600	1	5000	5000	1	1	250	YES	4000	1250	EL CENTRO	0.70	0.54	5.67	4.14
26	600	600	1	5000	5000	1	1	500	YES	4000	1250	EL CENTRO	0.70	0.54	5.67	4.14
27	600	600	1	5000	5000	1	1	1500	YES	4000	1250	EL CENTRO	0.70	0.54	5.67	4.14
28	600	600	1	5000	5000	1	1	2000	YES	4000	1250	EL CENTRO	0.70	0.54	5.67	4.14
29	600	600	1	5000	5000	1	1	2500	YES	4000	1250	EL CENTRO	0.70	0.54	5.67	4.14

CASE	K1 (k/in.)	K2 (k/in.)	K2/K1	W1 (k)	W2 (k)	REST. GAP (inch)	COMP. GAP (inch)	REST. STIFF. (k/in.)	FRICT.	ABUT. STIFF. (k/in.)	ABUT. STREN. (kips)	EARTHQ. RECORD	EARTHQ. INTEN. (g)	MAX REL. DISPL. HINGE (inch)	MAX REL. DISPL. ABUT. 1 (inch)	MAX REL. DISPL. ABUT. 2 (inch)
30	600	1200	2	5000	5000	1	1	0	YES	4000	1250	EL CENTRO	0.70	2.89	4.71	2.75
31	600	1200	2	5000	5000	1	1	250	YES	4000	1250	EL CENTRO	0.70	2.34	4.94	2.75
32	600	1200	2	5000	5000	1	1	500	YES	4000	1250	EL CENTRO	0.70	1.63	4.93	2.75
33	600	1200	2	5000	5000	1	1	1500	YES	4000	1250	EL CENTRO	0.70	1.39	4.89	2.75
34	600	1200	2	5000	5000	1	1	2000	YES	4000	1250	EL CENTRO	0.70	1.37	4.90	2.75
35	600	1200	2	5000	5000	1	1	2500	YES	4000	1250	EL CENTRO	0.70	1.43	4.95	2.75
36	600	2400	4	5000	5000	1	1	0	YES	4000	1250	EL CENTRO	0.70	5.02	3.67	1.76
37	600	2400	4	5000	5000	1	1	250	YES	4000	1250	EL CENTRO	0.70	2.92	4.13	1.94
38	600	2400	4	5000	5000	1	1	500	YES	4000	1250	EL CENTRO	0.70	2.91	4.23	2.09
39	600	2400	4	5000	5000	1	1	2000	YES	4000	1250	EL CENTRO	0.70	1.79	4.09	2.03
40	600	4200	7	5000	5000	1	1	0	YES	4000	1250	EL CENTRO	0.70	6.27	2.69	1.77
41	600	4200	7	5000	5000	1	1	250	YES	4000	1250	EL CENTRO	0.70	4.81	2.65	1.83
42	600	4200	7	5000	5000	1	1	500	YES	4000	1250	EL CENTRO	0.70	3.60	2.87	1.84
43	600	4200	7	5000	5000	1	1	2000	YES	4000	1250	EL CENTRO	0.70	2.11	2.80	1.70
44	600	6000	10	5000	5000	1	1	0	YES	4000	1250	EL CENTRO	0.70	6.23	2.44	1.39
45	600	6000	10	5000	5000	1	1	250	YES	4000	1250	EL CENTRO	0.70	4.36	2.44	1.40
46	600	6000	10	5000	5000	1	1	500	YES	4000	1250	EL CENTRO	0.70	3.48	2.47	1.38
47	600	6000	10	5000	5000	1	1	2000	YES	4000	1250	EL CENTRO	0.70	2.25	2.93	1.17
48	600	60	0.1	5000	5000	0	1	1000	YES	4000	1250	EL CENTRO	0.70	0.94	6.15	4.55
49	600	60	0.1	5000	5000	2	1	1000	YES	4000	1250	EL CENTRO	0.70	3.21	5.16	4.40
50	600	60	0.1	5000	5000	3	1	1000	YES	4000	1250	EL CENTRO	0.70	4.16	5.16	4.20
51	600	150	0.25	5000	5000	0	1	1000	YES	4000	1250	EL CENTRO	0.70	1.06	6.31	4.07
52	600	150	0.25	5000	5000	2	1	1000	YES	4000	1250	EL CENTRO	0.70	3.36	5.23	3.78
53	600	150	0.25	5000	5000	3	1	1000	YES	4000	1250	EL CENTRO	0.70	4.68	5.47	4.09
54	600	300	0.5	5000	5000	0	1	1000	YES	4000	1250	EL CENTRO	0.70	0.55	6.01	5.21
55	600	300	0.5	5000	5000	0.5	1	1000	YES	4000	1250	EL CENTRO	0.70	1.18	6.15	4.99
56	600	300	0.5	5000	5000	1.5	1	1000	YES	4000	1250	EL CENTRO	0.70	2.47	6.18	4.72
57	600	300	0.5	5000	5000	2	1	1000	YES	4000	1250	EL CENTRO	0.70	2.93	6.18	4.64
58	600	300	0.5	5000	5000	2.5	1	1000	YES	4000	1250	EL CENTRO	0.70	3.40	6.18	4.64
59	600	300	0.5	5000	5000	3	1	1000	YES	4000	1250	EL CENTRO	0.70	3.85	6.18	4.64
60	600	600	1	5000	5000	0	1	1000	YES	4000	1250	EL CENTRO	0.70	0.28	5.54	4.05
61	600	600	1	5000	5000	0.5	1	1000	YES	4000	1250	EL CENTRO	0.70	0.53	5.67	4.14
62	600	600	1	5000	5000	1.5	1	1000	YES	4000	1250	EL CENTRO	0.70	0.54	5.67	4.14

CASE	K1 (k/in.)	K2 (k/in.)	K2/K1	W1 (k)	W2 (k)	REST. GAP (inch)	COMP. GAP (inch)	REST. STIFF. (k/in.)	FRICT.	ABUT. STIFF. (k/in.)	ABUT. STREN. (kips)	EARTHQ. RECORD	EARTHQ. INTEN. (g)	MAX REL. DISPL. HINGE (inch)	MAX REL. DISPL. ABUT. 1 (inch)	MAX REL. DISPL. ABUT. 2 (inch)
63	600	600	1	5000	5000	2	1	1000	YES	4000	1250	EL CENTRO	0.70	0.54	5.67	4.14
64	600	600	1	5000	5000	2.5	1	1000	YES	4000	1250	EL CENTRO	0.70	0.54	5.67	4.14
65	600	600	1	5000	5000	3	1	1000	YES	4000	1250	EL CENTRO	0.70	0.54	5.67	4.14
66	600	1200	2	5000	5000	0	1	1000	YES	4000	1250	EL CENTRO	0.70	0.69	4.81	3.01
67	600	1200	2	5000	5000	0.5	1	1000	YES	4000	1250	EL CENTRO	0.70	1.11	4.92	2.75
68	600	1200	2	5000	5000	1.5	1	1000	YES	4000	1250	EL CENTRO	0.70	2.30	5.03	2.75
69	600	1200	2	5000	5000	2	1	1000	YES	4000	1250	EL CENTRO	0.70	2.61	4.85	2.75
70	600	1200	2	5000	5000	2.5	1	1000	YES	4000	1250	EL CENTRO	0.70	2.82	4.73	2.75
71	600	1200	2	5000	5000	3	1	1000	YES	4000	1250	EL CENTRO	0.70	2.89	4.71	2.75
72	600	2400	4	5000	5000	0	1	1000	YES	4000	1250	EL CENTRO	0.70	1.20	4.84	2.11
73	600	2400	4	5000	5000	2	1	1000	YES	4000	1250	EL CENTRO	0.70	2.87	3.93	1.78
74	600	2400	4	5000	5000	3	1	1000	YES	4000	1250	EL CENTRO	0.70	3.82	3.87	1.76
75	600	4200	7	5000	5000	0	1	1000	YES	4000	1250	EL CENTRO	0.70	1.72	3.90	0.87
76	600	4200	7	5000	5000	2	1	1000	YES	4000	1250	EL CENTRO	0.70	3.82	2.69	1.82
77	600	4200	7	5000	5000	3	1	1000	YES	4000	1250	EL CENTRO	0.70	4.76	2.69	1.77
78	600	6000	10	5000	5000	0	1	1000	YES	4000	1250	EL CENTRO	0.70	1.77	3.84	1.33
79	600	6000	10	5000	5000	2	1	1000	YES	4000	1250	EL CENTRO	0.70	3.89	2.44	1.40
80	600	6000	10	5000	5000	3	1	1000	YES	4000	1250	EL CENTRO	0.70	4.84	2.44	1.39
81	600	60	0.1	5000	5000	1	1	1000	NO	4000	1250	EL CENTRO	0.70	2.71	5.86	5.40
82	600	150	0.25	5000	5000	1	1	1000	NO	4000	1250	EL CENTRO	0.70	2.76	5.83	3.97
83	600	300	0.5	5000	5000	1	1	1000	NO	4000	1250	EL CENTRO	0.70	2.32	6.30	4.23
84	600	480	0.8	5000	5000	1	1	1000	NO	4000	1250	EL CENTRO	0.70	1.61	5.18	4.25
85	600	600	1	5000	5000	1	1	1000	NO	4000	1250	EL CENTRO	0.70	1.39	5.59	4.05
86	600	1200	2	5000	5000	1	1	1000	NO	4000	1250	EL CENTRO	0.70	1.87	4.88	3.02
87	600	2400	4	5000	5000	1	1	1000	NO	4000	1250	EL CENTRO	0.70	2.71	4.15	2.21
88	600	4200	7	5000	5000	1	1	1000	NO	4000	1250	EL CENTRO	0.70	2.49	2.82	1.55
89	600	6000	10	5000	5000	1	1	1000	NO	4000	1250	EL CENTRO	0.70	2.99	2.86	1.22
90	600	60	0.1	5000	5000	1	1	1000	YES	0	0	EL CENTRO	0.70	2.30	8.24	4.38
91	600	60	0.1	5000	5000	1	1	1000	YES	8000	2500	EL CENTRO	0.70	2.48	5.12	4.99
92	600	150	0.25	5000	5000	1	1	1000	YES	0	0	EL CENTRO	0.70	2.32	9.35	3.19
93	600	150	0.25	5000	5000	1	1	1000	YES	8000	2500	EL CENTRO	0.70	2.14	4.82	5.41
94	600	300	0.5	5000	5000	1	1	1000	YES	0	0	EL CENTRO	0.70	1.82	9.15	2.32
95	600	300	0.5	5000	5000	1	1	1000	YES	8000	2500	EL CENTRO	0.70	1.66	4.71	4.98

CASE	K1 (k/in.)	K2 (k/in.)	K2/K1	W1 (k)	W2 (k)	REST. GAP (inch)	COMP. GAP (inch)	REST. STIFF. (k/in.)	FRICT.	ABUT. STIFF. (k/in.)	ABUT. STREN. (kips)	EARTHQ. RECORD	EARTHQ. INTEN. (g)	MAX REL. DISPL. HINGE (inch)	MAX REL. DISPL. ABUT. 1 (inch)	MAX REL. DISPL. ABUT. 2 (inch)
96	600	600	1	5000	5000	1	1	1000	YES	0	0	EL CENTRO	0.70	0.00	7.30	3.81
97	600	600	1	5000	5000	1	1	1000	YES	8000	2500	EL CENTRO	0.70	0.78	4.46	4.47
98	600	1200	2	5000	5000	1	1	1000	YES	0	0	EL CENTRO	0.70	1.75	5.63	1.85
99	600	1200	2	5000	5000	1	1	1000	YES	8000	2500	EL CENTRO	0.70	1.84	4.06	3.51
100	600	2400	4	5000	5000	1	1	1000	YES	0	0	EL CENTRO	0.70	2.23	4.58	1.46
101	600	2400	4	5000	5000	1	1	1000	YES	8000	2500	EL CENTRO	0.70	2.23	3.56	3.03
102	600	4200	7	5000	5000	1	1	1000	YES	0	0	EL CENTRO	0.70	2.76	2.59	1.85
103	600	4200	7	5000	5000	1	1	1000	YES	8000	2500	EL CENTRO	0.70	2.78	2.96	1.74
104	600	6000	10	5000	5000	1	1	1000	YES	0	0	EL CENTRO	0.70	2.87	2.06	2.20
105	600	6000	10	5000	5000	1	1	1000	YES	8000	2500	EL CENTRO	0.70	2.64	3.05	0.70
106	600	60	0.1	5000	5000	0.6	1.4	1000	YES	4000	1250	EL CENTRO	0.70	1.92	5.66	4.33
107	600	60	0.1	5000	5000	1.3	0.7	1000	YES	4000	1250	EL CENTRO	0.70	2.58	5.88	4.70
108	600	150	0.25	5000	5000	0.6	1.4	1000	YES	4000	1250	EL CENTRO	0.70	1.70	6.87	3.61
109	600	150	0.25	5000	5000	1.3	0.7	1000	YES	4000	1250	EL CENTRO	0.70	2.61	6.05	4.17
110	600	300	0.5	5000	5000	0.6	1.4	1000	YES	4000	1250	EL CENTRO	0.70	1.51	6.07	4.54
111	600	300	0.5	5000	5000	1.3	0.7	1000	YES	4000	1250	EL CENTRO	0.70	1.94	5.83	5.02
112	600	600	1	5000	5000	0.6	1.4	1000	YES	4000	1250	EL CENTRO	0.70	0.88	4.95	4.39
113	600	600	1	5000	5000	1.3	0.7	1000	YES	4000	1250	EL CENTRO	0.70	1.53	4.43	4.02
114	600	1200	2	5000	5000	0.6	1.4	1000	YES	4000	1250	EL CENTRO	0.70	1.07	4.60	2.98
115	600	1200	2	5000	5000	1.3	0.7	1000	YES	4000	1250	EL CENTRO	0.70	1.88	4.63	2.64
116	600	2400	4	5000	5000	0.6	1.4	1000	YES	4000	1250	EL CENTRO	0.70	1.79	4.44	2.14
117	600	2400	4	5000	5000	1.3	0.7	1000	YES	4000	1250	EL CENTRO	0.70	2.52	3.84	2.04
118	600	4200	7	5000	5000	0.6	1.4	1000	YES	4000	1250	EL CENTRO	0.70	2.44	2.92	1.93
119	600	4200	7	5000	5000	1.3	0.7	1000	YES	4000	1250	EL CENTRO	0.70	3.09	2.48	1.82
120	600	6000	10	5000	5000	0.6	1.4	1000	YES	4000	1250	EL CENTRO	0.70	2.52	2.27	2.23
121	600	6000	10	5000	5000	1.3	0.7	1000	YES	4000	1250	EL CENTRO	0.70	3.18	2.25	1.37
122	600	60	0.1	2500	5000	1	1	1000	YES	4000	1250	EL CENTRO	0.70	2.65	5.51	4.36
123	600	60	0.1	10000	5000	1	1	1000	YES	4000	1250	EL CENTRO	0.70	1.82	7.56	3.50
124	600	150	0.25	2500	5000	1	1	1000	YES	4000	1250	EL CENTRO	0.70	2.52	5.04	5.32
125	600	150	0.25	10000	5000	1	1	1000	YES	4000	1250	EL CENTRO	0.70	1.84	7.59	2.86
126	600	150	0.25	10000	5000	1	1	0	YES	4000	1250	EL CENTRO	0.70	7.21	7.09	4.01
127	600	300	0.5	2500	5000	1	1	0	YES	4000	1250	EL CENTRO	0.70	2.99	2.65	3.42
128	600	300	0.5	10000	5000	1	1	0	YES	4000	1250	EL CENTRO	0.70	4.06	7.89	2.35

CASE	K1 (k/in.)	K2 (k/in.)	K2/K1	W1 (k)	W2 (k)	REST. GAP (inch)	COMP. GAP (inch)	REST. STIFF. (k/in.)	FRICT.	ABUT. STIFF. (k/in.)	ABUT. STREN. (kips)	EARTHQ. RECORD	EARTHQ. INTEN. (g)	MAX REL. DISPL. HINGE (inch)	MAX REL. DISPL. ABUT. 1 (inch)	MAX REL. DISPL. ABUT. 2 (inch)
129	600	300	0.5	2500	5000	1	1	1000	YES	4000	1250	EL CENTRO	0.70	2.35	3.45	5.99
130	600	300	0.5	10000	5000	1	1	1000	YES	4000	1250	EL CENTRO	0.70	1.64	7.89	2.35
131	600	600	1	2500	5000	1	1	0	YES	4000	1250	EL CENTRO	0.70	2.74	3.35	3.56
132	600	600	1	10000	5000	1	1	0	YES	4000	1250	EL CENTRO	0.70	4.06	6.04	1.70
133	600	600	1	2500	5000	1	1	1000	YES	4000	1250	EL CENTRO	0.70	2.08	2.74	4.60
134	600	600	1	10000	5000	1	1	1000	YES	4000	1250	EL CENTRO	0.70	2.14	6.37	2.28
135	600	1200	2	2500	5000	1	1	0	YES	4000	1250	EL CENTRO	0.70	2.22	3.54	3.38
136	600	1200	2	10000	5000	1	1	0	YES	4000	1250	EL CENTRO	0.70	6.22	4.93	1.84
137	600	1200	2	2500	5000	1	1	1000	YES	4000	1250	EL CENTRO	0.70	1.45	4.08	3.38
138	600	1200	2	10000	5000	1	1	1000	YES	4000	1250	EL CENTRO	0.70	2.49	6.26	1.78
139	600	2400	4	10000	5000	1	1	0	YES	4000	1250	EL CENTRO	0.70	7.02	3.54	1.66
140	600	2400	4	2500	5000	1	1	1000	YES	4000	1250	EL CENTRO	0.70	1.55	3.21	2.87
141	600	2400	4	10000	5000	1	1	1000	YES	4000	1250	EL CENTRO	0.70	2.73	5.32	1.78
142	600	4200	7	2500	5000	1	1	1000	YES	4000	1250	EL CENTRO	0.70	1.84	2.84	2.27
143	600	4200	7	10000	5000	1	1	1000	YES	4000	1250	EL CENTRO	0.70	3.18	4.55	1.04
144	600	6000	10	2500	5000	1	1	1000	YES	4000	1250	EL CENTRO	0.70	1.94	2.32	1.80
145	600	6000	10	10000	5000	1	1	1000	YES	4000	1250	EL CENTRO	0.70	3.50	3.61	1.39
146	300	30	0.1	5000	5000	1	1	1000	YES	4000	1250	EL CENTRO	0.70	2.06	9.17	4.29
147	1200	120	0.1	5000	5000	1	1	1000	YES	4000	1250	EL CENTRO	0.70	2.59	5.25	3.59
148	300	75	0.25	5000	5000	1	1	1000	YES	4000	1250	EL CENTRO	0.70	1.69	9.14	3.67
149	1200	300	0.25	5000	5000	1	1	1000	YES	4000	1250	EL CENTRO	0.70	2.36	4.04	5.07
150	300	75	0.25	5000	5000	1	1	0	YES	4000	1250	EL CENTRO	0.70	6.57	8.53	3.52
151	300	150	0.5	5000	5000	1	1	1000	YES	4000	1250	EL CENTRO	0.70	1.76	9.48	3.48
152	1200	600	0.5	5000	5000	1	1	1000	YES	4000	1250	EL CENTRO	0.70	1.58	4.63	3.31
153	300	300	1	5000	5000	1	1	1000	YES	4000	1250	EL CENTRO	0.70	1.10	7.59	3.57
154	1200	1200	1	5000	5000	1	1	1000	YES	4000	1250	EL CENTRO	0.70	1.19	4.67	2.38
155	300	600	2	5000	5000	1	1	1000	YES	4000	1250	EL CENTRO	0.70	1.53	5.47	4.08
156	1200	2400	2	5000	5000	1	1	1000	YES	4000	1250	EL CENTRO	0.70	1.59	3.71	2.48
157	300	1200	4	5000	5000	1	1	1000	YES	4000	1250	EL CENTRO	0.70	2.06	4.76	3.66
158	1200	4800	4	5000	5000	1	1	1000	YES	4000	1250	EL CENTRO	0.70	2.22	2.61	1.85
159	300	2100	7	5000	5000	1	1	1000	YES	4000	1250	EL CENTRO	0.70	2.76	4.14	2.57
160	1200	8400	7	5000	5000	1	1	1000	YES	4000	1250	EL CENTRO	0.70	2.22	2.48	1.07
161	300	3000	10	5000	5000	1	1	1000	YES	4000	1250	EL CENTRO	0.70	2.77	3.97	2.16

CASE	K1 (k/in.)	K2 (k/in.)	K2/K1	W1 (k)	W2 (k)	REST. GAP (inch)	COMP. GAP (inch)	REST. STIFF. (k/in.)	FRICT.	ABUT. STIFF. (k/in.)	ABUT. STREN. (kips)	EARTHQ. RECORD	EARTHQ. INTEN. (g)	MAX REL. DISPL. HINGE (inch)	MAX REL. DISPL. ABUT. 1 (inch)	MAX REL. DISPL. ABUT. 2 (inch)
162	1200	12000	10	5000	5000	1	1	1000	YES	4000	1250	EL CENTRO	0.70	2.42	1.89	0.74
163	600	60	0.1	5000	5000	1	0	1000	YES	4000	1250	EL CENTRO	0.70	2.28	5.62	4.38
164	600	60	0.1	5000	5000	1	0.5	1000	YES	4000	1250	EL CENTRO	0.70	2.22	5.80	4.86
165	600	60	0.1	5000	5000	1	1.5	1000	YES	4000	1250	EL CENTRO	0.70	2.43	5.69	4.76
166	600	150	0.25	5000	5000	1	0	1000	YES	4000	1250	EL CENTRO	0.70	2.59	5.84	3.62
167	600	150	0.25	5000	5000	1	0.5	1000	YES	4000	1250	EL CENTRO	0.70	2.98	6.04	4.00
168	600	150	0.25	5000	5000	1	1.5	1000	YES	4000	1250	EL CENTRO	0.70	2.98	6.05	4.30
169	600	300	0.5	5000	5000	1	0	1000	YES	4000	1250	EL CENTRO	0.70	0.67	5.77	5.46
170	600	300	0.5	5000	5000	1	0.5	1000	YES	4000	1250	EL CENTRO	0.70	1.18	6.15	4.99
171	600	300	0.5	5000	5000	1	1.5	1000	YES	4000	1250	EL CENTRO	0.70	1.96	5.75	4.64
172	600	600	1	5000	5000	1	0	1000	YES	4000	1250	EL CENTRO	0.70	0.63	4.87	3.86
173	600	600	1	5000	5000	1	0.5	1000	YES	4000	1250	EL CENTRO	0.70	1.39	4.66	4.05
174	600	600	1	5000	5000	1	1.5	1000	YES	4000	1250	EL CENTRO	0.70	0.44	5.82	4.41
175	600	1200	2	5000	5000	1	0	1000	YES	4000	1250	EL CENTRO	0.70	1.81	4.30	2.68
176	600	1200	2	5000	5000	1	0.5	1000	YES	4000	1250	EL CENTRO	0.70	1.75	4.46	2.65
177	600	1200	2	5000	5000	1	1.5	1000	YES	4000	1250	EL CENTRO	0.70	1.77	5.02	2.99
178	600	2400	4	5000	5000	1	0	1000	YES	4000	1250	EL CENTRO	0.70	2.90	3.77	1.81
179	600	2400	4	5000	5000	1	0.5	1000	YES	4000	1250	EL CENTRO	0.70	2.75	4.24	1.84
180	600	2400	4	5000	5000	1	1.5	1000	YES	4000	1250	EL CENTRO	0.70	2.46	4.35	2.01
181	600	4200	7	5000	5000	1	0	1000	YES	4000	1250	EL CENTRO	0.70	2.48	3.06	1.85
182	600	4200	7	5000	5000	1	0.5	1000	YES	4000	1250	EL CENTRO	0.70	2.61	2.87	1.33
183	600	4200	7	5000	5000	1	1.5	1000	YES	4000	1250	EL CENTRO	0.70	3.06	3.35	1.94
184	600	6000	10	5000	5000	1	0	1000	YES	4000	1250	EL CENTRO	0.70	2.72	2.72	1.45
185	600	6000	10	5000	5000	1	0.5	1000	YES	4000	1250	EL CENTRO	0.70	2.69	2.94	0.75
186	600	6000	10	5000	5000	1	1.5	1000	YES	4000	1250	EL CENTRO	0.70	2.96	2.66	1.75
187	600	150	0.25	5000	5000	1	1	0	YES	4000	1250	EL CENTRO	0.35	3.80	2.52	2.65
188	600	150	0.25	10000	5000	1	1	0	YES	4000	1250	EL CENTRO	0.35	2.17	4.04	2.64
189	300	75	0.25	5000	5000	1	1	0	YES	4000	1250	EL CENTRO	0.35	3.27	3.76	3.28
190	600	600	1	5000	5000	1	1	0	YES	4000	1250	EL CENTRO	0.35	1.21	2.64	2.33
191	600	2400	4	10000	5000	1	1	0	YES	4000	1250	EL CENTRO	0.35	4.64	2.01	0.91
192	600	2400	4	5000	5000	2	1	1000	YES	4000	1250	EL CENTRO	0.35	2.71	1.85	0.80
193	600	150	0.25	5000	5000	1	1	1000	YES	4000	1250	EL CENTRO	0.35	2.01	2.52	3.34
194	600	600	1	5000	5000	1	1	1000	YES	4000	1250	EL CENTRO	0.35	1.09	2.57	2.33

CASE	K1 (k/in.)	K2 (k/in.)	K2/K1	W1 (k)	W2 (k)	REST. GAP (inch)	COMP. GAP (inch)	REST. STIFF. (k/in.)	FRICT.	ABUT. STIFF. (k/in.)	ABUT. STREN. (kips)	EARTHQ. RECORD	EARTHQ. INTEN. (g)	MAX REL. DISPL. HINGE (inch)	MAX REL. DISPL. ABUT. 1 (inch)	MAX REL. DISPL. ABUT. 2 (inch)
195	600	2400	4	5000	5000	1	1	1000	YES	4000	1250	EL CENTRO	0.35	1.87	1.89	1.17
196	600	2400	4	5000	5000	1	1	0	YES	4000	1250	EL CENTRO	0.35	3.06	1.85	0.80
197	600	150	0.25	5000	5000	1	1	0	YES	4000	1250	OLYMPIA	0.56	2.20	3.33	2.41
198	600	150	0.25	10000	5000	1	1	0	YES	4000	1250	OLYMPIA	0.56	1.45	3.48	3.45
199	300	75	0.25	5000	5000	1	1	0	YES	4000	1250	OLYMPIA	0.56	1.46	2.49	3.49
200	600	600	1	5000	5000	1	1	0	YES	4000	1250	OLYMPIA	0.56	0.75	2.82	2.58
201	600	2400	4	10000	5000	1	1	0	YES	4000	1250	OLYMPIA	0.56	3.21	2.31	0.41
202	600	2400	4	5000	5000	2	1	1000	YES	4000	1250	OLYMPIA	0.56	2.73	2.59	0.51
203	600	150	0.25	5000	5000	1	1	1000	YES	4000	1250	OLYMPIA	0.56	1.39	2.75	2.32
204	600	600	1	5000	5000	1	1	1000	YES	4000	1250	OLYMPIA	0.56	0.75	2.82	2.58
205	600	2400	4	5000	5000	1	1	1000	YES	4000	1250	OLYMPIA	0.56	2.12	2.84	0.51
206	600	2400	4	5000	5000	1	1	0	YES	4000	1250	OLYMPIA	0.56	2.85	2.56	0.49
207	600	150	0.25	5000	5000	1	1	0	YES	4000	1250	JAMES	0.38	5.45	4.11	5.34
208	600	150	0.25	10000	5000	1	1	0	YES	4000	1250	JAMES	0.38	2.68	6.34	6.17
209	300	75	0.25	5000	5000	1	1	0	YES	4000	1250	JAMES	0.38	4.89	4.59	5.48
210	600	600	1	5000	5000	1	1	0	YES	4000	1250	JAMES	0.38	0.07	3.35	5.00
211	600	2400	4	10000	5000	1	1	0	YES	4000	1250	JAMES	0.38	6.71	4.24	0.53
212	600	2400	4	5000	5000	2	1	1000	YES	4000	1250	JAMES	0.38	2.62	2.27	0.66
213	600	150	0.25	5000	5000	1	1	1000	YES	4000	1250	JAMES	0.38	1.89	4.11	5.34
214	600	600	1	5000	5000	1	1	1000	YES	4000	1250	JAMES	0.38	0.07	3.35	5.00
215	600	2400	4	5000	5000	1	1	1000	YES	4000	1250	JAMES	0.38	2.02	2.19	1.48
216	600	2400	4	5000	5000	1	1	0	YES	4000	1250	JAMES	0.38	3.51	2.27	0.66